Development of Microdevice-Based Aptamer Sensors for Mycotoxin Analysis

DONNY NUGRAHA MAZAAFRIANTO

Graduate School of Chemical Sciences and Engineering

Hokkaido University

Doctor Dissertation

Title DEVELOPMENT OF MICRODEVICE-BASED APTAMER SENSORS FOR MYCOTOXIN ANALYSIS

Author Donny Nugraha Mazaafrianto

Supervisor Professor Manabu Tokeshi, Ph.D.

Abstract

Since the systematic evolution of ligands by exponential enrichment (SELEX) method was developed, aptamers have made significant contributions as bio-recognition sensors. The aptamer that affinity and specificity parallel those of antibody is expected to have a future impact on a biosensor. In addition, aptamers have an unleashed potential to circumvent limitations associated with antibodies and could be utilized in practical settings where their performance could be compared directly to that of antibodies. In this research, we have developed aptamer sensor on the microdevice system for detection of ochratoxin A (OTA), a carcinogenic toxin that produced by secondary metabolism of *Penicillium* and *Aspergillus* fungal strains. Microdevice systems allow for low reagent consumption, high-throughput of samples, and disposability. Due to these advantages, there has been an increasing demand to develop microdevice-based aptasensor for analytical technique application. Highly sensitive detection techniques, such as electrochemical and optical detection, have been integrated into lab-on-a-chip aptasensor devices towards the goal of establishing point-of-care diagnoses for target OTA analyses. In this context, the general introduction including present perspective are described in chapter 1.

In chapter 2, microdevice based aptamer sensor for the simple, portable, and low-cost detection system to quantitatively measure the ochratoxin A in real sample have been developed. First, a miniaturized electrochemical aptamer-based sensor was developed for the label-free with signal-off detection or TID (target induced dissociation) method. For the construction of the sensor, a gold thin-film three-electrode system was fabricated using standard microfabrication techniques on a polystyrene substrate (25 mm × 25 mm). Subsequently, the thiol-modified linker, 6-mercaptohexanol, DNA aptamer, and methylene blue (MB) were sequentially applied to the working electrode to construct a sensing layer. MB served as a redox indicator that interacted with the aptamer via the guanine bases and phosphate backbone to form complexes. The addition of OTA to the sensor induced the folding of the aptamer, which was accompanied by the release of the aptamer−MB−OTA complex from the sensor. Thus, the amount of MB decreased with increasing concentration of OTA. Differential pulse voltammetry (DPV) was used for monitoring the highly sensitive

detection. The standard curve for OTA exhibited a wide linearity ranging from 0.1 to 300 ng mL^{-1} with a detection limit of 78.3 pg mL^{-1} (S/N = 3). The selectivity test confirmed that the aptamer had high affinity only for the target. The OTA recoveries with the proposed sensor in commercial samples of coffee and beer were 86.4−107%.

Chapter 3 proposed the miniaturized electrochemical aptasensor by using a dithiol-modified aptamer which had a high stability on the gold electrode because of their two anchors. The sensor based on structure-switching of the aptamer upon the interaction with OTA, which produced the signal current. The non-covalent interaction of methylene blue (MB) with the aptamer was also used as an electrochemical indicator for the simple sensor fabrication. In this study, the performance of the sensor was characterized, including the dissociation constant of the aptamer-OTA complex. The proposed sensor exhibited high reproducibility and enough sensitivity to detect the minimum amount of OTA required for the analysis of real food samples with a limit of detection of 113 pM (45 pg mL^{-1}). The sensor holds great promise for a simple inexpensive technique with low-reagent consumption for on-site detection of OTA.

In chapter 4, describes competitive fluorescence polarization (FP) assay based on fluorescence polarization aptamerassay (FPAA). The FP method is a homogenous method which not required separation and washing step. In addition, integration of FP detection in the miniaturized device give more advantages such as low reagent consumption and portability. Different from conventional fluorescence polarization immunoassay (FPIA), here DNA aptamer against OTA was used as affinity ligand, and fluorescence-labeled OTA served as fluorescence tracer. The binding between tracer and aptamer gave large FP due to molecular volume increase and restricted rotation of the tracer. When OTA was present in the solution, the tracer and OTA was competitively bound with the aptamer, causing a decrease of FP intensity proportional with OTA concentration. The optimized FPAA had a wide detection range from 0.1 to 1500 ng mL^{-1} with detection limit 1 ng mL^{-1}. The selectivity of FP method was evaluated by using poly A-T-C-G and other mycotoxins such as AFB1 and DON, both tests presented good selectivity performance.

The final chapter is the summary of the results and findings during the research. In addition, future prospect and research for aptamer-based fluorescence polarization are described in this chapter.

Table of Contents

Abbreviations

The following abbreviations are used in this manuscript:

AFB1	aflatoxin
A-G-T-C	adenine – guanine – thymine – cytosine
AuNPs	aurum (gold) nanoparticles
CE	counter electrode
Cr	chrome
CTCs	circulating tumor cells
CV	cyclic voltammetry
DON	deoxynivalenol
DNA	deoxyribonucleic acid
DPV	differential pulse voltammetry
ELISA	enzyme-linked immune sorbent assay
FA	fluorescence anisotropy
FAM	fluorescein amidite
FC	ferrocene
FP	fluorescence polarization
FPAA	fluorescence polarization aptamerassay
FPIA	fluorescence polarization immunoassay
GO	graphene oxide
HCR	hybridization chain reaction
LOD	limit of detection

MB	methylene blue
MCH	mercaptohexanol
OTA	ochratoxin A
PBS	phosphate-buffered saline
PDMS	poly(dimethylsiloxane)
PMMA	poly (methyl methacrylate)
POCT	point-of-care-test
PS	poly styrene
PtNPs	platinum nanoparticles
RE	reference electrode
RNA	ribonucleic acid
SAM	self-assembly monolayer
SELEX	systematic evolution of ligands by exponential enrichment
SPE	solid phase extraction
SPR	surface plasmon resonance
SWV	square wave voltammetry
TCEP	tris-(2-carboxyethyl)- phosphine hydrochloride
TE	tris−ethylenediaminetetraacetic acid
Ti	titanium
WE	working electrode
4-PL	four parameter logistic

CHAPTER 1 General Introduction

1.1 Introduction

In the past decade, technologies for analytical detection sensors have undergone significant growth. Conventional sensors are robust, reliable, and provide high reproducibility of measurements. However, their main drawback is that they cannot be integrated into a compact packaging flow, which in many analysis cases is critical. Beyond this, expensive instrumentation and long analysis time are general problems to be considered. For these reasons, microdevice platforms offer an attractive alternative to conventional techniques [1]. Furthermore, microdevices are also important for reducing the amount of sample required, for alleviating interferences or cross-contamination by their disposable design, and for integrating multiple sensor arrays to increase the throughput. Sensors perform three functions: targeting an analyte, recognizing an element, and transducing a signal. The analyte interacts in a selective way with the recognition site, which shows some affinity or a catalytic reaction. In a biosensor, the recognition system is based on biochemical or biological sensing elements such as antibodies, enzymes, nucleic acids, or aptamers [2]. These elements are commonly immobilized on a physicochemical transducer and combined with a detector to generate an electronic signal readout that is proportional to the quantity of the target. Antibodies and enzymes have made a big contribution to a wide range of applications that are based on molecular recognition. The use of antibodies became widespread by the 1970s, when polyclonal techniques from immunized animals was a popular choice [3]. The catalytic enzyme-based recognition system is very attractive in biosensor applications due to a variety of measurable reaction products arising from the catalytic process, which includes protons, electrons, light, and heat. Despite the fact of antibodies and enzyme-based assays are established as a standard method for analytical detection, they are still restricted in

recognizing several small molecules or non-immunogenic targets, which are not easy to analyze and differentiate.

Oligonucleotides such as RNA, DNA or peptides can be used as the receptor for the recognition of specific small organic molecules or even as a complementary strand in the hybridization process. The name of such an oligonucleotide is aptamer (“aptus” meaning “fitted” and “meros” meaning “part”) [4]. Some aptamers contort into three-dimensional (3D) conformations that can bind to target molecules in stable complexes and they commonly rely on van der Waals forces, hydrogen bonds, or electrostatic interactions [5]. Aptamers play a role similar to antibodies. However, they are obtained by a chemical synthesis that is easily modified, more stable, and inexpensive. Also, aptamers can discriminate between highly similar molecules, such as theophylline and caffeine, which differ by only a methyl group [6]. In addition, after performing the recognition function, aptamers can be efficiently regenerated without loss of either sensitivity or selectivity [7]. All these features make aptamers very suitable as a receptor in bio-sensing applications than antibodies. As described in Figure 1-1, addresses the current state of research related to microdevice instruments and the advantage of emerging aptamer biosensor for numerous applications and target analysis. It is divided into three parts: (i) classification of microdevice platforms; (ii) detection methods and assay formats; and (iii) applications to actual samples.

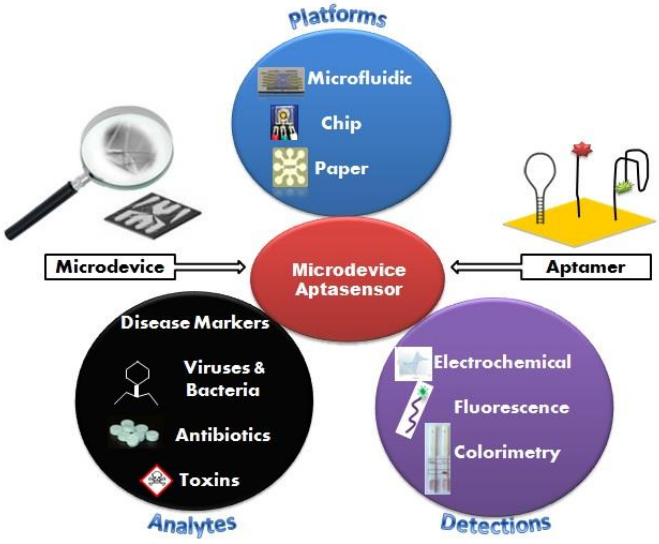

Figure 1-1. Schematic illustration of microdevice-based aptamer sensor with various platforms, detection methods and application to actual samples.

1.2 The SELEX Method (In-Vitro Selection)

Aptamers are oligonucleotides, commonly 12–80 nucleotides long, and they have a function to act as specific affinity receptors towards a broad spectrum of numerous targets including small organic molecules, proteins, cells, viruses, and bacteria. New aptamers are originated by an in vitro selection process known as the SELEX (systematic evolution of ligands by exponential enrichment) method. This method was simultaneously developed by Tuerk and Gold [8] and Ellington and Szostak [9], in 1990. The SELEX method contains several steps such as incubation, separation, amplification, and purification. Briefly, a library of randomized RNA or DNA sequences is incubated with the target of interest. The sequences with no affinity or only a weak affinity to the target are removed from the library, while the sequences that have strong binding are then recovered and amplified using a polymerase chain reaction (PCR), this process narrows down the aptamer candidates. The selection process is repeated approximately 7 to 15 times to create a sufficiently narrow pool of aptamer candidates that can then be characterized to determine their efficiency. A conventional SELEX method requires extensive manual handling of reagents, and it is time-

consuming, typically requiring a dozen or more rounds of repeating the method and weeks to months to achieve suitable affinity. The integration of several SELEX steps in a single small platform is an appealing trend in the field. It offers a range of capabilities of high-resolution separation between oligonucleotide candidates using small quantities of reagents and samples. A single-round screening of aptamers has been reported and this marked the innovation of a fully automated and integrated miniaturized SELEX process [10].

1.3 Classification of Microdevices

1.3.1 Microfluidic Devices

Microfluidics, also known as "lab-on-a-chip," is an emerging technology that represents a revolution in laboratory experimentation, bringing the benefits of integration, miniaturization, and automation to many research areas. It is the science and technology of systems that control small amounts (10^{-9}–10^{-18} L) of fluids in channels with dimensions of submillimeter to sub-micrometer [11]. The reduced dimensions and volumes in microfluidic channels allow all tasks to be done with much less sample than what otherwise might be used. It is beneficial to improve the transport of analyte from the sample volume to the biorecognition element, in particular for a surface-bound sensing element [12]. In recent years, the development of microfluidic chips as a miniaturized diagnostic platform has attracted the attention of researchers. The basic operating units of biochemistry analysis, e.g., sample preparation, reaction, and separation tests, can be integrated into a micron scale chip, and then the whole analysis process can be completed automatically.

1.3.1.1 Microfluidic SELEX Devices

One example that combines the advantages of the SELEX method and microfluidic systems into a compact platform design is a competitive assay test of the selected aptamer to

reduce the number of sequences subjected to sequencing and affinity characterization. The entire SELEX process is shortened and the possibility to produce the aptamer as a biorecognition element is increased [13]. Integration of the affinity selection and amplification steps in SELEX by combining bead-based biochemical reactions has been demonstrated [14–18]. A simple microfluidic SELEX device was developed by Olsen *et al* [17], this device was fabricated using single layer soft lithography (Figure 1-2). In this work, an electrokinetic microfluidic device for aptamer enrichment was demonstrated as an integrated microfluidic device without requiring an offline process. The electrokinetic microfluidic device features a microchamber and an electrokinetic transfer microchannel that allows oligonucleotide migration under an electric field. A heater and temperature sensor are used to control the target-aptamer binding and amplification process through PCR thermal cycling. In another example, Birch *et al* developed an inertia microfluidic SELEX or I-SELEX device to establish a system for continuous partitioning of cell-bound aptamers away from unbound nucleic acids in a bulk solution [19]. The device was fabricated from polydimethylsiloxane (PDMS) and bonded to microscopic glass slides and had bi-loop spiral with double inlets-outlets (Figure 1-3). The working process began by pumping the target-aptamer library and buffer through each inlet, then the unbound aptamers migrate along the outer wall towards the waste outlet. Using this strategy, they successfully identified a high-affinity aptamer that was a subset of specific interactions with distinct epitopes on malaria-parasite infected red blood cells. In order to improve efficiency and selectivity, some groups have developed techniques such as the volume dilution challenge microfluidic SELEX (VDC-MSELEX) [20], dielectrophoresis and electrophoresis SELEX [21], SELEX assisted by graphene oxide (GO) [22], surface plasmon resonance (SPR)-based SELEX methods [23,24]. SPR-based SELEX methods have attracted attention in recent years because selection and evaluation can be performed simultaneously without labeling the sensor.

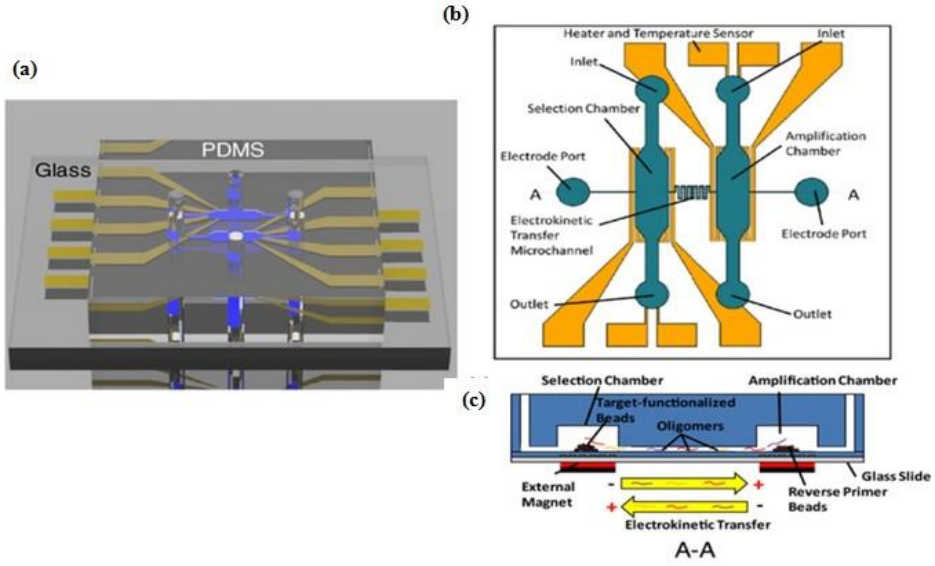

Figure 1-2. Schematic of microfluidic SELEX device which integrates selection and amplification steps. (**a**) Polydimethylsiloxane (PDMS) channel on glass substrate; (**b**) Top view with detailed features; (**c**) Selection and amplification microchamber connected by a single serpentine shaped microchannel. Reproduced with permission from reference [17]. Copyright 2017 Electrochemical Society

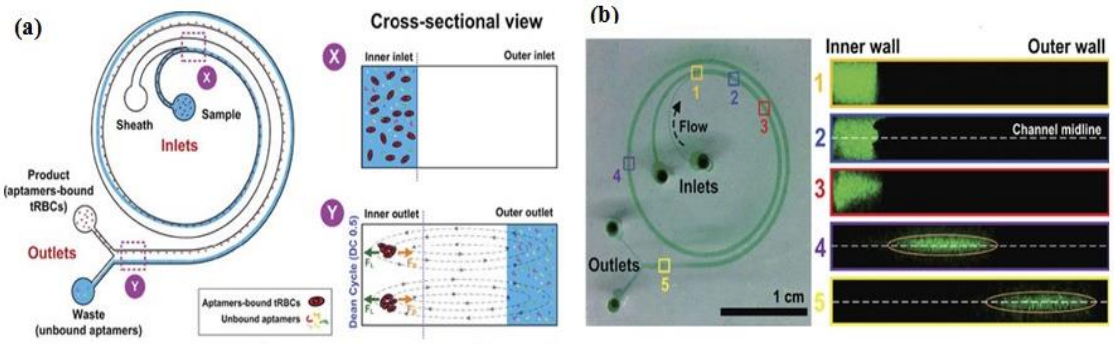

Figure1-3. Bi-loop spiral design of inertial microfluidic SELEX (I-SELEX) with dual inlets and outlets. (**a**) The unbound oligonucleotide/any particles migrate towards the outer-side wall (blue color) and are separated with the desired target; (**b**) Numbers 1–5 represent cross sections inside the channel. Fluorescence-labeled aptamer was used to identify each position. Reproduced with permission from reference [19]. Copyright 2015 Macmillan.

1.3.1.2 Microfluidic Chip Aptasensors

Microfluidic chips are a device or micro-channel that integrates a fluidic system including steps for transporting, mixing, preparing, and detecting a sample. Dimensions of the device must be in the range of a millimeter to a few square centimeters [25]. In recent years, microfluidic chips have aroused increasing interest for various application because of their desirable features, such as the smaller sample amount needed and lowered reagent consumption. The substrate materials of microfluidic chips such as polymers (e.g., PDMS, PMMA, PS) [26–34], ceramics (e.g., glass) [6,13,14,16–19,21,25,35–63], and semiconductors (e.g., silicon) [64–73], are currently used to obtain mechanical strength. Many researchers utilize PDMS and the soft lithography technique to fabricate microfluidic devices due to their easiness of use and simple process. Prototypes can be rapidly built and tested because researchers do not waste time with laborious fabrication protocols. Contrary to common beliefs, soft lithography does not require hundreds of square meters of clean room space. Indeed, a small bench space under a lab fume hood is sufficient for placing PDMS prototyping instruments to quickly assess a microfluidic technique. Recently, Ma *et al* developed a very attractive design for a volumetric bar chart chip (V-chip) aptasensor [62]. This group applied a distance-readout method combined with aptamer-responsive hydrogel. Platinum nanoparticles (PtNPs) were used to encapsulate aptamer and hydrogel. Upon introduction of the target, the aptamer bound with the target then induced disruption of the hydrogel and released the PtNPs. Subsequently, the hydrogel was loaded into the volumetric bar chart chip while the PtNPs catalyzed the reaction of H_2O_2 to produce O_2. The colored ink flow in the V-chip was triggered by O_2 and was quantitatively related to the concentration of the target. Although the instrument design was very simple, it still needs to treat the sample with an immunoaffinity column similar to conventional methods. Zhao *et al* fabricated an aptamer-grafted silicon nanowire substrate (SiNS) embedded microfluidic chip and chaotic

mixer PDMS for sensitive detection of circulating tumor cells (CTCs) [68]. As a cancer marker, the presence of CTCs in blood is very rare and it is difficult to repeatedly observe them during the treatment, so Zhao *et al*. developed an aptamer-cocktail form with a synergistic effect (two or more aptamers may work synergistically, this phenomenon leads to increased cell affinity) (Figure 1-4). They constructed the cell-SELEX to produce multiple aptamers that were immobilized on the microfluidic device. In order to ensure the synergistic effect, they switched the position and number of aptamers to examine optimal conditions. Furthermore, they also evaluated the cell capture efficiency as a function of aptamer density and found that the efficiency gradually increased with aptamer density.

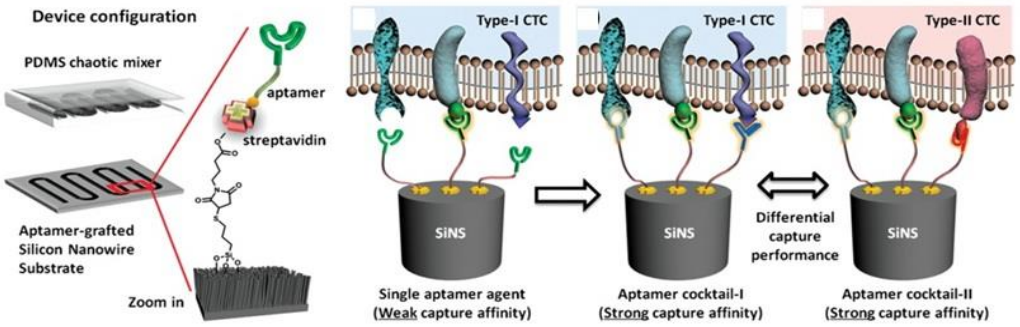

Figure 1-4. A representative chaotic mixer microfluidic device combined with an aptamer cocktail-grafted silicon nanowire substrate (SiNS). The different aptamers work synergistically to enhance capture affinity in a low-concentration target. Reproduced with permission from reference [68]. Copyright 2016 John Wiley and Son.

Automatic and integrated detection in a microfluidic device was demonstrated by Lee's group [46,47,56]. They fabricated two layers of PDMS structures and a glass substrate into a device having several chambers and including an external magnet, a micropump and a microvalve. As shown schematically in figure 1-5, the experiment started by immobilizing the first aptamer on magnetic beads (MBs) then incubating the

target in the micro chamber to form a complex aptamer-MBs-target. The external magnet was used to collect the complex molecules during the washing process, while the unbound and interfering molecules were washed away (Figure 1-5b step c–d). When the magnetic field was removed, the complex aptamer-MBs-target was remained at the micro-pump. In the next step, the FAM-labeled aptamer was introduced to determine the fluorescent intensity. Taking advantage of another feature of microfluidic design, Dou *et al*. developed microfluidic droplets-based aptamer-functionalized graphene oxide (GO) to detect low-solubility molecules [48]. The droplet-based design enables the rapid mixing of fluids in the droplet with a high reaction efficiency, even between two different phases of compounds like 17β-estradiol with solvent. The graphene oxide (GO) was used for fluorescence quenching and bonded with aptamer. Their microfluidic device consisted of two layers, the top layer was a PDMS channel with three inlets and one outlet (as the detection zone) and the bottom layer was a glass substrate. The target estradiol was dissolved in ethyl acetate as the oil phase, whereas an aptamer-GO was the aqueous phase. To generate droplets, Dou *et al*. used a T-junction channel. When the water and the oil phase introduced at different flow rates meet at the T-junction, water-in-oil emulsion droplets were generated and the aptamer-GO-target complex starts to form at this time. The principle detection of the microfluidic droplets is based on the distance-dependent fluorescence quenching properties of GO. Competitive binding of the aptamer and the target decrease the affinity of the adsorption by GO, this condition may release the aptamer from the GO surface, thus resulting in the fluorescence recovery ("turn-on" of fluorescence intensity). Giuffrida *et al*. [33] also used microfluidic droplets with a T-junction channel to detect lysozyme. However, their device had six inlets and was equipped with a mixing region and a chaotic mixer channel to allow chemiluminescence detection. The AuNPs was used to enhance chemiluminescence

intensity and it was conjugated with the aptamer. Giuffrida *et al*. reported that their device had several advantages over conventional devices, such as greater sensitivity (femtomolar level), faster detection (10 min), and a low background signal in the absence of the target. Several groups have utilized a microfluidic device for the separation process called microchip electrophoresis (MCE). Lin *et al*. [41] developed separation techniques on the MCE device based on a tunable aptamer. Different lengths of aptamers could modulate the electrophoretic mobility of proteins and promote effective separation in hydroxyethyl cellulose buffer. Pan *et al*. [37] proposed laser-induced fluorescence detection (LIF) on the MCE device to detect tumor marker carcinoembryonic antigen (CEA). The application of magnetic beads (MBs) to assist in the target-induced strand cycle would increase the sensitivity.

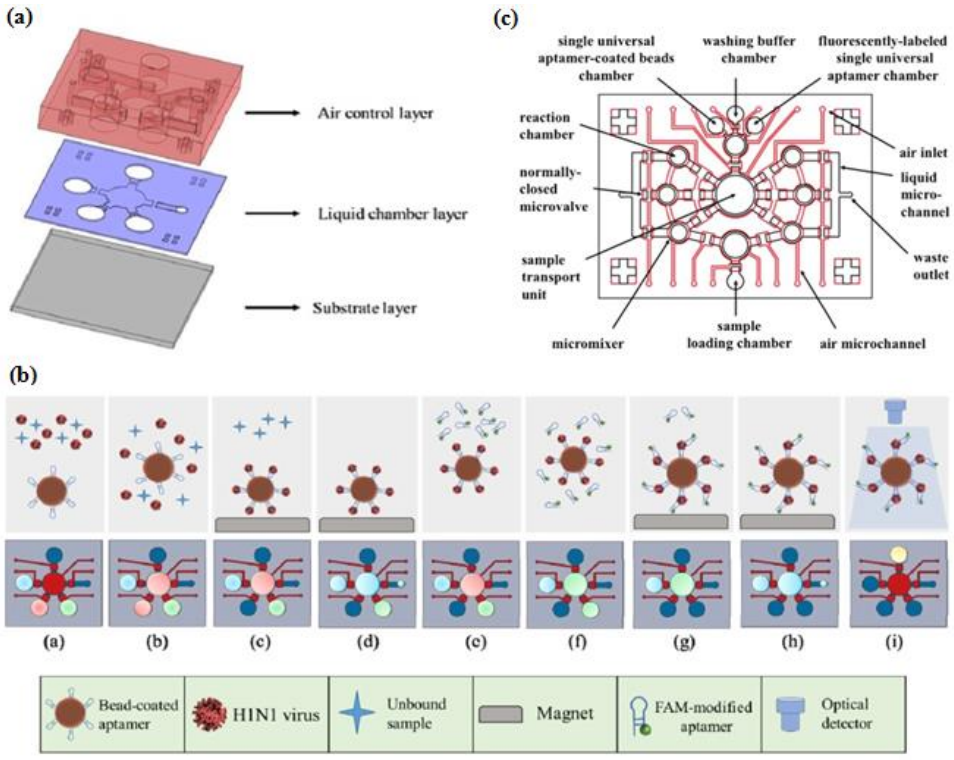

Figure 1-5. Integrated microfluidic chip system using a sandwich aptamer. (**a**) The device was composed of PDMS structures (air control layer & liquid chamber layer) and a glass substrate; (**b**) Schematic illustration of experimental procedure performed on the integrated microfluidic chip system. Reproduced with permission from reference [47]. Copyright 2016 Elsevier. (**c**) The configuration of the inlet-outlet, chambers, micromixers, and microvalve. Reproduced with permission from reference [46]. Copyright 2016 Elsevier.

1.3.2 Paper-Based Microdevice Aptasensors

Paper as a substrate in microdevices is a very promising material because its properties provide a versatility of functions. First of all, the cellulose structure allows a passive pump dispenser to be made; the fluid moves by capillary force, which precludes the need for an external instrument. Second, the porous cellulose structure serves to immobilize particles easily. Colorimetry is a common signaling method for obtaining qualitative or semiquantitative results [74]. Since Whitesides's group revitalized the field of microfluidic paper-based devices in 2007 [75], applications of paper devices have significantly increased due to their simple and low-cost fabrication. Paper-based microdevices can be classified into three main types: microfluidic paper analytical devices, dipstick assays, and lateral flow strip assays [76]. Integrating a paper analytical device and an aptamer to develop sensitive and efficient diagnosis point-of-care-test (POCT) devices for on-site detection was reported by Zhang *et al*. [77], who developed equipment-free quantitative aptamer-based assays with naked-eye readout to detection adenosine. The super-paramagnetic particles were modified with a short DNA strand for anchoring an aptamer probe. In the presence of the target, the complex aptamer-target was released from the magnetic surface, which then triggered a hybridization chain reaction (HCR) and glucose oxidase was activated to oxidize glucose to

H_2O_2 and glucose acid. The number of glucose oxidase molecules was proportional to the target concentration. The unique fabrication of a micro paper-based analytical device (μPAD) aptasensor was demonstrated by Fu *et al*. [78], who were inspired by Rubik's Cube (RC) toys and formed small iron components to generate hydrophobic barriers through a stamp-mode. The six-faced RCs have different patterns and can be tailored to make multiple combination channels. Fu *et al*. integrated the portable glucometer readout to detect signals (Figure 1-6a). During the stamping process, rosin (wax) penetrated into the paper, forming the hydrophobic channel and sample test zone. Although the RC stamp method has good potential for instrument-free sensing, preparing the aptamer sensor, supporting enzyme and carrying out reagent loading remain challenging tasks. Origami paper analytical devices (oPADs) have been introduced by several groups [79–81]. For example, Liu *et al*. [80] used a glucose oxidase tag to modify the relative concentrations of an electroactive redox couple, and a digital multimeter (DMM) to transduce the result. They folded the chromatography paper into two layers. The first layer, including the sample inlet, was fabricated by wax printing. The second layer was fabricated by screen printing conductive carbon ink. Furthermore, this paper was covered with plastic lamination to prevent fluid evaporation and any contamination. The biotin-labeled aptamer was immobilized on microbeads trapped within the paper fluidic channel and the electrochemical current rise with increasing adenosine concentration. This technique demonstrated a simple preparation when the aptamers immobilized on microbeads. However, the present challenges still occur when the aptamers directly immobilized on the cellulose structure. Yan *et al*. [79] presented a novel porous Au-paper working electrode on a compatible design origami-electrochemiluminescence (o-ECL). In order to amplify the signal, they used AuNPs, due to their large surface area, stability, and biocompatibility especially with aptamers. The ECL intensity increased only when ATP (adenosine triphosphate) was present. On the other hand, Ma *et al*. [81] developed the specific recognition of an aptamer

and the amplification strategy of a hybridization chain reaction (HCR) using an electrochemiluminescence (ECL) probe ($Ru(phen)_3^{2+}$). Lateral flow strip assays (LFSAs) are another type of paper-based microdevices. Their simple design allows for on-site detection. Several groups have successfully developed LFSAs combined with aptamer-functionalized AuNPs. As an example, Raston *et al*. [82] performed an easy fabrication of an LFSAs using a sandwich aptamer conjugated with AuNPs for sensitive vaspin detection. A strip contained three pads: sample pad, nitrocellulose membrane pad, and absorption pad. Two aptamers probes were used that basically functioned as a capturing probe and a signaling probe. When the sample containing vaspin was loaded on a sample pad, the primary aptamer in the test zone captured the vaspin. Thus, the color could be observed in the test zone. For the control experiment, a complementary aptamer in the control zone captured the remaining AuNP-labeled aptamer, thus the signal could always be observed as the control. The signal could only be observed in the presence of vaspin, while no signal was observed in the test zone for adiponectin, HSA (human serum albumin), and buffer as shown in Figure 1-6b. Wu *et al*. [83] and Zhou *et al*. [84] applied this assay strip to get a sensitive and rapid detection of Escherichia coli O157:H7 and Ochratoxin A. They covered the LFSA device with a plastic cover and utilized a portable strip reader to quantify the result.

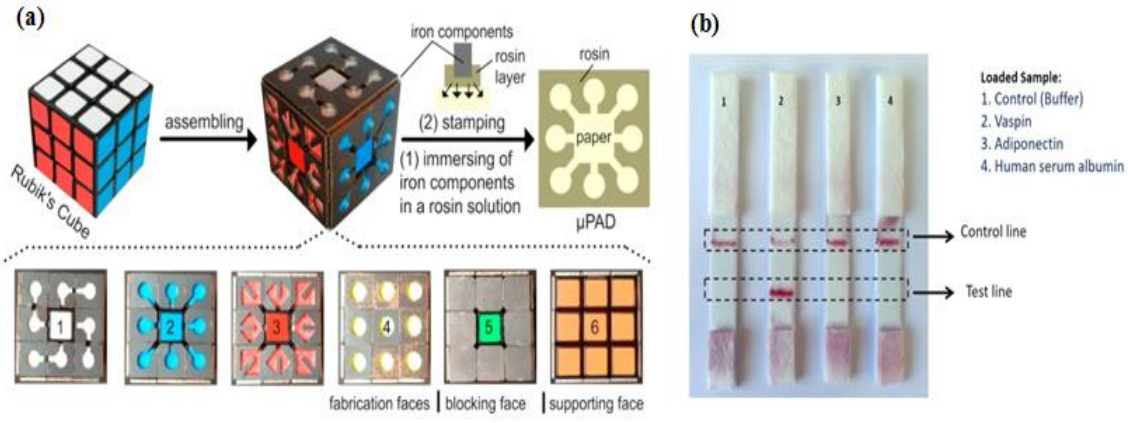

Figure 1-6. Paper-based analytical device aptasensor. (**a**) Rubik's cube-based μPAD aptasensor to generate a hydrophobic barrier and a testing zone. Parts 1–5 have different functions while the 6th part acts as a "bare" or support part only. Reproduced with permission from reference [78]. Copyright 2017 Elsevier. (**b**) Lateral strip test for specific detection of vaspin. This device was equipped with a control as indicator. Reproduced with permission from reference [82]. Copyright 2017 Elsevier.

1.4 Detection Method and Assay Format

1.4.1 Electrochemical Detection Methods

In general, an electrochemical reaction is defined as an electron transfer from a reactant to form a product that gives rise to an electrical current flowing through the cell. Electrochemical detection methods can be divided into three types of dynamic methods. The first type is known as the amperometric method and the current measured at a given electrode potential represents an analytical response that is dependent on the reactant concentration. The second type is known as the voltammetric method and the current is measured at a particular potential to obtain good sensitivity and low interference (the current-potential curve is archived for analytical purposes). The third type is called the galvanostatic method and the response is acquired in the form of a potential-time curve. Electrochemical measurements are typically performed using a cell comprised of three electrodes: (1) A working electrode (WE) where the main reaction, such as a redox and immobilization of a probe occur; (2) A reference electrode (RE) that measures the potential of the WE without passing the current through it; and (3) A counter electrode (CE) that serves to set the WE potential and balance current.

Many electrochemical techniques are used in analytical chemistry. The most commonly used ones for microfluidic devices or aptamer biosensors are amperometry [43], voltammetry [31,34,40,44,80,85], and electrochemical impedance spectroscopy [32,35,72,86–89]. Liu *et al*. [87] developed ZnO/graphene (ZnO/G) composite with S6 aptamer for a photoelectrochemical (PEC) detector. The AuNPs were electrodeposited on ZnO/G composite that was immobilized with the S6 aptamer, then indium tin oxide (ITO) was used as an electrode to facilitate the ZnO/G composite reaction. As a supporting electrolyte, Liu *et al*. utilized ascorbic acid as an electron donor for scavenging photogenerated holes under a mild solution medium. The electrochemical impedance spectra were applied to characterize the PEC biosensor and examine each condition (bare, after ZnO/G composite was dropped onto the ITO surface, and the aptamer-target complex form). Sanghavi *et al*. [40] proposed a unique microfluidic aptasensor that features glassy carbon electrodes and a nanoslit microwells on a glass substrate. Their method does not require a labeling, immobilizing, or a washing process. Aptamer-functionalized AuNPs were used to enhance the net area available for target cortisol capture and to enable the unhindered diffusion of analytes towards the binding surface. Square wave voltammetry (SWV) data were acquired by scanning the potential of the working electrode toward the positive direction in the −0.5 to −1.2 V range with frequency 100 Hz. Another electrochemical technique was developed by Chad *et al*. [66]. They proposed a microfluidic electrolyte-insulator-semiconductor (EIS) chip based on ion-sensitive field-effect transistor with capacitive detection. The working principle of the proposed device is the change of the gate voltage that occurs due to the release of protons or intrinsic charge biomolecules during biomolecule interactions. A thiolated aptameric peptide was immobilized on AuNPs for recognition of a protein kinase A (PKA) target. Interaction between the aptamer and target led to a shift in the gate voltage. Recently, Thiha *et al*. [72] presented a fabrication technique

for a suspended carbon nanowire sensor (sub-100 nm diameters) by simple electrospinning and applying carbon-microelectromechanical system (C-MEMS) techniques (Figure 1-7). The C-MEMS techniques provided patterning of the polymer (typically SU-8 photoresist) with a high aspect ratio and 3D structures shape. After the patterning process, the polymer was pyrolyzed and electrospun to obtain carbon nanostructures, then it was integrated with a microfluidic chip to form a label-free chemiresistive biosensor. The amine-functionalized aptamer was covalently attached to carboxylic groups with the assistance of sulfo-*N*-hydroxysuccinimide (sulfo-NHS) and *N*-(3-dimethylamnopropyl)-*N*-ethylcarbodiimide hydrochloride (EDC). The detection principle is based on conductivity changes that occur when the target binds on the suspended nanowire. The current-potential (I-V) was characterized before and after incubating with the target and the resistance value (R) was obtained from the inverse of the I-V curve slope. The percent ratio change of the resistance was calculated as $\Delta R/R_0$, where ΔR is the difference in resistance after incubation with target (R) and the original resistance (R_0).

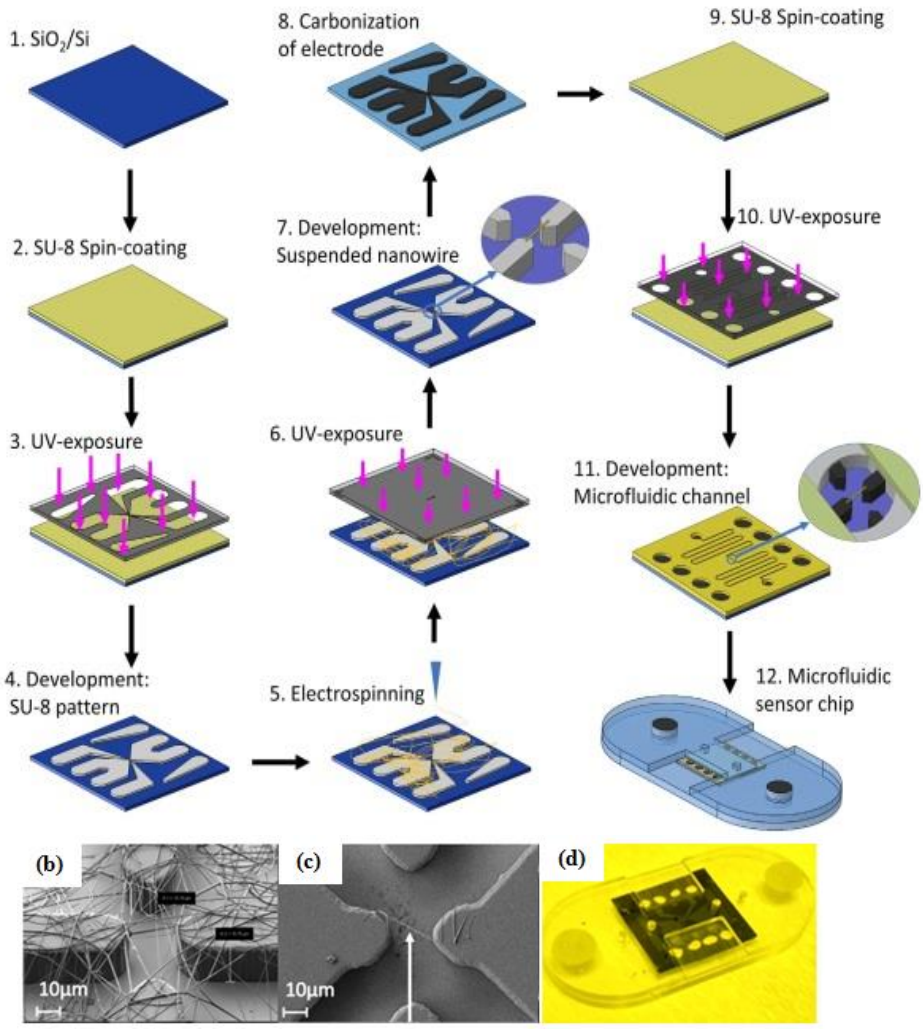

Figure 1-7. Fabrication steps of the carbon nanowire aptasensor. (a) The device was fabricated by integrating electrospinning and photolithography with carbon-microelectromechanical system (C-MEMS) technique; (b) Electrospun SU-8 nanowire; (c) Single SU-8 nanowire after photolithography and development; (d) Microfluidic platform containing the nanowire sensor. Reproduced with permission from reference [72]. Copyright 2018 Elsevier.

1.4.2 Optical Detection Methods

The analytical techniques based on light interaction with a sample are known as optical detection methods. To obtain an optical sensor, a specific reagent is involved in a sensing layer and its reaction process is monitored by a light beam that is conveyed by optical

fibers. An optical transducer was obtained after measuring the absorbed or emitted light power on the sensing layer. As the dependence of light power on the wavelength represents an optical spectrum, consequently the application of this method needs a component that enable to absorb or emit light. Otherwise, some external molecule may be used as an optical label. Fluorescent materials [13,17,19,21,28,37,38,42,45–48,50,53–56,60,61,68,69,90–96], and dyes (colorimetry) [25,64,74,77,78,82–84,97,98] are commonly used as labels in microdevices based on aptasensors.

1.4.2.1 Fluorescence Methods

Florescence methods consist of light emission by molecules previously excited through light absorption. Weng and Neethirajan [92] used 6-carboxyfluorescein (6-FAM) as the aptamer label and multi-walled carbon nanotubes (MWCNTs) or graphene oxide (GO) for the quencher in their device. When the target norovirus was present, fluorescence was recovered due to the release of the labeled aptamer from the MWCNT surface and it was detected at Ex/Em = 490 nm/520 nm by the multi-mode reader (Figure 1-8). The "signal-on" fluorescence aptasensor was also demonstrated by Ueno *et al*. [55]. They demonstrated a portable design with a multichannel chip for simultaneous detection of three to five samples. A recent update on a fluorescence aptasensor was presented by Jin *et al*. [95]. This group developed nanocomposites composed of magnetic Fe_3O_4-aptamer-carbon dots that exhibited down-conversion fluorescence (DCF) and up-conversion fluorescence (UCF) emissions simultaneously. The UCF emission wavelength is shorter than its corresponding excitation wavelength, whereas the DCF (usually called fluorescence) is the opposite. The high binding affinity between the target and aptamer could induce unwinding of the carbon dots from the target-aptamer complex and recovery of the UCF signal. Therefore, in the presence of the target, the UCF signal (peak at 475 nm) gradually increased.

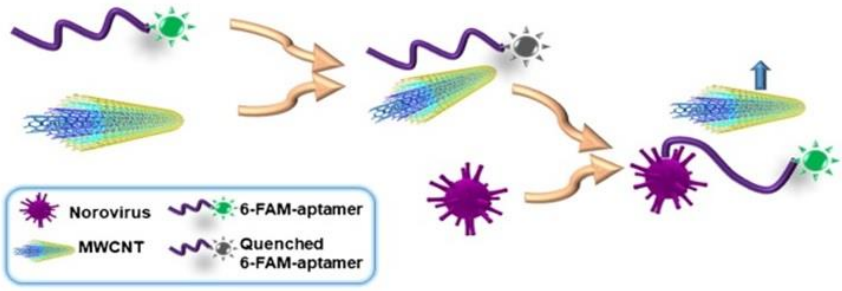

Figure 1-8. Schematic illustration of "signal-on" aptasensor based on MWCNT and fluorescence-labeled aptamer. Reproduced with permission from reference [92]. Copyright 2017 Springer.

1.4.2.2 Colorimetry Methods

Colorimetry methods are commonly used to determine the concentration of a solution by measuring the absorbance of at a specific wavelength, this approach is also applied in lateral strip detection with a control or known concentration [82–84]. Simple to enable and develop, instrument-free colorimetry is favorable. Wei *et al*. [98] and Zhang *et al*. [77] developed instrument-free detections using a microfluidic aptasensor: the colored result could be identified easily by the naked eye. Another advantage of a colorimetry-integrated microdevice was utilized by Fraser *et al*. [97]. They designed an integrated Aptamer-Tethered Enzyme Capture (APTEC) on a microfluidic device and applied it for a telemedicine application. The APTEC technique has three main steps: First, micromagnetic beads (µMBs) were coated with the aptamer via a streptavidin-biotin interaction. Then the coated beads were incubated on lysed sample of human blood. When the target was present, the aptamer-coated µMBs bound specifically to the target (protein PfLDH). Second, the unbound molecules and other contaminants were washed and removed by the mobile phase. Third, the aptamer-coated µMBs-target was transferred by mobile phase to the development chamber that contained the development reagent and a stronger colorimetry signal was generated. The

non-target sample would not develop a colorimetry signal in the described assay (Figure 1-9). For signal analysis, the microdevice was placed on the top of an iPad that displayed a homogenous white light then covered with an opaque box. The smartphone camera was used for capturing the images and coupled with supporting information such as time, date, and GPS coordinates for the telemedicine application. Furthermore, the receiver analyzed the images with *ImageJ* software.

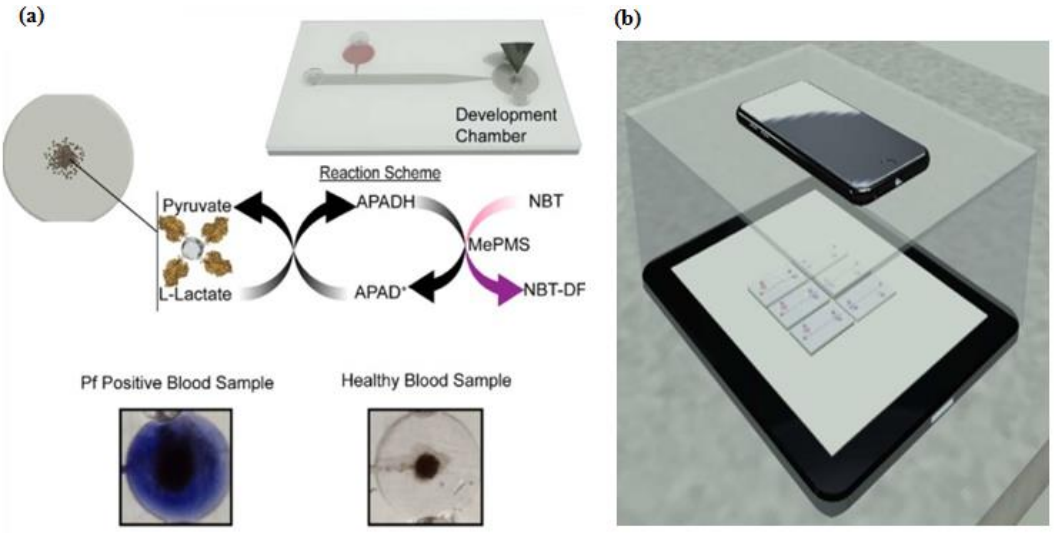

Figure 1-9. Microfluidic Aptamer-Tethered Enzyme Capture (APTEC) biosensor. (a) The reaction scheme of the reagents and redox reaction that results in the generation of an insoluble purple diformazan dye. There was a color difference between positive and negative samples; (b) The smartphone camera was used for capturing images in a telemedicine application. Reproduced with permission from reference [97]. Copyright 2018 Elsevier

1.4.3 Miscellaneous Methods

1.4.3.1 Surface Plasmon Resonance (SPR) Methods

Large groups of electrons in an oscillating state form a surface of plasmons, which is a phenomenon known as SPR. The SPR depends on three factors: angle of incident,

wavelength of the radiation, and refraction index of the sample. These methods are routinely used for investigating molecular interactions. Dausse *et al*. [23] demonstrated an SPR method for sequence selection during the SELEX method, called SPR-SELEX, that could perform selection and evaluation simultaneously. Other groups utilized a microfluidic aptasensor integrated with an SPR sensor to realize rapid and easy-to-use quantitative analysis [26,99].

1.4.3.2 Surface Acoustic Wave (SAW) Methods

These methods are based on acoustic excitation by means of two electrodes placed on the same surface interdigitated transducer (IDT) configuration. The acoustic wave induced by an IDT is propagated in a thin layer at a piezoelectric surface. Ahmad *et al*. [100] proposed a microfluidic device that applies acoustic waves to drive functionalized microparticles into a continuous flow microchannel to separate particle-conjugated target proteins from the sample. This platform utilized an IDT transducer (with an Au-Cr layer) that was patterned on top of the piezoelectric lithium niobate ($LiNbO_3$) substrate to generate high-frequency surface acoustic waves (SAWs). The aptamer was conjugated to streptavidin-functionalized polystyrene microparticles and incubated with a sample mixture. When the target thrombin was present, the aptamer formed a microparticle-target complex and other molecules remained in a free condition. Once the high-frequency SAWs were actuated, the complex aptamer was separated from the mixture due to the lateral migration of fluid under the influence of the acoustic radiation force and collected in outlet 2 (Figure 1-10). Furthermore, Zhang *et al*. [101] proposed a microfluidic love-wave sensor that is a special type of SAW sensor that uses a shear horizontal wave to reduce energy dissipation and to increase the surface sensitivity. The device was prepared on a $LiTaO_3$ (lithium tantalate) substrate with an aluminum IDT and functionalized with aptamer.

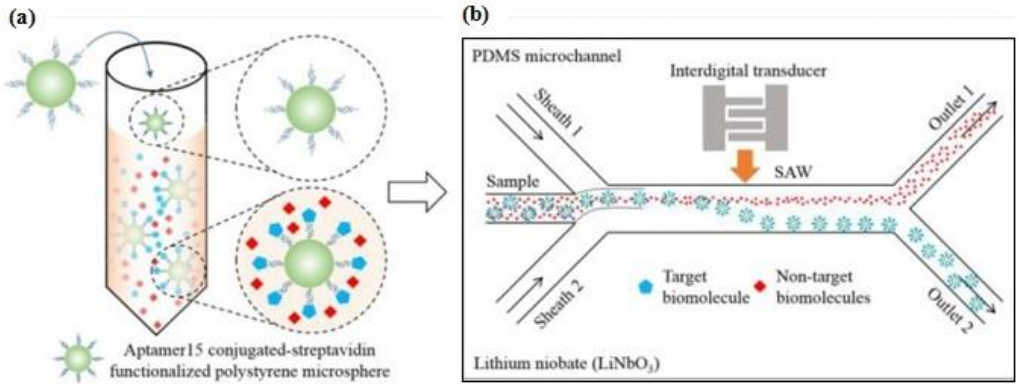

Figure 1-10. (a) Specific aptamer to form a microparticle−aptamer−target complex; the unbound particles remained in a free condition; (b) Separation process of the mixture solution through an acoustofluidic device. Reproduced with permission from reference [100]. Copyright 2017 American Chemical Society.

1.4.3.3 Chemiluminescence and Electrochemiluminescence Methods

Luminescence, as a general term is related to the energy transition between molecular orbitals that produces an emission of light. When the excitation of the molecules is caused by a chemical reaction, this light emission is chemiluminescence [27,33,36,58,71,81]. The emission that accompanies an electrochemical reaction is known as electrochemiluminescence [79]. Costantini *et al*. [58] developed an aptamer-linked immobilized sorbent assay (ALISA) that was performed in a microfluidic device that had a functionalized poly (2-hydroxyethyle methacrylate) PHEMA polymer brush layer on a glass substrate. The ALISA relied on the formation of a sandwich-like structure consisting of the target and two target related-aptamers. The first aptamer was bounded on PHEMA to capture the target and the other aptamer was a biotin-labeled probe. The avidin-labeled HRP (horseradish peroxidase) would give a chemiluminescent signal after binding with the biotin, this signal indicated that PHEMA-aptamer was interacting with the target.

1.5 Target Analytes

1.5.1 Disease Markers

As described in previous section, microfluidic aptasensor have numerous advantages for point-of-care detection, mostly as disease markers. Thrombin is a critical biomarker for Alzheimer's and it is a well-known target for a microfluidic aptasensor and every year several researchers have reported updates for thrombin detection that offer more sensitivity. Lin *et al*. [64] proposed a very sensitive detection of thrombin from human plasma serum with a detection limit 0.082 $pg{\cdot}mL^{-1}$ and a linear range 0.1–50.000 $pg{\cdot}mL^{-1}$. On the other hand, some groups focused on improving the detection method. For example, Zhao *et al*. [25] developed a microfluidic chip without signal amplification and using only naked-eye detection. The detection limit was 20 pM, this result is quite satisfying for simple detection purposes. Song *et al*. [60] used a sandwich aptamer-target-aptamer to assay thrombin with high selective detection even in the presence of concentrated bovine serum albumin (BSA). They obtained a thrombin detection limit of 25 pM. Uddin *et al*. [29] used a device with attractive disk and microbeads to reduce the sample-to-result time from 40 min to 15 min while using only 10 µL of sample volume. They obtained a thrombin detection limit of 25 pM.

1.5.2 Viruses and Bacteria

The detection of viruses and bacteria in real samples is important for dealing with environmental contamination or foodborne diseases. Commonly, their detection relies on culture-based tests, antibody-based tests, and polymerase chain reaction (PCR)-based tests. Despite their usefulness, these methods are costly and time-consuming. Neethiarajan group's [31,92] successfully developed a simple microfluidic aptasensor for norovirus detection with low detection limits (100 pM). The device not only had good of sensitivity but was also

selective to norovirus even in the present of interferon. Moreover, the total analysis time was significantly reduced compared with the conventional method. Wang *et al*. [46] demonstrated a fluorescent-labeled universal aptamer to determine three different influenza viruses (influenza A-H1N1, H3N2, and influenza B) at the same time in 20 min. Another multiple detection was developed by Zuo *et al*. [90]. Their microdevice was able to detect multiple bacteria (Lactobacillus acidophilus, Staphylococcus aureus, Salmonella enterica) at the same time. This device was consisted of a ready-to-use microfluidic aptasensor with a detection limit of 11.0 $CFU \cdot mL^{-1}$ and total time for detection was about 10 min.

1.5.3 Antibiotics

Antibiotic residues in foodstuffs pose certain hazards to human health among people who are sensitive to antibiotics, have an imbalance of intestinal microbiota or have bacterial resistance. Unfortunately, many of these residues are unintentionally consumed because some of the conventional methods may not meet the need for fast and high throughput analysis in food safety screening. Recently, the detection of multiple antibiotic residues based on a microfluidic aptasensor has been developed to fulfill these needs in food safety screening. The detection principle is based on microchip electrophoresis (MCE) and the target is a catalyzed hairpin assembly. The device could simultaneously detect kanamycin and oxytetracycline with detection limits of 0.7 $pg \cdot mL^{-1}$ and 0.9 $pg \cdot mL^{-1}$, respectively [102]. Using a similar MCE method, Zhou *et al.* [103] developed a label-free and sensitive detection of chloramphenicol that reached a detection limit of 0.003 $ng \cdot mL^{-1}$. Hou *et al*. [86] reported the fast detection of tetracycline using an interdigital array microelectrode (IDAM). The IDAM was integrated with impedance detection into a miniaturized conventional electrode and it was able to detect 1 nM of tetracycline in a milk sample.

1.5.4 Toxins

A rapid, sensitive, and specific assay technique was developed for routine analysis in foods and animal feedstuffs. Several researchers proposed a microfluidic aptasensor assay to analyze mycotoxin [50,58,62]. A lateral flow strip aptasensor assay was developed to detect ochratoxin A more easily. To perform a test, only the minimum sample volume and reagent volume were needed. The whole process was completed within 15 mins and a visual detection limit of 1 $ng{\cdot}mL^{-1}$ was obtained [84]. This assay was suitable for rapid and on-site detection, especially for screening raw materials in the animal feed production industry. Another challenging factor to analyze these toxins is isolation from the real samples. The uneven distribution of mycotoxin in matrix samples should be considered to apply additional steps on sample preparation. In recent years, marine toxins have drawn the attention of scientists due to the increased consumption of sea products. Certain toxins have been identified: saxitoxins, tetrodotoxin, okadaic acid, brevetoxins, and gonyautoxin ¼. Although these toxins are mostly produced by microalgae, especially dinoflagellates, it is now clear that bacteria are responsible for the production of some toxins. Handy *et al*. [24] published the first article related to marine toxin detection with an aptasensor, specifically saxitoxin. They developed saxitoxin-aptamer sequences by the SELEX method and evaluated the binding affinity with the SPR method. Tetrodotoxin is one famous marine toxin because of its involvement in the fatal food poisoning found in puffer fish, starfish, and blue-ringed octopus. Recently, a sensitive detection of tetrodotoxin using a microfluidic aptasensor was developed by Jin *et al*. [95], with a detection limit of 0.06 $ng{\cdot}mL^{-1}$. Okadaic acid is known as diarrhetic shellfish toxin (DST) and is found in contaminated shellfish. Various microfluidic techniques for okadaic acid detection have been developed, including interdigitated microelectrodes with AuNPs [73], a paper-based aptasensor [61], and an enzyme-linked aptamer assay (ELAA) [22]. In the ELAA competitive assay, the lowest limit of detection reached 0.01 $ng{\cdot}mL^{-1}$ and

the widest detection range was from 0.025 to 10 ng·mL^{-1} in spiked clam samples. The binding affinity of an aptamer to detect brevetoxins and gonyautoxin-1/4 has been tested. The lowest dissociation constants for brevetoxin were 4.83 μM [104] and for gonyautoxin ¼ 17.7 nM [105].

1.6 Present Perspective

Applications of aptasensors on microdevices have led to positive outcomes in bioanalysis. The review article on recent microdevice-based aptamer sensors has been discussed and published in *Micromachines*. Table 1-1 summarizes device features, including their classifications and assay formats. Microdevice sensors in flow analysis systems deals with the control and manipulation of fluid volumes in the sub-microliter region that are constrained to very small size channels. The fluid flow can be prompted by applied pressure or electrokinetic. What distinguishes microdevice systems from the conventional analysis systems is the integration of a large network of channels and other microdevices (such as actuators and valves) on a small chip. The major concepts and principles of device fabrication still rely on photolithography, etching, bonding, screen printing, doping, and thin film formation. These fabrication techniques give rise to various collaborations in multidisciplinary research. The utilization of new nanomaterials (metal nanoparticles, polymer nanoparticles, carbon dots, magnetic beads, and micro beads) has promoted the development of aptamer sensors that offer high throughput and good sensitivity. Many innovations presented in the literature are still at the proof-of-concept state. However, some have already been applied to commercial applications, such as the lateral flow strip assay. This technique does not require a sophisticated instrument or may even be instrument-free as a result of naked-eye detection. Based on the current circumstances in the field of bioanalysis, several points that can be considered in the future are noted: (1) Despite their many advantages over other conventional methods, the scaling down of existing procedures to use

microdevice-based aptasensors sometimes needs to be improved from the onset; (2) The simplest design is not always related to the smallest dimension. The movement towards ergonomic design, easy to handle, and cost-effective devices will certainly occur; (3) Marine toxins have attracted attention due to the increased human consumption of marine products. However, detections using microfluidic-based aptasensor are still limited to only a few toxins. The continued developments of such methods are expected in the future.

Developing relatively simple and sensitive microdevices that are easily fabricated and combining them with automatic and embedded elements in compatible substrates by micro-total analytical systems (μTAS) will certainly increase in the coming years.

This dissertation then describes the experimental procedures and results obtaining during the time of research. A label-free electrochemical aptasensor using microfabricated electrode to detection ochratoxin A was developed and described in chapter 2. The fabrication of microelectrode and immobilization of aptamer were investigated to determine the optimum condition of the proposed sensor. The methylene blue (MB) was used as redox probe that attached on the aptamer through π-π interaction with guanine base. This work suggests that the proposed electrochemical aptasensor makes simple and sensitive to on-site detection of ochratoxin A.

In chapter 3. the immobilization strategy of the aptamer is optimized with dithiol modification. Besides, detection with "signal-on" method is developed to increase the accuracy of measurement by reducing the false-positive result.

The ochratoxin A analysis also performed with microchip based on fluorescence polarization aptamerassay (FPAA). When OTA was present in the solution, the tracer and OTA was competitively bound with the aptamer, causing a decrease of FP intensity proportional with OTA concentration. The selectivity of FP method was evaluated by using poly A-T-C-G and other mycotoxins such as AFB1 and DON, both tests presented good

selectivity performance. The results for the fluorescence polarization were described in chapter 4.

To overall findings of the present research are summarized in chapter 5.

Table 1-1. Summary of microdevice-based aptasensors on several platforms and target analytes.

Detection Method	Substrate	Aptamer	Target	Matrix Sample	LOD or Linear Range	Device Features	Reference
Electrochemical							
Chronoamperometry	Glass	Peptide	Thrombin	-	10 fg·mL^{-1} to 1 µg·mL^{-1}	Plasma-functionalized SWCNT	[43]
DPV	PDMS	Biotin-Aptamer-Ferrocene	Norovirus	Bovine Blood	100 pM 100 pM to 3.5 nM	Integrated PDMS-SPCE Graphene-Au composite Switch-off signal	[31]
SWV	Glass	Competitive aptamer	Cortisol	Saliva glucocorticoids in serum	10 pg·mL^{-1} 30 pg·mL^{-1} to 10 µg·mL^{-1}	Sample volume (<1 µL) Graphene modified electrode	[40]
SWV	Glass	MB-labeled Aptamer	TGF-β1	Human hepatic stellate cell	1 ppb	PDMS layer with microcup Comparing with ELISA	[44]
Digital multimeter	Chromatography paper	-	Adenosine	-	11.8 µM	Origami paper device Attractive design	[80]
DPV	Paper	Peptide	Renin	-	300 ng·mL^{-1}	DEP (disposable electrochemical printed) Uses SPR to check binding affinity	[85]
EIS	Poly-imide film	-	Bisphenol A (BPA)	Food (canned)	152.93 aM 1 fM to 10 pM	Printed circuit board material	[32]

Detection Method	Substrate	Aptamer	Target	Matrix Sample	LOD or Linear Range	Device Features	Reference
EIS	Glass	-	Avian Influenza Virus	Virus culture	0.0128 hemagglutinin units (HAU)	Interdigitated electrode On site detection SELEX on Chip	[35]
Resistance	Si-Wafer	Amine-functionalized aptamer	Salmonella typhimurium	Fresh beef	10 CFU·mL^{-1}	Carbon nanowire sensors C-MEMS Rapid detection (5 min)	[72]
EIS	Glass	-	Tetracycline	Milk	1 pM	Multi-walled carbon nanotubes Interdigital array microelectrode	[86]
Photoelectrochemical	Indium Tin Oxide (ITO)	S6 aptamer	SK-BR-3	-	58 cell·mL^{-1} 10^2 to 10^6 cells·mL^{-1}	ITO-based SPEs device Disposable ITO device	[87]
EIS	Cyclic olefin copolymer	Short strand aptamer	Ampicillin Kanamycin A	UHT low fatm milk	10 pM A = 100 pM to 1 mM K = 10 nM to 1 mM	PEDOT-OH:TsO All polymer substrate	[88]
EIS	Glass	Sgc8 TD05	CCRF-CEM Ramos cells	T-cell acute lymphoblastic leukemia (ALL)	-	Logic aptamer sensor (LAS) Simple detection with digital multimeter	[89]
Optical							
Fluorescence	Glass	Aptamer-antibody sandwich	Cancer stem-like cells	-	-	Cell-SELEX Automatic device Heater—cooling chip	[13]

Detection Method	Substrate	Aptamer	Target	Matrix Sample	LOD or Linear Range	Device Features	Reference
Fluorescence	Glass	Aptamer sandwich with magnetic beads	Human immunoglobulin A (IgA)	Random oligonucleotides	-	Microfludic SELEX Fully integrated platform	[17]
Fluorescence	Glass	-	Malaria parasite	Red blood cells	-	I-SELEX Only requires syringe pump	[19]
Fluorescence	Glass	-	-	Mixed cells	-	Cell-SELEX Dielectrophoresis and electrophoresis	[21]
Fluorescence	PDMS	Hair pin aptamer	Protein tyrosine kinase-7	Cell culture	0.4 nM	Laser-induced fluorescence detector (LIFD) Microfluidic droplet	[28]
Fluorescence	Glass	FAM-aptamer	Carcinoembryonic antigen (CEA)	Human serum	68 ng·mL^{-1} 130 pg·mL^{-1} to 8 ng·mL^{-1}	Micro chip electrophoresis (MCE)	[37]
Fluorescence	Glass	Cy3-aptamer	Thrombin	Human serum	0.4 fM	Avidin-biotin interaction Use 2 kinds of aptamer	[38]
Fluorescence	Glass	Photoluminescent GOQD-aptamer	Lead ion (Pb^{2+})	Drinking water Tap water Lake water	0.64 nM 1 to 1000 nM	Packed with cation exchange resins Peristaltic PDMS Micropump	[42]
Fluorescence	Glass	G-quadruplex	VEGF-165 protein	DMEM cell media	0.17 pM 0.52 to 52.00 pM	Label-free In the presence of Ir(III) no signal	[45]

Detection Method	Substrate	Aptamer	Target	Matrix Sample	LOD or Linear Range	Device Features	Reference
Fluorescence	Glas	FAM-aptamer universal	Influenza virus	Random oligonucleotides	3.2 HAU	Automatic process Rapid detection	[46]
Fluorescence	Glass	FAM-aptamer sandwich	Influenza A (InfA/H1N1)		0.032 HAU	Magnet external Rapid detection	[47]
Fluorescence	Glass	Fluorescence-labeled	17β-estradiol	Estradiol solution	0.07 pM	Microfluidic droplet Turn-on signal	[48]
Fluorescence	Glass	G-quadruplex structure	Ochratoxin A	-	-	Fluorescence polarization	[50]
Fluorescence	Glass	Multivalent DNA aptamer nanospheres	Human acute leukemia cells	Human blood	-	Flow cytometry analysis Rapid detection	[53]
Fluorescence	Glass	FAM-aptamer	Thrombin Prostate specific antigen (PSA)	-	-	FRET Longer spacer gives good sensitivity	[54]
Fluorescence	Glass	FAM-aptamer	Thrombin Prostate specific antigen (PSA) Hemagglutinin	-	-	FRET Multiple target Aptamer immobilize on GO flakes	[55]
Fluorescence	Glass	Sandwich aptamer FITC	Glycated hemoglobins (HbA1c) & Total hemoglobin (Hb)	Blood	-	Automated microfluidic system Low reagent consumption	[56]
Fluorescence	Glass	Sandwich aptamer	Thrombin	-	27 pM	Gold nanohole array Nanoimprinting technology	[60]

Detection Method	Substrate	Aptamer	Target	Matrix Sample	LOD or Linear Range	Device Features	Reference
Fluorescence	Glass	Aptamer functionalize QD	Lysozyme, OA, Brevetoxin, ß-conglutin lupine	Fresh egg white Mussel tissue Sausage	Lysozyme (343 ppb); OA (0.4 ppb); Brevetoxin (0.56 ppb); ß-cl(2.5 ppb)	Quantum Dots (QD) GO-quencher Comparing with ELISA	[61]
Fluorescence	Si-nanowire	Cocktail aptamer	Non-small cell lung cancer	Blood	-	PDMS chaotic mixer Aptamer grafted Si-nano wire substrate	[68]
Fluorescence	Glass	FAM-aptamer	ss-DNA	-	-	Isolating ssDNA from dsDNA PC membrane	[69]
Fluorescence	Chromatography paper	Aptamer-functionalized GO	Staphylococcus aureus	Buffer (Bacterial colonies)	11.0 CFU·mL^{-1}	PDMS/paper/glass microfludic device Fast detection	[90]
Fluorescence	Paper	-	Cancer cells	Cell culture	MCF-7: 6270 cell·mL^{-1} HL-60 : 65 cell·mL^{-1}	Mesoporous silica nanoparticles (MSNs) Naked-eye detection	[91]
Fluorescence	Paper	FAM-aptamer	Norovirus	Spiked mussel sample	MWCNT: 4.4 ng·mL^{-1} GO: 3.3 ng·mL^{-1} 13 ngmL^{-1} to 13 µg·mL^{-1}	Multi-walled carbon nanotubes Graphene oxide	[92]
Fluorescence	Printed circuit board (PCB)	-	Cocaine Adenosine	Human blood serum	Cocaine : 0.1 pM Adenosine: 0.5	MECAS-chip Simultaneous detection	[93]
Fluorescence	Glass	FAM-aptamer	Lysozyme	-	-	Electrophoresis frontal mode FACME method	[94]

Detection Method	Substrate	Aptamer	Target	Matrix Sample	LOD or Linear Range	Device Features	Reference
Fluorescence	-	Amine-aptamer	Tetrodotoxin (TTX)	Human blood Urine	0.06 ng·mL^{-1} 0.1 ng·mL^{-1} to mg·mL^{-1}	Marine toxin Fe_3O_4/apt/CD composite	[95]
Colorimetry							
Colorimetry	Glass	Sandwich aptamer	Thrombin	-	20 pM	Naked-eye & Flatbed detection Micro pump	[25]
Colorimetry	Si-wafer	G-quadruplex structure	Thrombin	Human blood	0.083 pg·mL^{-1} 0.1 to 50.000 pg·mL^{-1}	Rolling circle amplification Micro channel	[64]
Colorimetry	Paper	Cross-linking aptamer	Cocaine	Urine	7.3 µM	Utilizes ImageJ software Hydrogel-µPAD	[74]
Colorimetry	Paper	Hybridization chain reaction	Adenosine	Human serum	1.5 µM 1.5 µM to 19.3 mM	Naked eyes detection Uses superparamagnetism	[77]
Colorimetry	Paper	Aptamer attached microbeads	Adenosine	Urine	-	Rubik's cube stamp Stamping method	[78]
Colorimetry	Paper Cellulose fiber	Sandwich aptamer	Vaspin	Buffer & serum	Buffer: 0.137 nM Serum: 0.105 nM	Lateral strip assay Naked-eye detection	[82]
Colorimetry	Paper Cellulose fiber	Biotin modified aptamer	*E. coli* O157: H7	Culture E.coli	10 CFU·mL^{-1}	Lateral strip assay Naked-eye detection	[83]
Colorimetry	Paper Cellulose fiber	Competitive aptamer	Ochratoxin A	-	1 ppb	Lateral strip assay Naked-eye detection Rapid detection	[84]

Detection Method	Substrate	Aptamer	Target	Matrix Sample	LOD or Linear Range	Device Features	Reference
Colorimetry	Clear resin	Biotinylated aptamer	PfLDH enzyme (Malaria)	Human blood serum	0.01%	Telemedicine Ipad - Iphone detection 3D printing resin	[97]
Colorimetry	Paper	Hydrogel-aptamer	Cocaine Adenosine Pt^{+2}	Urine	-	Naked-eye detection Signal off-on by interaction apt-target	[98]
Miscellaneous							
Surface Plasmon Resonance		Hairpin RNA aptamer	Aptamer candidate	Random library	K_D = 8 nM	SPR-SELEX SELEX on chip	[23]
Surface Acoustic Wave	PDMS	Polystyrene aptamer conjugate	Thrombin	Buffer	-	Acoustic wave driven Interdigitated transducer	[100]
Surface Acoustic Wave	$LiTaO_3$ substrate with SiO_2 film	Aptamer beacon	Prostate specific antigen (PSA) ATP	-	PSA = 10 ppb 10 ppb to 1 ppm ATP = 0.1 pM 0.5 pM to 7 nM	Interdigitated transducer Utilized AuNPs	[101]
Chemiluminescence	PDMS	Aptamer-antibody sandwich	free prostate specific antigen (fPSA)	Human semen	0.5 $ng \cdot mL^{-1}$	Performed in parallel Antibody labeled HRP	[27]
Chemiluminescence	PDMS	Thiolated aptamer	Lysozyme	Human serum	44.6 fM	Droplet microfluidic Digital microfluidic Low sample volume	[33]
Chemiluminescence	Glass	Aptamer-antibody sandwich	HbA1c	Blood	0.65 $g \cdot dL^{-1}$	Three-layer chips Detection time 25 min Utilizes magnetic beads	[36]

Detection Method	Substrate	Aptamer	Target	Matrix Sample	LOD or Linear Range	Device Features	Reference
Chemiluminescence	Glass	-	Ochratoxin A	Beer	0.82 $mg \cdot L^{-1}$	Polymer brush ALISA	[58]
Electrochemiluminescence	Paper	Sandwich aptamer	ATP	-	0.1 pM 0.5 pM to 7 nM	Origami design Modified porous paper	[79]

References

[1] Ansari, M.I.H.; Hassan, S.; Qurashi, A.; Khanday, F.A. Microfluidic-integrated DNA nanobiosensors. *Biosens. Bioelectron*. 2016, 85, 247–260.

[2] Hung, L.Y.; Wu, H.W.; Hsieh, K.; Lee, G. Bin Microfluidic platforms for discovery and detection of molecular biomarkers. *Microfluid. Nanofluid*. 2014, 16, 941–963.

[3] Jayasena, S.D. Aptamers: An emering class of molecules that rival antibodies. *Clin. Chem.* 1999, 45, 1628–1650.

[4] Gopinath, S.C.B.; Lakshmipriya, T.; Chen, Y.; Phang, W.M.; Hashim, U. Aptamer-based "point-of-care testing". *Biotechnol. Adv*. 2016, 34, 198–208.

[5] Hu, J.; Ye, M.; Zhou, Z. Aptamers: Novel diagnostic and therapeutic tools for diabetes mellitus and metabolic diseases. *J. Mol. Med*. 2016, 95, 249–256.

[6] Feng, S.; Chen, C.; Wang, W.; Que, L. An aptamer nanopore-enabled microsensor for detection of theophylline. *Biosens. Bioelectron*. 2018, 105, 36–41.

[7] Chen, A.; Yang, S. Replacing antibodies with aptamers in lateral flow immunoassay. *Biosens. Bioelectron*. 2015, 71, 230–242.

[8] Tuerk, C.; Gold, L. Systematic evolution of ligands by exponential enrichment: RNA ligands to bacteriophage T4 DNA polymerase. *Science.* 1990, 249, 505–510.

[9] Ellington, A.D.; Szostak, J. In vitro selection of RNA molecules that bind specific ligands. *Nature*. 1990, 346, 818–822.

[10] Dembowski, S.K.; Bowser, M.T. Microfluidic methods for aptamer selection and characterization. *Analyst*. 2018, 143, 21–32.

[11] Marques, M.P.; Szita, N. Bioprocess microfluidics: Applying microfluidic devices for bioprocessing. *Curr. Opin. Chem. Eng*. 2017, 18, 61–68.

[12] Luka, G.; Ahmadi, A.; Najjaran, H.; Alocilja, E.; Derosa, M.; Wolthers, K.; Malki, A.; Aziz, H.; Althani, A.; Hoorfar, M. Microfluidics integrated biosensors: A leading

technology towards lab-on-a-chip and sensing applications. *Sensors*. 2015, 15, 30011–30031.

[13] Weng, C.H.; Hsieh, I.S.; Hung, L.Y.; Lin, H.I.; Shiesh, S.C.; Chen, Y.L.; Lee, G. Bin An automatic microfluidic system for rapid screening of cancer stem-like cell-specific aptamers. *Microfluid. Nanofluid*. 2013, 14, 753–765.

[14] Olsen, T.; Zhu, J.; Kim, J.; Pei, R.; Stojanovic, M.N.; Lin, Q. An integrated microfluidic selex approach using combined electrokinetic and hydrodynamic manipulation. SLAS TECHNOL. *Transl. Life Sci. Innov*. 2017, 22, 63–72.

[15] Huang, C.J.; Lin, H.I.; Shiesh, S.C.; Lee, G. Bin An integrated microfluidic system for rapid screening of alpha-fetoprotein-specific aptamers. *Biosens. Bioelectron*. 2012, 35, 50–55.

[16] Kim, T.K.; Lee, S.W.; Ahn, J.Y.; Laurell, T.; Kim, S.Y.; Jeong, O.C. Fabrication of microfluidic platform with optimized fluidic network toward on-chip parallel systematic evolution of ligands by exponential enrichment process. Jpn. *J. Appl. Phys*. 2011, 50.

[17] Olsen, T.R.; Tapia-Alveal, C.; Yang, K.-A.; Zhang, X.; Pereira, L.J.; Farmakidis, N.; Pei, R.; Stojanovic, M.N.; Lin, Q. Integrated Microfluidic Selex Using Free Solution Electrokinetics. *J. Electrochem. Soc*. 2017, 164, B3122–B3129.

[18] Lai, H.-C.; Wang, C.-H.; Liou, T.-M.; Lee, G.-B. Influenza A virus-specific aptamers screened by using an integrated microfluidic system. *Lab Chip*. 2014, 14, 2002–2013.

[19] Birch, C.M.; Hou, H.W.; Han, J.; Niles, J.C. Identification of malaria parasite-infected red blood cell surface aptamers by inertial microfluidic SELEX (I-SELEX). *Sci. Rep*. 2015, 5, 11347.

[20] Oh, S.S.; Ahmad, K.M.; Cho, M.; Kim, S.; Xiao, Y.; Soh, H.T. Improving aptamer selection efficiency through volume dilution, magnetic concentration, and continuous washing in microfluidic channels. *Anal. Chem*. 2011, 83, 6883–6889.

[21] Stoll, H.; Kiessling, H.; Stelzle, M.; Wendel, H.P.; Schütte, J.; Hagmeyer, B.; Avci-Adali, M. Microfluidic chip system for the selection and enrichment of cell binding aptamers. *Biomicrofluidics*. 2015, 9, 034111.

[22] Gu, H.; Duan, N.; Wu, S.; Hao, L.; Xia, Y.; Ma, X.; Wang, Z. Graphene oxide-assisted non-immobilized SELEX of okadaic acid aptamer and the analytical application of aptasensor. *Sci. Rep*. 2016, 6, 21665.

[23] Dausse, E.; Barré, A.; Aimé, A.; Groppi, A.; Rico, A.; Ainali, C.; Salgado, G.; Palau, W.; Daguerre, E.; Nikolski, M.; et al. Aptamer selection by direct microfluidic recovery and surface plasmon resonance evaluation. *Biosens. Bioelectron*. 2016, 80, 418–425.

[24] Handy, S.M.; Yakes, B.J.; DeGrasse, J.A.; Campbell, K.; Elliott, C.T.; Kanyuck, K.M.; DeGrasse, S.L. First report of the use of a saxitoxin-protein conjugate to develop a DNA aptamer to a small molecule toxin. *Toxicon*. 2013, 61, 30–37.

[25] Zhao, Y.; Liu, X.; Li, J.; Qiang, W.; Sun, L.; Li, H.; Xu, D. Microfluidic chip-based silver nanoparticles aptasensor for colorimetric detection of thrombin. *Talanta*. 2016, 150, 81–87.

[26] Loo, J.F.C.; Lau, P.M.; Kong, S.K.; Ho, H.P. An assay using localized surface plasmon resonance and gold nanorods functionalized with aptamers to sense the cytochrome-c released from apoptotic cancer cells for anti-cancer drug effect determination. *Micromachines*. 2017, 8, 338.

[27] Jolly, P.; Damborsky, P.; Madaboosi, N.; Soares, R.R.G.; Chu, V.; Conde, J.P.; Katrlik, J.; Estrela, P. DNA aptamer-based sandwich microfluidic assays for dual quantification

and multi-glycan profiling of cancer biomarkers. *Biosens. Bioelectron*. 2016, 79, 313–319.

[28] Li, L.; Wang, Q.; Feng, J.; Tong, L.; Tang, B. Highly sensitive and homogeneous detection of membrane protein on a single living cell by aptamer and nicking enzyme assisted signal amplification based on microfluidic droplets. *Anal. Chem*. 2014, 86, 5101–5107.

[29] Uddin, R.; Burger, R.; Donolato, M.; Fock, J.; Creagh, M.; Hansen, M.F.; Boisen, A. Lab-on-a-disc agglutination assay for protein detection by optomagnetic readout and optical imaging using nano- and micro-sized magnetic beads. *Biosens. Bioelectron*. 2016, 85, 351–357.

[30] Wang, H.; Liu, Y.; Liu, C.; Huang, J.; Yang, P.; Liu, B. Microfluidic chip-based aptasensor for amplified electrochemical detection of human thrombin. *Electrochem. Commun*. 2010, 12, 258–261.

[31] Chand, R.; Neethirajan, S. Microfluidic platform integrated with graphene-gold nano-composite aptasensor for one-step detection of norovirus. *Biosens. Bioelectron*. 2017, 98, 47–53.

[32] Mirzajani, H.; Cheng, C.; Wu, J.; Chen, J.; Eda, S.; Najafi Aghdam, E.; Badri Ghavifekr, H. A highly sensitive and specific capacitive aptasensor for rapid and label-free trace analysis of Bisphenol A (BPA) in canned foods. *Biosens. Bioelectron*. 2017, 89, 1059–1067.

[33] Giuffrida, M.C.; Cigliana, G.; Spoto, G. Ultrasensitive detection of lysozyme in droplet-based microfluidic devices. *Biosens. Bioelectron*. 2018, 104, 8–14.

[34] Mazaafrianto, D.N.; Maeki, M.; Ishida, A.; Tani, H.; Tokeshi, M. Label-free electrochemical sensor for ochratoxin A using microfabricated electrode with an immobilized aptamer. 2018, *ACS omega*, 3, 16823-16830.

[35] Lum, J.; Wang, R.; Hargis, B.; Tung, S.; Bottje, W.; Lu, H.; Li, Y. An Impedance Aptasensor with Microfluidic Chips for Specific Detection of H5N1 Avian Influenza Virus. *Sensors*, 2015, 15, 18565–18578.

[36] Chang, K.W.; Li, J.; Yang, C.H.; Shiesh, S.C.; Lee, G. Bin An integrated microfluidic system for measurement of glycated hemoglobin Levels by using an aptamer-antibody assay on magnetic beads. *Biosens. Bioelectron*. 2015, 68, 397–403.

[37] Pan, L.; Zhao, J.; Huang, Y.; Zhao, S.; Liu, Y.M. Aptamer-based microchip electrophoresis assays for amplification detection of carcinoembryonic antigen. *Clin. Chim. Acta*, 2015, 450, 304–309.

[38] Chen, F.Y.; Wang, Z.; Li, P.; Lian, H.Z.; Chen, H.Y. Aptamer-based thrombin assay on microfluidic platform. *Electrophoresis*. 2013, 34, 3260–3266.

[39] Sheng, W.; Chen, T.; Kamath, R.; Xiong, X.; Tan, W.; Fan, Z.H. Aptamer-enabled efficient isolation of cancer cells from whole blood using a microfluidic device. *Anal. Chem*. 2012, 84, 4199–4206.

[40] Sanghavi, B.J.; Moore, J.A.; Chávez, J.L.; Hagen, J.A.; Kelley-Loughnane, N.; Chou, C.F.; Swami, N.S. Aptamer-functionalized nanoparticles for surface immobilization-free electrochemical detection of cortisol in a microfluidic device. *Biosens. Bioelectron*. 2016, 78, 244–252.

[41] Lin, X.; Chen, Q.; Liu, W.; Yi, L.; Li, H.; Wang, Z.; Lin, J.M. Assay of multiplex proteins from cell metabolism based on tunable aptamer and microchip electrophoresis. *Biosens. Bioelectron*. 2015, 63, 105–111.

[42] Park, M.; Ha, H.D.; Kim, Y.T.; Jung, J.H.; Kim, S.H.; Kim, D.H.; Seo, T.S. Combination of a Sample Pretreatment Microfluidic Device with a Photoluminescent Graphene Oxide Quantum Dot Sensor for Trace Lead Detection. *Anal. Chem*. 2015, 87, 10969–10975.

[43] Kim, J.H.; Jin, J.H.; Lee, J.Y.; Park, E.J.; Min, N.K. Covalent attachment of biomacromolecules to plasma-patterned and functionalized carbon nanotube-based devices for electrochemical biosensing. *Bioconjug. Chem*. 2012, 23, 2078–2086.

[44] Matharu, Z.; Patel, D.; Gao, Y.; Haque, A.; Zhou, Q.; Revzin, A. Detecting transforming growth factor-β release from liver cells using an aptasensor integrated with microfluidics. *Anal. Chem*. 2014, 86, 8865–8872.

[45] Lin, X.; Leung, K.H.; Lin, L.; Lin, L.; Lin, S.; Leung, C.H.; Ma, D.L.; Lin, J.M. Determination of cell metabolite VEGF165and dynamic analysis of protein-DNA interactions by combination of microfluidic technique and luminescent switch-on probe. *Biosens. Bioelectron*. 2016, 79, 41–47.

[46] Wang, C.H.; Chang, C.P.; Lee, G. Bin Integrated microfluidic device using a single universal aptamer to detect multiple types of influenza viruses. *Biosens. Bioelectron*. 2016, 86, 247–254.

[47] Tseng, Y.T.; Wang, C.H.; Chang, C.P.; Lee, G. Bin Integrated microfluidic system for rapid detection of influenza H1N1 virus using a sandwich-based aptamer assay. *Biosens. Bioelectron*. 2016, 82, 105–111.

[48] Dou, M.; Mireles Garcia, J., Jr.; Zhan, S.; Li, X. Interfacial nano-biosensing in microfluidic droplets for high-sensitivity detection of low-solubility molecules. *Chem. Commun*. 2016, 52, 3470–3473.

[49] Hilton, J.P.; Olsen, T.; Kim, J.; Zhu, J.; Nguyen, T.H.; Barbu, M.; Pei, R.; Stojanovic, M.; Lin, Q. Isolation of thermally sensitive protein-binding oligonucleotides on a microchip. *Microfluid. Nanofluid*. 2015, 19, 795–804.

[50] Galarreta, B.C.; Tabatabaei, M.; Guieu, V.; Peyrin, E.; Lagugné-Labarthet, F. Microfluidic channel with embedded SERS 2D platform for the aptamer detection of ochratoxin A. *Anal. Bioanal. Chem*. 2013, 405, 1613–1621.

[51] Du, Y.; Chen, C.; Zhou, M.; Dong, S.; Wang, E. Microfluidic electrochemical aptameric assay integrated on-chip: A potentially convenient sensing platform for the amplified and multiplex analysis of small molecules. *Anal. Chem*. 2011, 83, 1523–1529.

[52] Liu, Y.; Yan, J.; Howland, M.C.; Kwa, T.; Revzin, A. Micropatterned aptasensors for continuous monitoring of cytokine release from human leukocytes. *Anal. Chem*. 2011, 83, 8286–8292.

[53] Sheng, W.; Chen, T.; Tan, W.; Fan, Z.H. Multivalent DNA nanospheres for enhanced capture of cancer cells in microfluidic devices. *ACS Nano*. 2013, 7, 7067–7076.

[54] Ueno, Y.; Furukawa, K.; Tin, A.; Hibino, H. On-chip FRET Graphene Oxide Aptasensor: Quantitative Evaluation of Enhanced Sensitivity by Aptamer with a Double-stranded DNA Spacer. *Anal Sci*. 2015, 31, 875–879.

[55] Ueno, Y.; Furukawa, K.; Matsuo, K.; Inoue, S.; Hayashi, K.; Hibino, H. On-chip graphene oxide aptasensor for multiple protein detection. *Anal. Chim. Acta*. 2015, 866, 1–9.

[56] Li, J.; Chang, K.W.; Wang, C.H.; Yang, C.H.; Shiesh, S.C.; Lee, G. Bin On-chip, aptamer-based sandwich assay for detection of glycated hemoglobins via magnetic beads. *Biosens. Bioelectron*. 2016, 79, 887–893.

[57] Kawano, R.; Osaki, T.; Sasaki, H.; Takinoue, M.; Yoshizawa, S.; Takeuchi, S. Rapid detection of a cocaine-binding aptamer using biological nanopores on a chip. *J. Am. Chem. Soc*. 2011, 133, 8474–8477.

[58] Costantini, F.; Sberna, C.; Petrucci, G.; Reverberi, M.; Domenici, F.; Fanelli, C.; Manetti, C.; De Cesare, G.; Derosa, M.; Nascetti, A.; et al. Aptamer-based sandwich assay for on chip detection of Ochratoxin A by an array of amorphous silicon photosensors. *Sens. Actuators B Chem*. 2016, 230, 31–39.

[59] Yang, J.; Zhu, J.; Pei, R.; Oliver, J.A.; Landry, D.W.; Stojanovic, M.N.; Lin, Q. Integrated microfluidic aptasensor for mass spectrometric detection of vasopressin in human plasma ultrafiltrate. *Anal. Methods*. 2016, 8, 5190–5196.

[60] Song, H.Y.; Wong, T.I.; Guo, S.; Deng, J.; Tan, C.; Gorelik, S.; Zhou, X. Nanoimprinted thrombin aptasensor with picomolar sensitivity based on plasmon excited quantum dots. *Sens. Actuators B Chem*. 2015, 221, 207–216.

[61] Weng, X.; Neethirajan, S. Paper-based microfluidic aptasensor for food safety. *J. Food Saf*. 2018, 38.

[62] Ma, Y.; Mao, Y.; Huang, D.; He, Z.; Yan, J.; Tian, T.; Shi, Y.; Song, Y.; Li, X.; Zhu, Z.; et al. Portable visual quantitative detection of aflatoxin B1 using a target-responsive hydrogel and a distance-readout microfluidic chip. *Lab Chip*. 2016, 16, 3097–3104.

[63] Song, C.; Chen, C.; Che, X.; Wang, W.; Que, L. Detection of plant hormone abscisic acid (ABA) using an optical aptamer-based sensor with a microfluidics capillary interface. In Proceedings of the 2017 IEEE 30th International Conference on Micro Electro Mechanical Systems (MEMS), Las Vegas, NV, USA, 22–26 January 2017; pp. 370–373.

[64] Lin, X.; Chen, Q.; Liu, W.; Li, H.; Lin, J.M. A portable microchip for ultrasensitive and high-throughput assay of thrombin by rolling circle amplification and hemin/G-quadruplex system. *Biosens. Bioelectron*. 2014, 56, 71–76.

[65] Lim, Y.C.; Kouzani, A.Z.; Duan, W.; Dai, X.J.; Kaynak, A.; Mair, D. A surface-stress-based microcantilever aptasensor. IEEE *Trans. Biomed. Circuits Syst*. 2014, 8, 15–24.

[66] Chand, R.; Han, D.; Neethirajan, S.; Kim, Y.S. Detection of protein kinase using an aptamer on a microchip integrated electrolyte-insulator-semiconductor sensor. *Sens. Actuators B Chem*. 2017, 248, 973–979.

[67] Wang, L.; Zheng, Q.; Zhang, Q.; Xu, H.; Tong, J.; Zhu, C.; Wan, Y. Detection of single tumor cell resistance with aptamer biochip. *Oncol. Lett*. 2012, 4, 935–940.

[68] Zhao, L.; Tang, C.; Xu, L.; Zhang, Z.; Li, X.; Hu, H.; Cheng, S.; Zhou, W.; Huang, M.; Fong, A.; et al. Enhanced and Differential Capture of Circulating Tumor Cells from Lung Cancer Patients by Microfluidic Assays Using Aptamer Cocktail. *Small*. 2016, 12, 1072–1081.

[69] Sheng, Y.; Bowser, M.T. Isolating single stranded DNA using a microfluidic dialysis device. *Analyst.* 2014, 139, 215–224.

[70] White, S.P.; Sreevatsan, S.; Frisbie, C.D.; Dorfman, K.D. Rapid, Selective, Label-Free Aptameric Capture and Detection of Ricin in Potable Liquids Using a Printed Floating Gate Transistor. *ACS Sens*. 2016, 1, 1213–1216.

[71] Pasquardini, L.; Pancheri, L.; Potrich, C.; Ferri, A.; Piemonte, C.; Lunelli, L.; Napione, L.; Comunanza, V.; Alvaro, M.; Vanzetti, L.; et al. SPAD aptasensor for the detection of circulating protein biomarkers. *Biosens. Bioelectron*. 2015, 68, 500–507.

[72] Thiha, A.; Ibrahim, F.; Muniandy, S.; Dinshaw, I.J.; Teh, S.J.; Thong, K.L.; Leo, B.F.; Madou, M. All-carbon suspended nanowire sensors as a rapid highly-sensitive label-free chemiresistive biosensing platform. *Biosens. Bioelectron*. 2018, 107, 145–152.

[73] Pan, Y.; Wan, Z.; Zhong, L.; Li, X.; Wu, Q.; Wang, J.; Wang, P. Label-free okadaic acid detection using growth of gold nanoparticles in sensor gaps as a conductive tag. *Biomed. Microdevices*. 2017, 19, 33.

[74] Tian, T.; Wei, X.; Jia, S.; Zhang, R.; Li, J.; Zhu, Z.; Zhang, H.; Ma, Y.; Lin, Z.; Yang, C.J. Integration of target responsive hydrogel with cascaded enzymatic reactions and microfluidic paper-based analytic devices (μPADs) for point-of-care testing (POCT). *Biosens. Bioelectron*. 2016, 77, 537–542.

[75] Martinez, A.W.; Phillips, S.T.; Butte, M.J.; Whitesides, G.M. Patterned Paper as a Platform for Inexpensive, Low Volume, Portable Bioassays. *Angew. Chem. Int. Ed*. 2007, 46, 1318–1320.

[76] Ren, K.; Zhou, J.; Wu, H. Materials for microfluidic chip fabrication. *Acc. Chem. Res*. 2013, 46, 2396–2406.

[77] Zhang, Y.; Gao, D.; Fan, J.; Nie, J.; Le, S.; Zhu, W.; Yang, J.; Li, J. Naked-eye quantitative aptamer-based assay on paper device. *Biosens. Bioelectron*. 2016, 78, 538–546.

[78] Fu, H.; Yang, J.; Guo, L.; Nie, J.; Yin, Q.; Zhang, L.; Zhang, Y. Using the Rubik's Cube to directly produce paper analytical devices for quantitative point-of-care aptamer-based assays. *Biosens. Bioelectron*. 2017, 96, 194–200.

[79] Yan, J.; Yan, M.; Ge, L.; Yu, J.; Ge, S.; Huang, J. A microfluidic origami electrochemiluminescence aptamer-device based on a porous Au-paper electrode and a phenyleneethynylene derivative. *Chem. Commun*. 2013, 49, 1383–1385.

[80] Liu, H.; Xiang, Y.; Lu, Y.; Crooks, R.M. Aptamer-based origami paper analytical device for electrochemical detection of adenosine. *Angew. Chem. Int. Ed*. 2012, 51, 6925–6928.

[81] Ma, C.; Liu, H.; Zhang, L.; Li, L.; Yan, M.; Yu, J.; Song, X. Microfluidic Paper-Based Analytical Device for Sensitive Detection of Peptides Based on Specific Recognition of Aptamer and Amplification Strategy of Hybridization Chain Reaction. *Chem. Electro. Chem*., 2017, 4, 1744–1749.

[82] Ahmad Raston, N.H.; Nguyen, V.T.; Gu, M.B. A new lateral flow strip assay (LFSA) using a pair of aptamers for the detection of Vaspin. *Biosens. Bioelectron*. 2017, 93, 21–25.

[83] Wu, W.; Zhao, S.; Mao, Y.; Fang, Z.; Lu, X.; Zeng, L. A sensitive lateral flow biosensor for Escherichia coli O157: H7 detection based on aptamer mediated strand displacement amplification. *Anal. Chim. Acta*., 2015, 861, 62–68.

[84] Zhou, W.; Kong, W.; Dou, X.; Zhao, M.; Ouyang, Z.; Yang, M. An aptamer based lateral flow strip for on-site rapid detection of ochratoxin A in Astragalus membranaceus. *J. Chromatogr. B Anal. Technol. Biomed. Life Sci*. 2016, 1022, 102–108.

[85] Biyani, M.; Kawai, K.; Kitamura, K.; Chikae, M.; Biyani, M.; Ushijima, H.; Tamiya, E.; Yoneda, T.; Takamura, Y. PEP-on-DEP: A competitive peptide-based disposable electrochemical aptasensor for renin diagnostics. *Biosens. Bioelectron*. 2016, 84, 120–125.

[86] Hou, W.; Shi, Z.; Guo, Y.; Sun, X.; Wang, X. An interdigital array microelectrode aptasensor based on multi-walled carbon nanotubes for detection of tetracycline. *Bioprocess Biosyst. Eng*. 2017, 40, 1419–1425.

[87] Liu, F.; Zhang, Y.; Yu, J.; Wang, S.; Ge, S.; Song, X. Application of ZnO/graphene and S6 aptamers for sensitive photoelectrochemical detection of SK-BR-3 breast cancer cells based on a disposable indium tin oxide device. *Biosens. Bioelectron*. 2014, 51, 413–420.

[88] Daprà, J.; Lauridsen, L.H.; Nielsen, A.T.; Rozlosnik, N. Comparative study on aptamers as recognition elements for antibiotics in a label-free all-polymer biosensor. *Biosens. Bioelectron*. 2013, 43, 315–320.

[89] Lou, B.; Zhou, Z.; Du, Y.; Dong, S. Resistance-based logic aptamer sensor for CCRF-CEM and Ramos cells integrated on microfluidic chip. *Electrochem. Commun*. 2015, 59, 64–67.

[90] Zuo, P.; Li, X.; Dominguez, D.C.; Ye, B.-C. A PDMS/paper/glass hybrid microfluidic biochip integrated with aptamer-functionalized graphene oxide nano-biosensors for one-step multiplexed pathogen detection. *Lab Chip*., 2013, 13, 3921–3928.

[91] Liang, L.; Su, M.; Li, L.; Lan, F.; Yang, G.; Ge, S.; Yu, J.; Song, X. Aptamer-based fluorescent and visual biosensor for multiplexed monitoring of cancer cells in microfluidic paper-based analytical devices. *Sens. Actuators B Chem*. 2016, 229, 347–354.

[92] Weng, X.; Neethirajan, S. Aptamer-based fluorometric determination of norovirus using a paper-based microfluidic device. *Microchim. Acta*., 2017, 184, 4545–4552.

[93] Zhang, H.; Hu, X.; Fu, X. Aptamer-based microfluidic beads array sensor for simultaneous detection of multiple analytes employing multienzyme-linked nanoparticle amplification and quantum dots labels. *Biosens. Bioelectron*. 2014, 57, 22–29.

[94] Girardot, M.; D'Orlyé, F.; Descroix, S.; Varenne, A. Aptamer-conjugated nanoparticles: Preservation of targeting functionality demonstrated by microchip electrophoresis in frontal mode. *Anal. Biochem*. 2013, 435, 150–152.

[95] Jin, H.; Gui, R.; Sun, J.; Wang, Y. Facilely self-assembled magnetic nanoparticles/aptamer/carbon dots nanocomposites for highly sensitive up-conversion fluorescence turn-on detection of tetrodotoxin. *Talanta*., 2018, 176, 277–283.

[96] Ni, X.; Xia, B.; Wang, L.; Ye, J.; Du, G.; Feng, H.; Zhou, X.; Zhang, T.; Wang, W. Fluorescent aptasensor for 17β-estradiol determination based on gold nanoparticles quenching the fluorescence of Rhodamine B. *Anal. Biochem*. 2017, 523, 17–23.

[97] Fraser, L.A.; Kinghorn, A.B.; Dirkzwager, R.M.; Liang, S.; Cheung, Y.W.; Lim, B.; Shiu, S.C.C.; Tang, M.S.L.; Andrew, D.; Manitta, J.; et al. A portable microfluidic

Aptamer-Tethered Enzyme Capture (APTEC) biosensor for malaria diagnosis. *Biosens. Bioelectron*. 2018, 100, 591–596.

[98] Wei, X.; Tian, T.; Jia, S.; Zhu, Z.; Ma, Y.; Sun, J.; Lin, Z.; Yang, C.J. Target-responsive DNA hydrogel mediated stop-flow microfluidic paper-based analytic device for rapid, portable and visual detection of multiple targets. *Anal. Chem*. 2015, 87, 4275–4282.

[99] Chuang, T.-L.; Chang, C.-C.; Chu-Su, Y.; Wei, S.-C.; Zhao, X.; Hsueh, P.-R.; Lin, C.-W. Disposable surface plasmon resonance aptasensor with membrane-based sample handling design for quantitative interferon-gamma detection. *Lab Chip*., 2014, 14, 2968–2977.

[100] Ahmad, R.; Destgeer, G.; Afzal, M.; Park, J.; Ahmed, H.; Jung, J.H.; Park, K.; Yoon, T.S.; Sung, H.J. Acoustic Wave-Driven Functionalized Particles for Aptamer-Based Target Biomolecule Separation. *Anal. Chem*. 2017, 89, 13313–13319.

[101] Zhang, F.; Li, S.; Cao, K.; Wang, P.; Su, Y.; Zhu, X.; Wan, Y. A microfluidic love-wave biosensing device for PSA detection based on an aptamer beacon probe. *Sensors* (Switzerland) 2015, 15, 13839–13850.

[102] Wang, Y.; Gan, N.; Zhou, Y.; Li, T.; Hu, F.; Cao, Y.; Chen, Y. Novel label-free and high-throughput microchip electrophoresis platform for multiplex antibiotic residues detection based on aptamer probes and target catalyzed hairpin assembly for signal amplification. *Biosens. Bioelectron*. 2017, 97, 100–106.

[103] Zhou, L.; Gan, N.; Zhou, Y.; Li, T.; Cao, Y.; Chen, Y. A label-free and universal platform for antibiotics detection based on microchip electrophoresis using aptamer probes. *Talanta*., 2017, 167, 544–549.

[104] Tian, R.Y.; Lin, C.; Yu, S.Y.; Gong, S.; Hu, P.; Li, Y.S.; Wu, Z.C.; Gao, Y.; Zhou, Y.; Liu, Z.S.; et al. Preparation of a specific ssDNA aptamer for brevetoxin-2 using SELEX. *J. Anal. Methods Chem*. 2016, 2016.

[105] Gao, S.; Hu, B.; Zheng, X.; Cao, Y.; Liu, D.; Sun, M.; Jiao, B.; Wang, L. Gonyautoxin 1/4 aptamers with high-affinity and high-specificity: From efficient selection to aptasensor application. *Biosens. Bioelectron*. 2016, 79, 938–944.

CHAPTER 2 Label-Free Aptamer-based "Signal-off" Sensor for Determination Ochratoxin A Using Microfabricated Electrode

2.1 Introduction

Ochratoxin A (OTA) is a toxin produced by the secondary metabolism of *Penicillium* and *Aspergillus* fungal strains. As OTA is potentially carcinogenic to humans, the International Agency for Research on Cancer (IARC) has classified it as a group 2B carcinogen. Structurally, the OTA molecule is a derivative of phenylalanine-dihydroisocoumarin, which is stable to high temperatures and hydrolysis. This toxin is frequently found in food and feedstuff such as coffee, cereals, dried fruits, and beverages such as beer and wine [1, 2]. Several researchers have reported that OTA causes acute and chronic nephropathies, tubulointerstitial diseases, and immunosuppression [3 – 6]. The fungus proliferates during harvest and storage. Hence, storage conditions in the warehouse are a major determining factor for the growth of mold and ochratoxinogenesis.

It is not feasible to test for contaminated food products simply by evaluating their appearance because even apparently moldy products may not necessarily contain OTA. Therefore, these products should be tested with laboratory analytical methods. Recently, a detection method of this toxin involving liquid chromatography with fluorescence detection and immunoaffinity column clean-up was established for routine analysis in several laboratories [7, 8]. However, this method required sophisticated instrument and a centralized laboratory test, which disqualified it for on-site analysis. Consequently, the sample should be delivered to the laboratory, although fresh samples ensure constant results and that future contamination is avoided. Enzyme-linked immunosorbent assay (ELISA) in a lateral-strip form is an alternative for real-time analysis outside the laboratory [9]. This assay technique

usually re-quires no sample clean-up other than filtration and dilution of the sample. However, the disadvantage is the necessity of stable antibodies and the narrow detection range (typically 1–40 ng mL^{-1}).

Therefore, electrochemical detection is an attractive option because of its high specificity and sensitivity. Unfortunately, the conventional electrochemical techniques require high reagent consumption and specialized laboratory space [10, 11]. Hence, at present, they are unfeasible for rapid-on-site detection. For these reasons, there have been several attempts to miniaturize the electrochemical platforms [12, 13]. An oligonucleotide that has high affinity to a specific target is called an aptamer, which has been used as a promising replacement of antibody. An aptamer can be modified with a thiol group for immobilization on a gold surface as a self-assembled monolayer (SAM). Cruz-Aguado and Penner isolated the first aptamer that showed a specific binding affinity with OTA through the systematic evolution of ligands by exponential enrichment (SELEX) technique [14]. To enhance the sensitivity of the aptamer sensors, various techniques have been proposed, including redox labeling, using enzymes, metal nanoparticles (MNPs), and magnetic beads [15-18]. Despite their advantage of high sensitivity, the reagents and materials used in these techniques are expensive and require complex preparations. An integrated electrochemical detection technique with OTA aptamer has been reported previously, which employed rod electrodes that were cleaned using hazardous reagents such as piranha solution and a silicon-based device containing three planar microelectrodes with a two-layer format (adhesion layer prior to the gold material) and involved screen printing [19-21]. Screen-printing is a common technique for the fabrication of carbon or silver electrodes. However, for a gold electrode, screen printing is not appropriate because gold ink is expensive. Microfabrication technologies including vacuum deposition and photolithography are suitable methods to fabricate a gold electrode, because of the efficient use of gold, good precision of shape and

size especially for microelectrodes, and exceptional smoothness of the electrode surface, which are essential for DNA immobilization.

In this study, a miniaturized electrochemical label-free sensor based on an aptamer was developed. The construction of the sensor and the measurements were simple, with enough sensitivity to detect OTA in food samples. The electrode system was integrated on a polystyrene (PS) substrate (1 $in.^2$), which was fabricated by patterning after depositing gold directly onto the substrate without a Cr or Ti layer, unlike electrodes fabricated on glass substrates. This sensor required lower amounts of reagents and a small volume of the sample, compared with previous studies. Furthermore, methylene blue (MB) was used as a redox indicator, because it can undergo two-electron- and one-proton-transfer oxidation or reduction, which can be detected as a signal from the sensor (figure 2-1). Modified redox indicators, such as the covalently modified indicator oligonucleotide conjugates employed in previous studies, were not required for this proposed sensor [15,22]. Instead, we utilized the ability of MB to interact with the guanine base and the backbone of DNA. Although there are several aptamer-based sensors for OTA exhibiting such interactions with MB, the proposed sensor has a simple design even without any signal enhancers, and hence can be prepared without complicated procedures [23−27]. The electrode of the sensor was reusable as it could be regenerated. Consequently, the cost of analysis could be significantly reduced. Additionally, this technique offered the possibility of the onsite detection of OTA with good sensitivity and selectivity without signal amplification. The highly sensitive detection of OTA was made possible by differential pulse voltammetry (DPV). The proposed sensor was successfully applied to the detection of OTA in real samples such as beer and coffee.

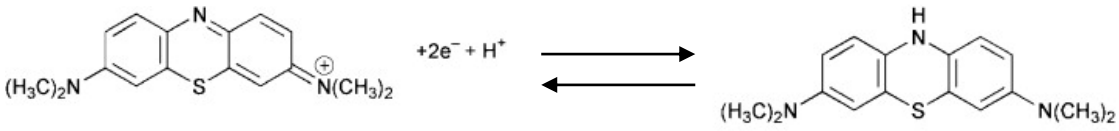

Methylene blue Leucomethylene blue

Figure 2-1. Reduction-oxidation reaction of methylene blue

2.2 Experimental

2.2.1 Reagents and Materials

The sequences of the oligonucleotides used in this study were as follows:

DNA aptamer: 5'–GAT CGG GTG TGG GTG GCG TAA AGG GAG CAT CGG ACA GGG TCC AAG AGA–3'

DNA linker : 5'–SH-C3-TCT CTT GGA CCC–3'

DNA 1 : 5'–CCC CCC CCC CCC CCC CCC CCC CCC CCC CCC CCC CCC GGG TCC AAG AGA–3'

DNA 2 : 5'–GGG GGG GGG GGG GGG GGG GGG GGG GGG GGG GGG GGG GGG GGG TCC AAG AGA–3'

DNA 3 : 5'–TTT TTT TTT TTT TTT TTT TTT TTT TTT TTT TTT TTT TTT GGG TCC AAG AGA–3'

DNA 4 : 5'–AAA AAA AAA AAA AAA AAA AAA AAA AAA AAA AAA AAA AAA GGG TCC AAG AGA–3'

The DNA oligonucleotides were synthesized by Integrated DNA Technologies (Coralville) and purified by high-performance liquid chromatography. The oligonucleotides were received lyophilized and resuspended in Tris−ethylenediaminetetraacetic acid (Tris−EDTA or TE) buffer at a final concentration of 100 μM. The sequence of the aptamer-identifying OTA was adopted from the literature [14]. A thiol modification at the 5′-end and

the spacer −C3− of the nucleotide was used as a linker to attach it perpendicularly to the gold surface. The DNAs 1−4 containing poly C, G, T, and A, and the complementary sequence with the linker at the 3′-end were used to test the selectivity of the aptamer.

The buffer solutions used in this study were TE buffer for DNA dilution comprising 10 mM Tris−HCl and 1.0 mM EDTA and phosphate-buffered saline (PBS) as the working buffer containing 1 mM $MgCl_2$ (10 mM phosphate with 1.0 M NaCl, pH 7.0). Components of the buffer solutions, ochratoxin A (10 μgmL−1 in acetonitrile, ≥99%), methylene blue (MB, ≥98.5%) powder, and tris-(2-carboxyethyl)- phosphine hydrochloride (TCEP, ≥98%) powder were purchased from Wako Pure Chemical Industries, Ltd., and 6-mercaptohexanol (MCH, ≥97%) was procured from Sigma- Aldrich. Unless otherwise stated, all other reagents were of analytical grade. A Milli-Q water purification system (Millipore, 18 MΩ cm at 25 °C) was used for preparing all solutions. A PS plate of 1.7 mm thickness (Tamiya Inc., Japan) was used as the substrate.

2.2.2 Fabrication of Electrodes

The electrode system consists of three integrated electrodes, namely, the working electrode, reference electrode, and counter electrode. The working electrode was 5 mm in diameter. The electrodes were fabricated on a PS substrate by thermal vacuum evaporation according to a previously reported procedure [38,39]. The schematic process is illustrated in figure 2-2. Briefly, a gold layer was directly evaporated on a 5 cm × 5 cm PS substrate and patterned photolithographically with an OFPR-800 photoresist (Tokyo Ohka Kogyo Co. Ltd., Japan). Subsequently, wet etching using a potassium iodide solution was performed to reveal the patterned electrode and the remaining photoresist was removed with methanol. The substrate was cut into a piece of size 2.5 cm × 2.5 cm. A small amount of AgCl paste (BAS

Inc., Japan) was placed and cured to form a reference electrode. Screws were fixed at the contact pads of the electrodes for electric terminals to connect to an electrochemical analyzer.

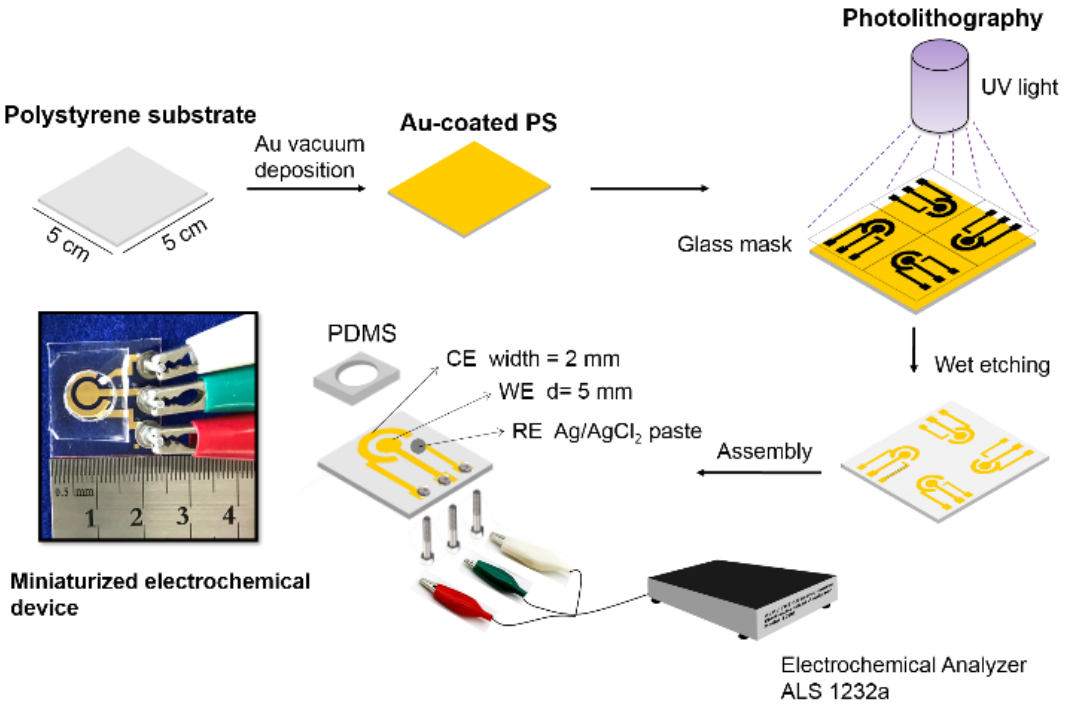

Figure 2-2. Schematic diagram for the fabrication of a miniaturized electrode for the present sensor and its experimental setup.

2.2.3 DNA Immobilization and Hybridization

Before DNA was immobilized, the Au working electrode was cleaned only by repeatedly applying cyclic potentials [40]. First, cleaning was performed under basic conditions (0.5 M NaOH) at a scan rate of 2 V s^{-1} and an overpotential of −0.35 to −1.35 V versus Ag/AgCl; typically, 100−200 repeat scans were performed until the current was at a minimum constant value. Next, potential scans were obtained under acidic conditions (0.5 M H_2SO_4) in the range of −0.35 to 1.5 V versus Ag/AgCl at a scan rate of 0.1 V s^{-1} for 20 scans. Lastly, a final round of scans was performed under acidic conditions (0.1 M H_2SO_4 and 0.01 M KCl) with four different potential ranges versus Ag/AgCl in a sequential manner: (1) 0.2−0.75 V; (2) 0.2−1.0 V; (3) 0.2− 1.25 V; and (4) 0.2−1.5 V versus Ag/AgCl (Table 2-1).

After the final step, the electrode was rinsed with water and dried under a stream of nitrogen. Punched poly(dimethylsiloxane) (PDMS) (the diameter of the hole was 5 mm) was attached to the substrate to form a well that contained only the working electrode.

Table 2-1. Parameters for electrode cleaning

	First step	Second step	Third step
Cleaning solution	0.5 M NaOH	0.5 M H_2SO_4	0.01M KCl/0.1 M H_2SO_4
Potential (V vs Ag/AgCl)	–0.35 to –1.35	–0.35 to 1.5	a) 0.2–0.75 b) 0.2–1.0 c) 0.2–1.25 d) 0.2–1.5
Segment	100–200	20	8 (each potential)
Scan Rate (V s^{-1})	2	0.1	0.1

The thiolated aptamer was immobilized on a gold working electrode to form SAMs. Before the SAM process, 2 μL of 100 μM linker was incubated with 2 μL of 10 mM TCEP for 60 min to reduce the disulfide bond of the linker. After this treatment, the mixture was diluted in PBS to a final volume of 200 μL. This solution was then transferred to the working electrode fixed with a PDMS well and incubated for 60 min as described in figure 2-3. Subsequently, the modified electrode was rinsed with a copious amount of PBS and further passivated with 50 μL of 2 mM MCH in PBS for 60 min to block the uncovered gold surface [41]. The aptamer solution was heated at 90 °C on a thermal block, exposed to ice for cooling, and then incubated at 25 °C. As a result, the aptamer was renatured and attained the most stable conformation, which is an essential condition for the aptamer to bind to the target molecule. Furthermore, 50 μL of 1 μM aptamer was added onto the electrode and hybridized with the linker. As a signal indicator, 200 μL of 20 μM MB containing 20 mM KCl was dropped onto the working electrode and incubated for 10 min to allow interaction with the oligonucleotides. Finally, the assembly was rinsed with PBS.

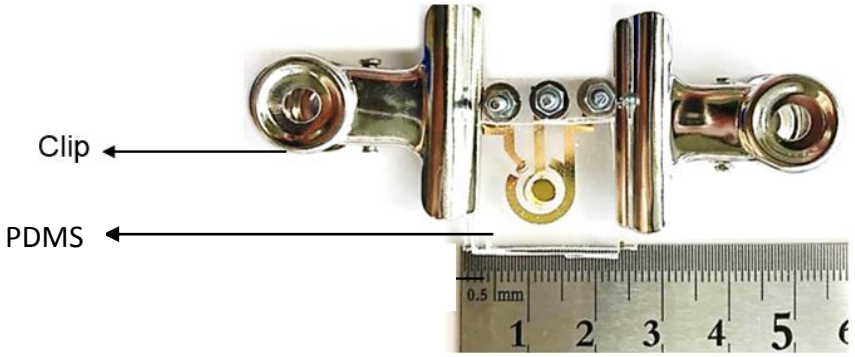

Figure 2-3. The miniaturized electrode covered with PDMS well. The PDMS well confines the area to localize the immobilization process.

2.2.4 Electrochemical Measurement

Cyclic voltammetry (CV) and differential pulse voltammetry (DPV) were performed at room temperature using an electrochemical analyzer ALS 1232a (BAS Inc., Japan) with parameters provided in table 2-2. A calibration curve for OTA was constructed based on DPV measurements, in which the negative peak current in a DPV response curve served as the signal (ordinate).

Table 2-2. Optimum parameters for measurement

Parameters	Cyclic Voltammetry	Parameters	Different Pulse Voltammetry
Initial E (V)	0	Initial E (V)	0
High E (V)	0	Final E (V)	–0.7
Low E (V)	–0.7	Incr E (V)	0.01
Init P/N	N	Amplitude (V)	0.04
Scan Rate (V s^{-1})	0.1	Pulse Width (sec)	0.06
Segment	2	Sample Width (sec)	0.02
Sample Interval (V)	0.001	Pulse Period (sec)	0.2
Sensitivity (A V^{-1})	0.0001	Sensitivity (A.V^{-1})	0.0001

2.2.5 Preparation of Spiked Real Sample

For validation of the proposed sensor with real samples, coffee and nonalcoholic beer were used. For the preparation of the coffee sample, commercially available milled coffee was used. First, 5 g of coffee was extracted with PBS (50 mL) for 60 min using a magnetic stirrer. To this extract, a known amount of OTA was added, and the solution was stirred for another 30 min. Next, the coffee sample was filtered with a solid-phase extraction (SPE) column packed with Wakosil 25C18 (particle size 15−30 μm; Wako Pure Chemical Industries, Japan) in-house, and approximately 500 μL of the filtrate was collected (Figure 2-4). For analysis of the beer sample, commercially available nonalcoholic canned beer was used, and the sample preparation was carried out by following a protocol presented by Hayat *et al* [42]. Briefly, OTA was spiked into the cooled beer, which was then degassed by sonicating for 60 min. This was followed by pH adjustment of the solution to 7.2−7.4 using NaOH solution to ensure the stability of the beer samples and appropriate aptamer binding. In the final step, the beer sample was filtered through a 0.45 μm syringe filter to separate particulate impurities.

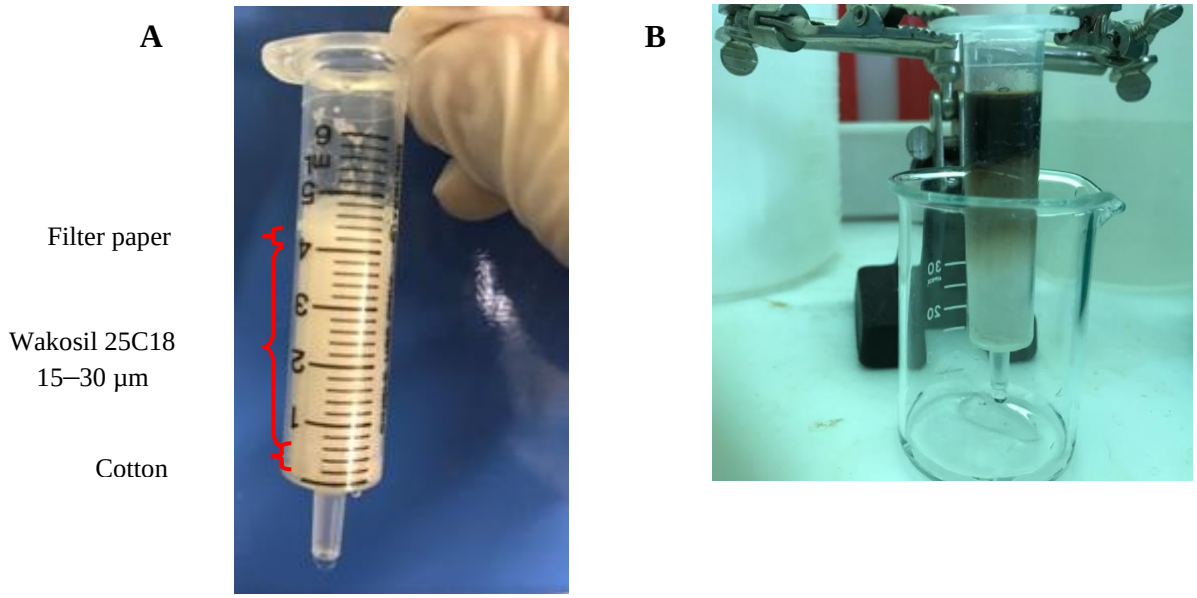

Figure 2-4. Preparation of a coffee sample by solid phase extraction. (A) In-house SPE column (syringe volume 5 mL and diameter 12 mm) and (B) The gravity force was used to filter the coffee sample and approximately 500 μL of the filtrate was collected.

2.3 Result and Discussion

2.3.1 Working Principle of the Proposed Sensor

This sensor comprises four components, namely a linker, 6-mercaptohexanol (MCH), aptamer, and MB; the process of building the sensor with each of these components is illustrated in Figure 2-4. The working principle of the proposed sensor is based on the target-induced dissociation of the aptamer from the linker on the electrode surface. In this sensor, MB does not covalently bond to the 5′- end of the aptamer as previously reported [22,28]. Instead, the aptamer-modified electrode was simply incubated with the MB solution and then washed to remove unbound MB molecules. The incubation resulted in the formation of an MB−aptamer complex and produced a label-free sensor (Figures 2-5C). After the addition of OTA to the sensor, the aptamer−MB−OTA complex was formed and dissociated from the linker on the electrode surface (Figures 2-5D). Although the aptamer was probably folded into an antiparallel G-quadruplex upon binding with OTA, the binding site for the aptamer and OTA is not known yet [29]. However, as shown in the original work by Cruz-Aguado and Penner, this aptamer has a rather high affinity to OTA, and binding depends on the presence of divalent cations such as Mg^{2+}, which are possibly responsible for the bridge-mediated interactions between the aptamer and the OTA molecules [14]. Therefore, this cation was used in phosphate-buffered saline (PBS) to achieve an optimum result.

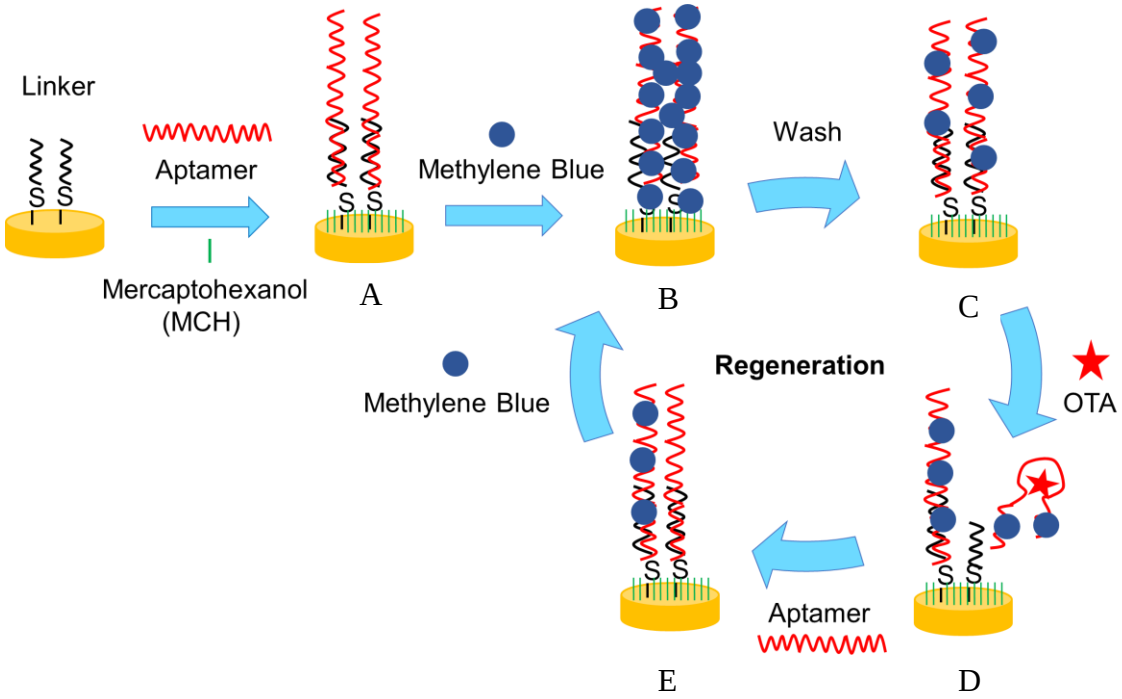

Figure 2-5. Schematic illustration of the modification of the electrode, detection of OTA, and regeneration of the sensor.

2.3.2 DNA Aptamer Immobilization

The schematics of electrode modification are illustrated in figure 2-6. Prior to DNA immobilization, the surface of the working electrode was not polished with alumina and underwent no treatment with highly oxidizing solutions such as piranha solution and aqua regia, for the sake of safety and ease. Instead, the electrode surface was cleaned by repeated potential scanning under acidic and basic conditions to remove ambient contaminants. This process was complete when the scan current became constant (Figure 2-7).

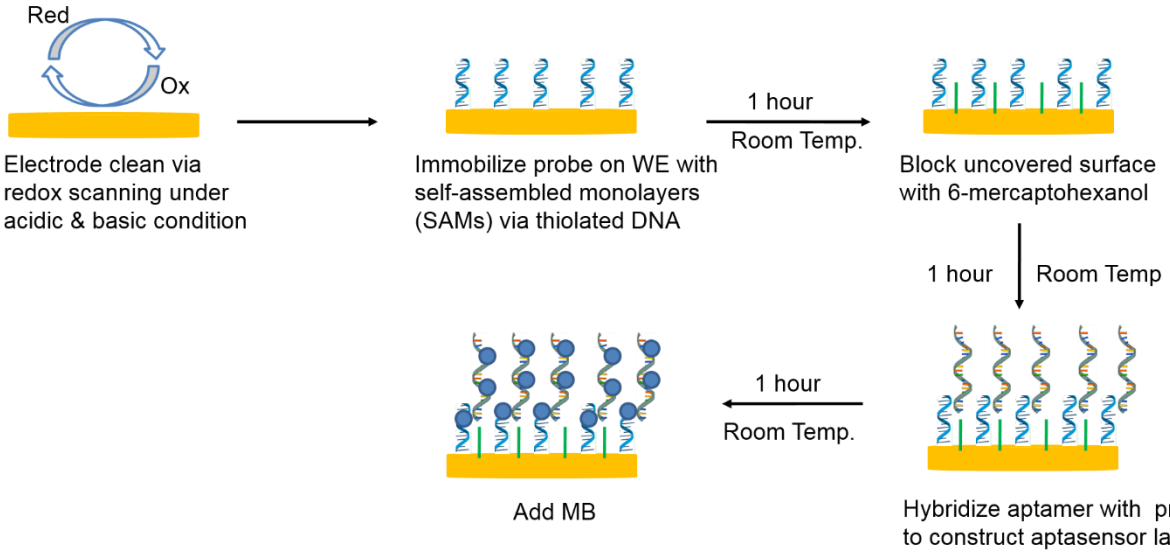

Figure 2-6. Schematic diagram of electrode modification. All processes were performed at room temperature.

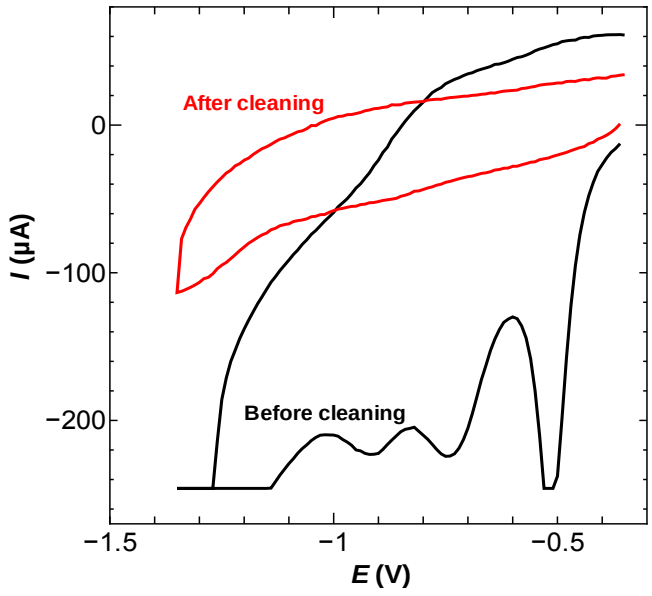

Figure 2-7. Potential scanning under basic condition (0.5 M NaOH) to clean the electrode before sensor fabrication. Voltammogram before cleaning (black) and after 200 times scanning completion (red) is shown.

Cyclic voltammetry (CV) and DPV were conducted in PBS to verify the electrode surface condition before and after immobilization (formation of the aptamer−linker electrode; MB is not included). As shown in figure 2-8, both CV and DPV voltammograms possess large current peaks for a bare gold electrode before immobilization. However, the current decreases significantly after the immobilization, which suggests that the electrode surface was successfully covered by thiolated oligonucleotides, including the aptamer−linker and MCH. Thus, the modified electrode blocked the nonspecific adsorption of electroactive substances that would have reduced the background signal.

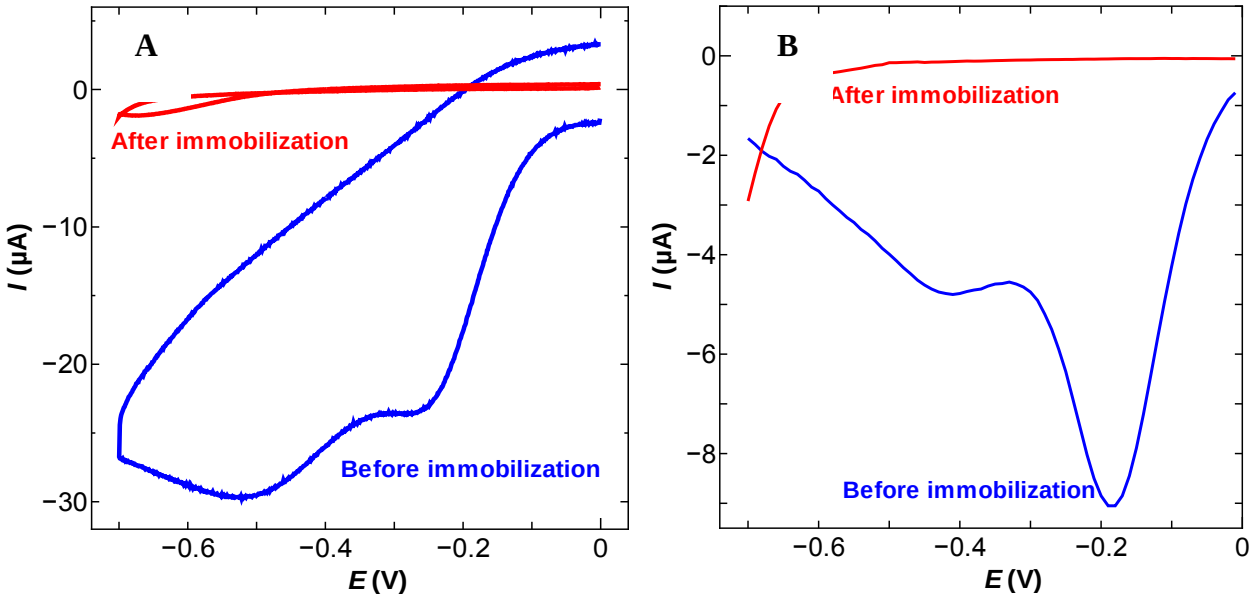

Figure 2-8. Background currents measured with electrodes before and after modification without MB by (A) cyclic voltammetry (CV) and (B) differential pulse voltammetry (DPV). The voltammograms were obtained in PBS buffer containing 1 mM MgCl.

We also examined the current signal of the proposed sensor in terms of reproducibility. The current signal was measured at various concentrations of OTA with three separately fabricated sensors (Table 2-3). Each sensor was regenerated after every measurement at each

concentration in a manner that will be described later. The coefficient of variation among the three sensors ranged from 0.3 to 11.8%. Table 2-3 shows the reproducibility of the regeneration of the sensor (detailed explanation follows later). The coefficient of variation of the current value was less than 5%. These results indicate that the sensor was reproducibly fabricated and regenerated. Consequently, we concluded that the density of the aptamer was also successfully controlled.

Table 2-3. Reproducibility test of the proposed sensor

OTA concentration (ng/mL)	Peak current (μA)			CV %
	Sensor #1	Sensor #2	Sensor #3	
0	-1.19	-1.18	-1.18	0.3
0.1	-1.10	-1.08	-1.07	1.1
1	-0.904	-0.898	-0.886	0.8
10	-0.804	-0.908	-0.901	5.4
100	-0.797	-0.683	-0.698	7.0
300	-0.743	-0.605	-0.568	11.8

Table 2-4. The current values of sensor after regeneration

Run #	Current (μA)
1	–0.4015
2	–0.3649
3	–0.3637
4	–0.3627
5	–0.3598
6	–0.3698
Average	–0.3704
SD	0.0142
RSD	3.84%

2.3.3 Detection of OTA

As illustrated in figure 2-9A, the blue curve shows the current response measured by DPV just after the addition of MB solution to the modified electrode; the peak current occurs at a potential of −0.3 V versus Ag/AgCl. This current was attributed to the reduction of the excess free MB in the proximity of the electrode surface rather than the MB molecules intercalated with the oligonucleotides. After rinsing the electrode to remove the free MB, DPV was performed in the PBS without OTA. As shown in figure 2-9A, the peak current was reduced and observed at −0.22 V versus Ag/AgCl (red curve). This current could be attributed to the remaining MB molecules that interacted with the oligonucleotides immobilized on the electrode surface. The same tendency of MB molecules intercalating with DNA was revealed in previous research [30−33]. The authors observed that MB could interact with ss-DNA or ds-DNA via face-to-face interactions with guanine bases, and the positively charged MB molecules interacted electrostatically with the negatively charged phosphate backbone of DNA to generate specific signals. Furthermore, adding 100 ng mL^{-1} of OTA to the modified electrode decreased the current (Figure 2-9B). The lower peak current signal could still be observed (black curve in Figure 2-9A) and indicated that a small amount of the MB−aptamer complex remained along with the formation of the MB−linker complex. This result also indicated that the capacity of the sensor was more than 100 ng mL^{-1}. The proposed sensor also demonstrated an ability to differentiate the specific form of the aptamer, between an MB−aptamer complex form and an MB−aptamer−OTA form, on the basis of the potential and current values. For further experiments, the potential used to measure the current signal was −0.22 V versus Ag/AgCl.

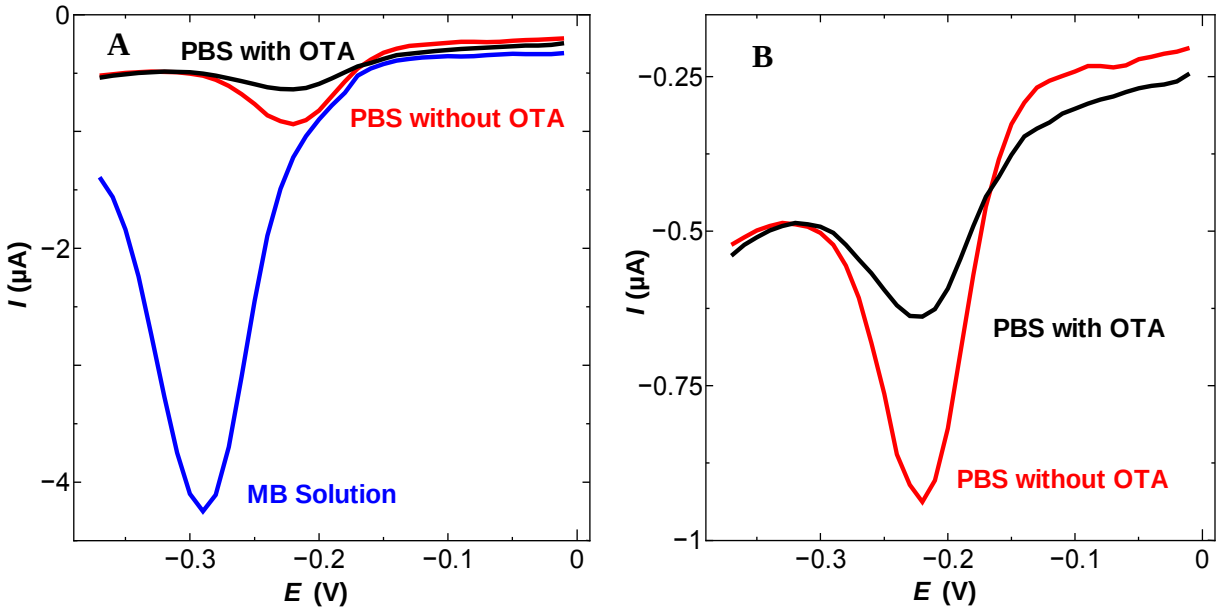

Figure 2-9. DPV curves of the sensor obtained with MB solution (blue curve), PBS buffer without OTA (red curve), and PBS buffer containing 100 ng mL^{-1} OTA (black curve). (B) Enlarged view of the curve for PBS with and without OTA in (A). Specific peak potential (-0.22 V vs Ag/AgCl) and the gap of currents indicates the presence of OTA.

2.3.4 Sensitivity of the Sensor to OTA

The current response of the proposed sensor was evaluated for a wide range of OTA concentrations. Figure 2-10A demonstrates that the peak current decreased with increasing OTA concentration. The peak voltage slightly shifted from −0.22 to −0.21 V with an increase in the OTA concentration. We attributed this to the variation of measurements. However, the differences were very small (10 mV); hence, their effect on the sensitivity and precision could be negligible. Furthermore, the plot of the peak current against OTA concentration (Figure 2-10B) exhibited a wide range of linearity from 0.1 to 300 ng mL^{-1} with an R^2 of 0.986. Thus, the proposed method improved the linear range as compared with conventional detection methods [7−9]. The limit of detection (LOD) was 78.3 pg mL^{-1} (defined as S/N =

3). This value was higher than those obtained in previous works (Table A1, Additional Information). However, it is noteworthy that this sensor, with its simple and label-free detection, satisfies the required minimum amount of OTA considered safe for human consumption (2−10 ng mL^{-1}) [34].

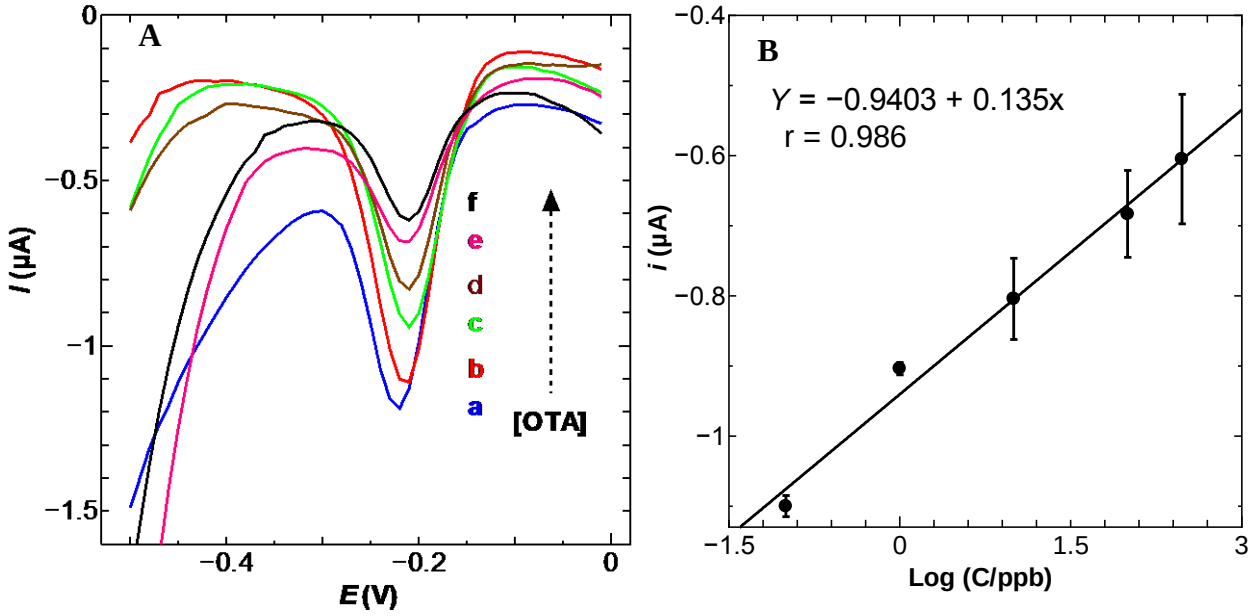

Figure 2-10. (A) Current responses measured by DPV at various concentrations of OTA: (a) 0, (b) 0.1, (c) 1, (d) 10, (e) 100, (f) 300 ng mL^{-1}. (B) Plot of current vs logarithmic concentration of OTA. Error bars represent ± standard deviations of means (n = 3).

2.3.5 Selectivity of the Aptamer

To verify the selectivity of the aptamer to OTA, the current responses were measured using sensors immobilized with several oligonucleotides (poly-C, poly-G, poly-T, and poly-A) possessing the complementary sequence with the linker in the absence and presence of OTA (Figure 2-11). These DNAs were treated under the same conditions as the aptamer. As shown in figure 2-12, changes in the current between the absence and presence of OTA were less than 6% for the DNAs containing poly-C, poly-G, poly-T, and poly-A, whereas the current changed by 45% in the case of the aptamer. This result indicated that the binding of

OTA to the oligonucleotides took place only because of the aptamer. Poly-G demonstrated the highest current signal (Figure 2-12). This was attributed to the binding of MB molecules to the G-rich oligonucleotide. Several studies have reported that the peak current increases with the number of guanine bases [35,36].

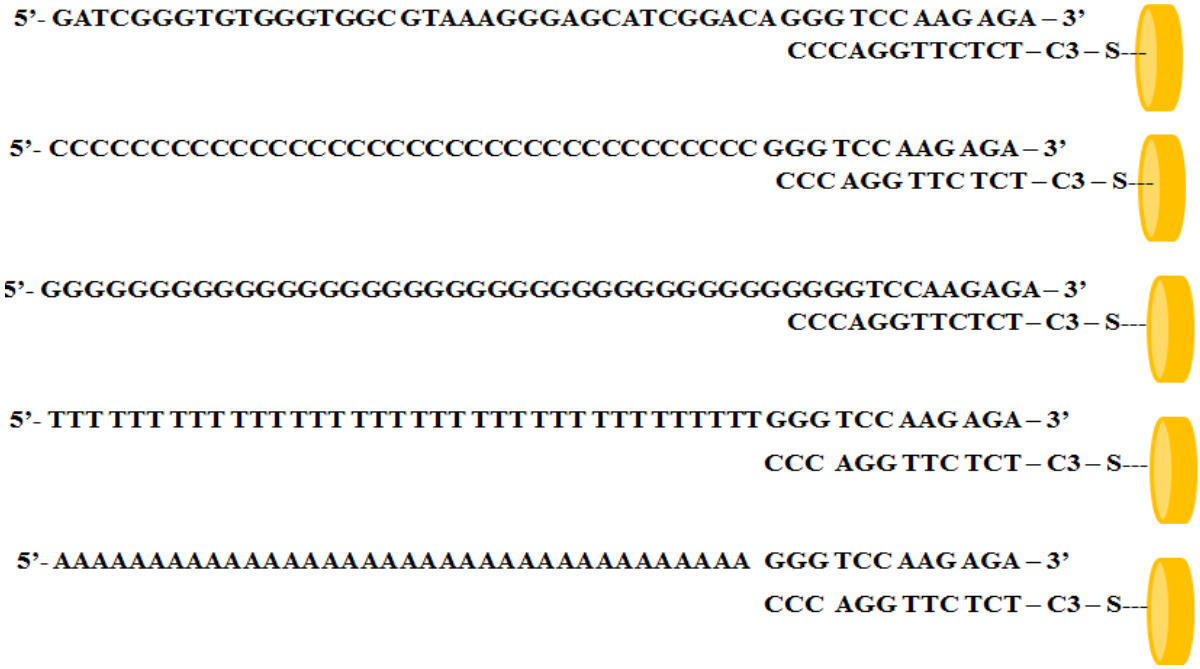

Figure 2-11. Sequences of oligonucleotides analogue to DNA aptamer used for selectivity test.

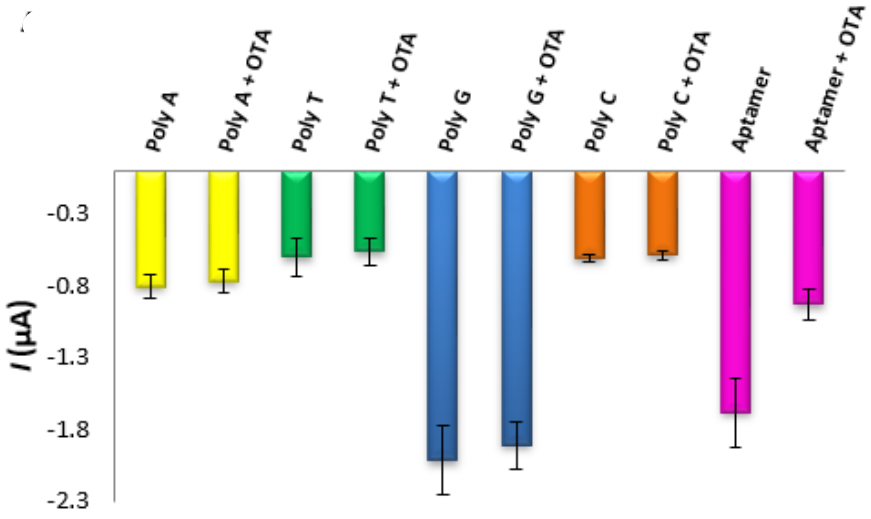

Figure 2-12. Selectivity test with Poly-C, Poly-G Poly-T, and Poly-A. All these oligonucleotides were treated under the same conditions as the aptamer.

In contrast, the current responses observed with G-poor sequences (poly-C, poly-T, and poly-A) were lower than that with poly-G despite the same base length. Since many fungi can grow and produce their mycotoxins under similar environmental conditions, OTA is rarely found as a single contaminant in foodstuffs [37]. Aflatoxin B1 (AFB1) is the most common toxin that was present in the samples used in this study. Furthermore, AFB1 possesses similar functional groups such as phenyl, hydroxyl, and methyl groups and a low molecular weight (less than 500 g mol^{-1}) as depicted in figure 2-13. Therefore, the effect of AFB1 on the assay results was also examined. The current responses of OTA were measured in the absence and presence of AFB1 at the same final concentrations (50 ng mL^{-1}) (Figure 2-14). The differences observed between both current signals (see curves b and c) were not statistically significant. This result suggested that the proposed sensor has good selectivity toward OTA.

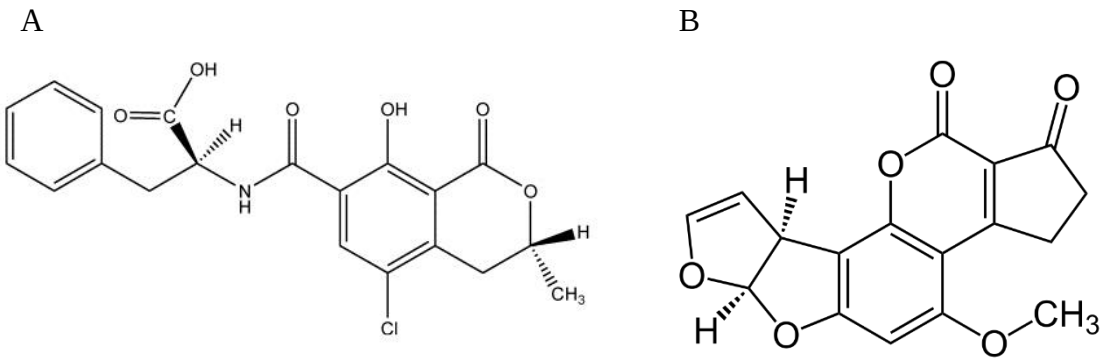

Figure 2-13. Chemical structure of (A) ochratoxin A and (B) aflatoxin B1

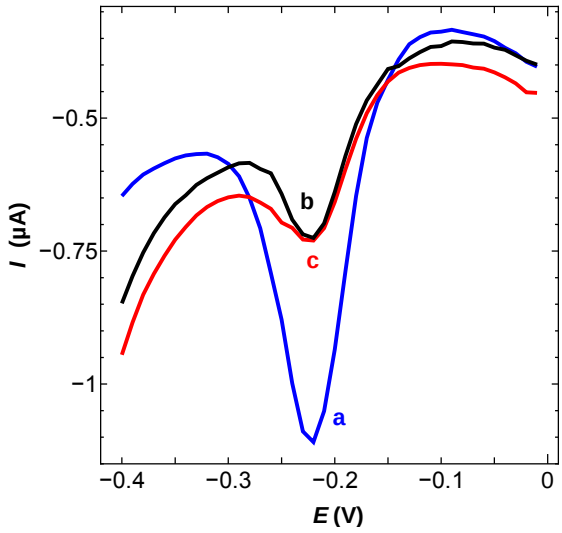

Figure 2-14. Selectivity of the sensor to (a) 0 ng mL^{-1} OTA and 0 ng mL-1 AFB1, (b) 50 ngmL^{-1} OTA and 50 ng mL^{-1} AFB1, and (c) 50 ng mL^{-1} OTA.

2.3.6 Real Sample Analysis

The proposed sensor was applied for the determination of OTA in two kinds of spiked samples (coffee and nonalcoholic beer) with a different matrix and phase. The samples were prepared as described in the Experimental Section. The concentration recovery was calculated using the standard curve after measurements were performed in triplicate. Table 2-5 lists the percentage recovery obtained with coffee and beer samples. For both these samples, favorable values of recovery were obtained (86.4−107%). These results confirmed that the

proposed sensor is suitable for the quantitative analysis of OTA in real samples. The lower recoveries for beer samples were attributed to the sample preparation, which was conducted without pH buffers, or, alternatively, to the effect of the sample matrix.

Table 2-5. Recovery test performed with spiked coffee and beer samples

Sample	Amount added ($ng\ mL^{-1}$)	Amount detected* ($ng\ mL^{-1}$)	Recovery (%)
Coffee	0	ND†	-
	10	10.8 ± 2.3	107
	100	95.4 ± 7.1	95.4
Non-alcoholic Beer	0	ND†	-
	10	8.6 ± 0.9	86.4
	100	88.4 ± 3.6	88.4

* Values revealed as the mean of three repeated measurements ± standard deviation (SD)
† ND, not detected (< LOD)

2.3.7 Regeneration of the Sensor

After OTA detection, the regeneration of the sensor was examined. For sensor regeneration, the used sensor was rinsed in deionized water and PBS, followed by incubation with an aptamer and MB solution, as described in figure 2-5 and the Experimental Section. The regeneration steps were repeated six times and the current response was measured at the OTA concentration of 50 ng mL^{-1} after every regeneration. As shown in figure 2-15, the signal response curves obtained with the regeneration sensors overlap with each other. Table 2-4 indicates that the differences in the current signals obtained with the sensor after the first to sixth regeneration were less than 5%. This result confirmed that the sensor could be successfully regenerated at least six times without any significant loss of sensitivity; note, however, that we did not carry out further tests.

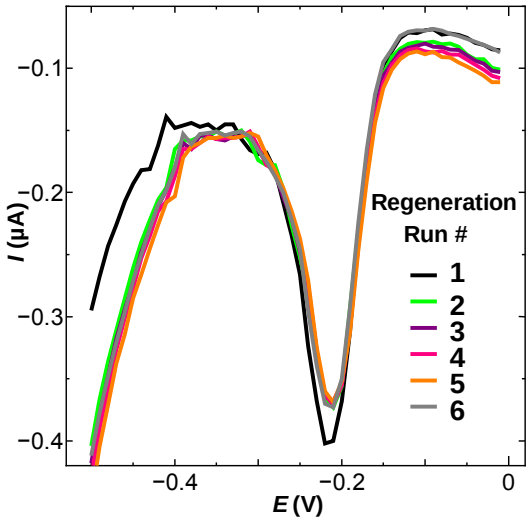

Figure 2-15. Signal responses for six times regeneration of sensor.

2.4 Conclusion

In this study, a label-free miniaturized electrochemical aptamer sensor was developed for the detection of OTA in real samples. The construction of an integrated gold electrode on a polystyrene substrate proved to be rather cost-effective and easy to use. Specifically, the ability of MB to bind specifically and with high affinity to guanine bases was utilized. With the proposed label-free sensor, the detection range was greatly improved from 0.1 to 300 ng mL^{-1}, and the LOD of 78.3 pg mL^{-1} was achieved without signal amplifiers. The proposed sensor was successfully applied to the analysis of spiked coffee and beer samples. A good recovery was obtained within the acceptable range (86.4−107%). Finally, the selectivity test with aflatoxin B1 and the regeneration test of the proposed sensor offer a potential tool for the simple onsite monitoring of food safety. The proposed sensor is applicable for the routine analysis of OTA without signal amplifiers.

2.5 Additional Information

Table A1. Summary of aptasensor for OTA detection

Authors	Detection	Linear range	Limit of detection	Signal indicator	Remarks	Ref
Tong, P. *et al*.	Electrochemical [a]	0.005–10.0 ng/mL	1 pg/mL	Ferrocene-label	Exonuclease enzyme	15
Yang, X. *et al*.	Electrochemical [a]	1.00 – 1000 pg/mL	0.3 pg/mL	Gold nanoparticles	Two-level cascade with four DNAs	17
Wu, J. *et al*.	Electrochemical [a]	0.1 – 1000 pg/mL	0.0095 pg/mL	MB-label	-	26
Liu, LH. *et al*.	Optical	0.73 – 12.50 ng/mL	0.39 ng/mL	-	-	A1
Wang, R. *et al*.	Optical	2.4 – 202 ng/mL	1.2 ng/mL	-	Evanescent wave	A2
Gu, C. *et al*.	Electrochemical [a]	not shown	3.31 ng/mL	Fluorescence-label	A personal glucose sensor was used for the measurement	18
Mazaafrianto, D. *et al*.	Electrochemical (miniaturized electrode)	0.1-300 ng/mL	78.3 pg/mL	MB but not labeled	Not needed	This study

[(a)]Conventional electrodes were used.

(A1) Wang, R.; Xiang, Y.; Zhou, X.; Liu, L. hua; Shi, H. A Reusable Aptamer-Based Evanescent Wave All-Fiber Biosensor for Highly Sensitive Detection of Ochratoxin A. Biosens. Bioelectron. 2015, 66, 11–18.

(A2) Liu, L. hua; Zhou, X. hong; Shi, H. chang. Portable Optical Aptasensor for Rapid Detection of Mycotoxin with a Reversible Ligand-Grafted Biosensing Surface. Biosens. Bioelectron. 2015, 72, 300–305.

References

[1] Monaci, L. Palmisano, F. Determination of Ochratoxin a in Foods: State-of-the-Art and Analytical Challenges. *Anal. Bioanal. Chem*. 2004, 378, 96−103.

[2]. Anli, E.; Alkis, I. M. Ochratoxin A and Brewing Technology: A Review. *J. Inst. Brew*. 2010, 116, 23−32.

[3] Marin, S.; Ramos, A. J.; Cano-Sancho, G.; Sanchis, V. Mycotoxins: Occurrence, Toxicology, and Exposure Assessment. *Food Chem. Toxicol*. 2013, 60, 218−237.

[4] Pfohl-Leszkowicz, A.; Manderville, R. A. Ochratoxin A: An Overview on Toxicity and Carcinogenicity in Animals and Humans. *Mol. Nutr. Food Res*. 2007, 51, 61−99.

[5] Mateo, R.; Medina, A.; Mateo, E. M.; Mateo, F.; Jiménez, M. An Overview of Ochratoxin A in Beer and Wine. *Int. J. Food Microbiol*. 2007, 119, 79−83.

[6] Lea, T.; Steien, K.; Størmer, F. C. Mechanism of Ochratoxin A Induced Immunosuppression. *Mycopathologia*., 1989, 107, 153−159.

[7] Chan, D.; MacDonald, S. J.; Boughtflower, V.; Brereton, P. Simultaneous Determination of Aflatoxins and Ochratoxin A in Food Using a Fully Automated Immunoaffinity Column Clean-up and Liquid Chromatography - Fluorescence Detection. *J. Chromatogr. A*., 2004, 1059, 13−16.

[8] Wan Ainiza, W. M.; Jinap, S.; Sanny, M. Simultaneous Determination of Aflatoxins and Ochratoxin A in Single and Mixed Spices. *Food Control*. 2015, 50, 913−918.

[9] Anfossi, L.; Giovannoli, C.; Giraudi, G.; Biagioli, F.; Passini, C.; Baggiani, C. A Lateral Flow Immunoassay for the Rapid Detection of Ochratoxin A in Wine and Grape Must. *J. Agric. Food Chem*. 2012, 60, 11491−11497.

[10] Xiao, Y.; Lai, R. Y.; Plaxco, K. W. Preparation of Electrode- immobilized, Redox-modified Oligonucleotides for Electrochemical DNA and Aptamer-based Sensing. *Nat. Protoc*. 2007, 2, 2875−2880.

[11] Zhao, W. W.; Wang, J.; Zhu, Y. C.; Xu, J. J.; Chen, H. Y. Quantum Dots: Electrochemiluminescent and Photoelectrochemical Bioanalysis. *Anal. Chem*. 2015, 87, 9520−9531.

[12] Karajić, A.; Reculusa, S.; Ravaine, S.; Mano, N.; Kuhn, A. Miniaturized Electrochemical Device from Assembled Cylindrical Macroporous Gold Electrodes. *Chem. Electro. Chem*., 2016, 3, 2031− 2035.

(13) Malecka, K.; Stachyra, A.; Góra-Sochacka, A.; Sirko, A.; Zagórski-Ostoja, W.; Radecka, H.; Radecki, J. Electrochemical Genosensor Based on Disc and Screen-Printed Gold Electrodes for Detection of Specific DNA and RNA Sequences Derived from Avian Influenza Virus H5N1. *Sens. Actuators, B*., 2016, 224, 290−297.

[14] Cruz-Aguado, J. A.; Penner, G. Determination of Ochratoxin A with a DNA aptamer. *J. Agric. Food Chem*. 2008, 56, 10456−10461.

[15] Tong, P.; Zhang, L.; Xu, J. J.; Chen, H. Y. Simply Amplified Electrochemical Aptasensor of Ochratoxin A Based on Exonuclease- catalyzed Target Recycling. *Biosens. Bioelectron*. 2011, 29, 97−101.

[16] González-Fernández, E.; Avlonitis, N.; Murray, A. F.; Mount, A.R.; Bradley, M. Methylene Blue Not Ferrocene: Optimal Reporters for Electrochemical Detection of Protease Activity. *Biosens. Bioelectron*. 2015, 84,82−88.

[17] Yang, X.; Jing, Q.; Ling, J.; Yuting, Y.; Kan, W.; Qian, L.; Kun, W. Ultrasensitive Electrochemical Aptasensor for Ochratoxin A Based on Two-Level Cascaded Signal Amplification Strategy. *Bioelectrochemistry*., 2014, 96, 7−13.

[18] Gu, C.; Long, F.; Zhou, X.; Shi, H. Portable Detection of Ochratoxin A in Red Wine Based on a Structure-Switching Aptamer using a Personal Glucometer. *RSC Adv*. 2016, 6, 29563−29569.

[19] Xuan, X.; Hossain, M. F.; Park, J. Y. A Fully Integrated and Miniaturized Heavy-metal-detection Sensor Based on Micro- patterned Reduced Graphene Oxide. *Sci. Rep*. 2016, 6, No. 33125.

[20] Zhu, L.; Zhou, X.; Shi, H. A Potentiometric Cobalt-Based Phosphate Sensor Based on Screen-Printing Technology. *Front. Environ. Sci. Eng.* 2014, 8, 945−951.

[21] Song, L.; Zhu, L.; Liu, Y.; Zhou, X.; Shi, H. A Disposable Cobalt-Based Phosphate Sensor Based on Screen Printing Technology. *Sci. China Chem*. 2014, 57, 1283−1290.

[22] Catanante, G.; Mishra, R. K.; Hayat, A.; Marty, J. L. Sensitive Analytical Performance of Folding Based Biosensor using Methylene Blue Tagged Aptamers. *Talanta*., 2016, 153, 138−144.

[23] Wei, M.; Zhang, W. The Determination of Ochratoxin A Based on the Electrochemical Aptasenor by Carbon Aerogels and Methylene Blue Assisted Signal Amplification. *Chem. Cent. J*. 2018, 12, 45.

[24] Kuang, H.; Chen, W.; Xu, D.; Xu, L.; Zhu, Y.; Liu, L.; Chu, H.; Peng, C.; Xu, C.; Zhu, S. Fabricated Aptamer-Based Electrochemical "Signal-off" Sensor of Ochratoxin A. *Biosens. Bioelectron*. 2010, 26, 710−716.

[25] Wei, M.; Feng, S. A Signal-off Aptasensor for the Determination of Ochratoxin A by Differential Pulse Voltammetry at a Modified Au Electrode Using Methylene Blue as an Electrochemical Probe. *Anal. Methods*., 2017, 9, 5449−5454.

[26] Abnous, K.; Danesh, N. M.; Alibolandi, M.; Ramezani, M.; Taghdisi, S. M. Amperometric Aptasensor for Ochratoxin A Based on the Use of a Gold Electrode Modified with Aptamer, Complementary DNA, SWCNTs and the Redox Marker Methylene Blue. *Microchim. Acta*., 2017, 184, 1151−1159.

[27] Xie, S.; Chai, Y.; Yuan, Y.; Bai, L.; Yuan, R. Development of an Electrochemical Method for Ochratoxin A Detection Based on Aptamer and Loop-Mediated Isothermal Amplification. *Biosens. Bioelectron*. 2014, 55, 324−329.

[28] Wu, J.; Chu, H.; Mei, Z.; Deng, Y.; Xue, F.; Zheng, L.; Chen, W. Ultrasensitive One-Step Rapid Detection of Ochratoxin A by the Folding-Based Electrochemical Aptasensor. *Anal. Chim. Acta*., 2012, 753, 27−31.

[29] Fadock, K. L.; Manderville, R. A. DNA Aptamer−Target Binding Motif Revealed Using a Fluorescent Guanine Probe: Implications for Food Toxin Detection. *ACS Omega*., 2017, 2, 4955−4963.

[30] Erdem, A.; Kerman, K.; Meric, B.; et al. Novel Hybridization Indicator Methylene Blue for the Electrochemical Detection of Short DNA Sequences Related to the Hepatitis B Virus. *Anal. Chim. Acta*., 2000, 422, 139−149.

[31] Tani, A.; Thomson, A. J.; Butt, J. N. Methylene Blue as an Electrochemical Discriminator of Single- and Double-Stranded Oligonucleotides Immobilized on Gold Substrates. *Analyst*., 2001, 126, 1756−1759.

[32] Ferapontova, E. E. Electrochemical Indicators for DNA Electroanalysis. *Curr. Anal. Chem*. 2011, 7,51−62.

[33] Gooding, J. J. Electrochemical DNA Hybridization Biosensors. *Electroanalysis*., 2002, 14, 1149−1156.

[34] European Commission. COMMISSION REGULATION (EC) No 1881/2006 of 19 December 2006 setting maximum levels for certain contaminants in foodstuffs. *Off. J. Eur. Union*., 2006, L364/5.

[35] Yang, W.; Ozsoz, M.; Hibbert, D. B.; Gooding, J. J. Evidence for the Direct Interaction between Methylene Blue and Guanine Bases Using DNA-modified Carbon Paste Electrodes. *Electroanalysis*., 2002, 14, 1299−1302.

[36] Lin, C.; Wu, Y.; Luo, F.; Chen, D.; Chen, X. A Label-free Electrochemical DNA Sensor using Methylene Blue as Redox Indicator Based on an Exonuclease III-aided Target Recycling Strategy. *Biosens. Bioelectron*. 2014, 59, 365−369.

[37] Battacone, G.; Nudda, A.; Pulina, G. Effects of Ochratoxin A on Livestock Production. *Toxins.,* 2010, 2, 1796−1824.

[38] Ishida, A.; Natsume, M.; Kamidate, T. Microchip Reversed- Phase Liquid Chromatography with Packed Column and Electro- chemical Flow Cell Using Polystyrene/poly(dimethylsiloxane). *J. Chromatogr. A.*, 2008, 1213, 209−217.

[39] Ishida, A.; Fujii, M.; Fujimoto, T.; Sasaki, S.; Yanagisawa, I.; Tani, H.; Tokeshi, M. A Portable Liquid Chromatograph with a Battery-operated Compact Electroosmotic Pump and a Microfluidic Chip Device with a Reversed Phase Packed Column. *Anal. Sci*. 2015, 31, 1163−1169.

[40] Fischer, L. M.; Maria, T.; Arto, R. H.; Noriyuki, M.; Jaime, C.; Anders, B.; Jenny, É.; Mogens, H. J.; Anja, B. Gold Cleaning Methods for Electrochemical Detection Applications. *Microelectron. Eng*. 2009, 86, 1282−1285.

[41] Jambrec, D.; Gebala, M.; La Mantia, F.; Schuhmann, W. Potential-Assisted DNA Immobilization as a Prerequisite for Fast and Controlled Formation of DNA Monolayers. *Angew. Chem., Int. Ed*. 2015, 54, 15064−15068.

[42] Hayat, A.; Andreescu, S.; Marty, J. L. Design of PEG-Aptamer Two Piece Macromolecules as Convenient and Integrated Sensing Platform: Application to the Label Free Detection of Small Size Molecules. *Biosens. Bioelectron*. 2013, 45, 168−173

CHAPTER 3 A "Signal-on" Detection of Ochratoxin A with Dithiol Modification Aptamer to Improve the Sensor Performance

3.1 Introduction

Development of microdevice sensor has special attention recently in connection with research discovery for drug-delivery, detection of pathogen or food contaminants, and quality control of certain products. Many techniques have been developed according to the main purpose including electrochemical [1, 2], chromatography [3, 4], spectroscopy [5, 6], and quartz crystal microbalance [7, 8], which had a prospect to future expanded as a microdevice or integrated microfluidics. Among the various sensing techniques, electrochemical sensors show great promise owing to their high sensitivity, low-cost, simplicity in instrumentation and operation [9, 10]. The use of alternative material for sensor substrate, such as polystyrene (PS) with a scale of a few millimeter and lightweight, has enabled a new type of microdevice sensors that capable of on-site detection and low cost [3].

An emerging class of biorecognition molecule that potentially replace the antibody in the sensor was called aptamer. The aptamer had the ability to bind tightly to their targets with high specificity, it is proven by dissociation constants (Kd) value in the range of micro to nanomolar [11, 12].

Detection of mycotoxins by using miniaturized electrochemical aptasensor has been reported which consists of labeled agents such as redox, fluorescence, and enzyme [13, 14, 15]. In addition, the number of strategies to enhance the sensitivity of detection has increased by using metal nanoparticles, carbon nanotube, and magnetic beads [10, 16, 17]. Despite impressing in sensitivity and detection speed, most of them require complex, multistep

preprocessing and addition of covalently labeled redox probe. In many cases, several strands of aptamer were immobilized to construct a sensing layer on the electrode and special treatment in every step was still needed.

Ferrocene and methylene blue (MB) have been widely used as redox reporter in electrochemical aptasensor owing to benefit from the electrochemically reversible behavior and differences in performance of both redox reporters have been reported. González-Fernández *et al* reported that the MB has good electrochemical performance when compared to the ferrocene by a stable background and reproducible response [18]. Moreover, the advantages of MB regarding to the ability to interact with guanine bases of DNA via $\pi - \pi$ interaction has been reported by several experiments and makes the MB become more favorable redox probe [19, 20].

Though sensitivity of reported electrochemical aptasensor was very high (lowest limit detection), the stability of immobilized sensing layer was still a challenging aspect to obtain reproducible results. Several investigations including our own research experience suggested that the alkanethiol layers consisting monothiols were not attached strongly on the gold surface. This phenomenon was observed as a decreased peak current after exposure with other thiol molecules, such as 6-mercaptohexanol (MCH) due to the displacement of main thiol molecules form the surface [21, 22]. Based on this condition, a new strategy is necessary to obtain more robust linkages between alkanethiol molecules and gold surface.

In this work, we proposed the different modification of alkanethiol with two thiols per unit aptamer. Our rationale is that by increasing the number of thiols in the anchoring site will produce much stronger interaction between aptamer and gold surface, and hence the sensor can produce the reproducible result. Indeed, dithiol modification have been shown to bind more strongly to the gold surface than mono thiol [21.28].

To the best of our knowledge, a simple microfabricated electrochemical basis on dithiol aptamer modification and non-covalently redox probe has never been reported so far. Motivated by this circumstance, we attempted to develop an approach which integrates of microfabricated electrochemical sensor with dithiol modified aptamer to improve the stability of sensor. In order to simple detection, we utilize non-covalently MB probe on the aptamer with a signal-on mechanism. Ochratoxin A was selected as the target of this study because of potentially carcinogenic to human and frequently found in food and beverage products.

3.2 Experimental

3.2.1 Reagents and Materials

The DNA aptamer is designed according to the literature [23] with some modifications. It contains 36 bases, modified with dithiol phosphoramidite (DTPA) at the 5'-end, incorporated through 3-carbon spacer (5'- DTPA-C3-GAT CGG GTG TGG GTG GCG TAA AGG GAG CAT CGG ACA-3') and was purified with high-performance liquid chromatography. This aptamer received as lyophilized powder from Integrated DNA Technologies (Coralville, USA) and rehydration by Tris−ethylenediaminetetraacetic acid (10 mM Tris−HCl and 1.0 mM EDTA) buffer at a final concentration of 100 μM. Then, the concentration was rechecked using NanoDrop One/One^{C} spectrophotometer (Thermo Fisher) to confirm actual concentration. The buffer for hybridization and electrochemical measurement is phosphate-buffered saline (PBS buffer, pH 7.2) containing 1 mM $MgCl_2$ (Thermo Fisher). Aflatoxin B1 (AFB1, 2 μg mL^{-1} in acetonitrile, ≥99%) and 6-mercaptohexanol (MCH, ≥ 97%) was procured from Sigma Aldrich. Deoxynivalenol (DON, 99.83 μg mL^{-1} in acetonitrile, ≥ 99%) was procured from Aokin AG., Germany. Methylene blue (MB, ≥ 98.5%), tris-(2-carboxyethyl) phosphine hydrochloride (TCEP, ≥ 99%), Ochratoxin A (OTA, 10 μg mL^{-1} in acetonitrile, ≥ 99%) and other unspecified chemicals and

reagents were of analytical purity and all purchased from Wako Pure Chemical Industries, Ltd., Japan. Solutions were prepared with ultrapure water processed with a Milli-Q water purification system (Millipore, 18 MΩ cm at 25 °C). A 1.7-mm thick polystyrene plate was used as a substrate (Tamiya Inc., Japan). The Au rod electrode, Ag/AgCl saturated with 3M NaCl reference electrode, Ag/AgCl paste, and platinum wire for conventional electrode set was purchased from BAS Inc., Japan.

3.2.2 Fabrication of Electrochemical Aptasensor

Aptasensor were constructed on a microfabricated electrode and a commercially available electrode. The procedures for surface treatment prior to self-assembly of aptamer monolayer on the gold surface was the electrode cleaning, this process is very crucial to provide a smooth surface for immobilization of aptamer. Especially for gold rod electrode was cleaned by mechanical polishing with 1.0 μm followed 0.5 μm alumina slurry on micro cloth pads (Buehler). Next, trace alumina particles on the electrodes were removed by sonicated with deionized water-ethanol mixture solution for 5 min. Both electrodes were cleaned by electrochemical oxidation and reduction by scanning repeatedly the potential from -0.35 to -1.35 V at a scan rate of 2 V s^{-1} in 0.5 M NaOH. Typically, 100-200 scans provided a steady state of the current. Then followed with 0.5 M H_2SO_4 in the range of −0.35 to 1.5 V at a scan rate of 0.1 V s^{-1} for 20 scans. A final round of electrochemical scans was performed in 0.1 M H_2SO_4 containing 0.01 M KCl with four different potential ranges: (1) 0.2−0.75 V; (2) 0.2−1.0 V; (3) 0.2−1.25 V; and (4) 0.2−1.5 V [24]. All cleaning process for microfabricated electrode was conducted on PDMS well.

Before immobilization process, the aptamer was incubated with TCEP solution followed by dilution with PBS to a final concentration of 1 μM. The 50 μL of this solution was transferred to the working electrode and incubated for 60 min. The electrode was then

thoroughly rinsed with PBS and further passivated with 50 µL of 2 mM MCH in PBS for 60 min to back-fill the uncovered gold surface. Methylene blue solution (50 µL) at 200 µM containing 20 mM KCl was dropped onto the electrode. The PBS buffer was thoroughly flowed over the modified electrode to remove any excess modifiers. Both electrodes were treated with the same manner, except for the incubation of conventional electrode in 2 mL conical tube, while integrated microelectrode using a PDMS well (Figure 3-1).

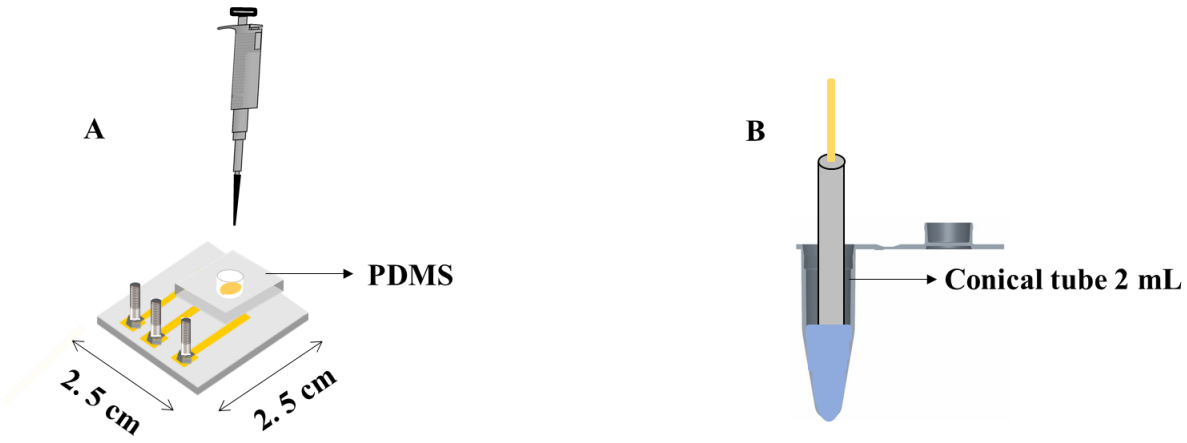

Figure 3-1. Incubation technique for microfabricated electrode (A) and conventional electrode (B). Indicated the volume of solutions.

3.2.3 Electrochemical Measurements

All electrochemical experiments were performed with an ALS 1232a electrochemical analyzer (BAS Inc., Japan). The conventional electrode system composed of a gold electrode (d = 2 mm), an Ag/AgCl electrode, and a platinum wire as working, reference, and counter electrode, respectively. The working electrode was built in a PEEK rod (69 mm × 6 mm). The microfabricated electrode system consisted of three gold thin film electrodes (Figure 3-2). The working electrode had a diameter d = 5 mm and the surface of the reference electrode was modified with Ag/AgCl paste. Notably, the electrochemical signal was obtained from electron transfer of MB that intercalated on aptamer. In addition, the distance of MB to the

electrode surface influence the current strength measured by differential pulse voltammetry (DPV). The DPV measurement was taken: the potential range was from -0.7 to 0 V vs Ag/AgCl, modulation amplitude was 0.04 V, a pulse width was 0.06 s, and sample width was 0.02 s.

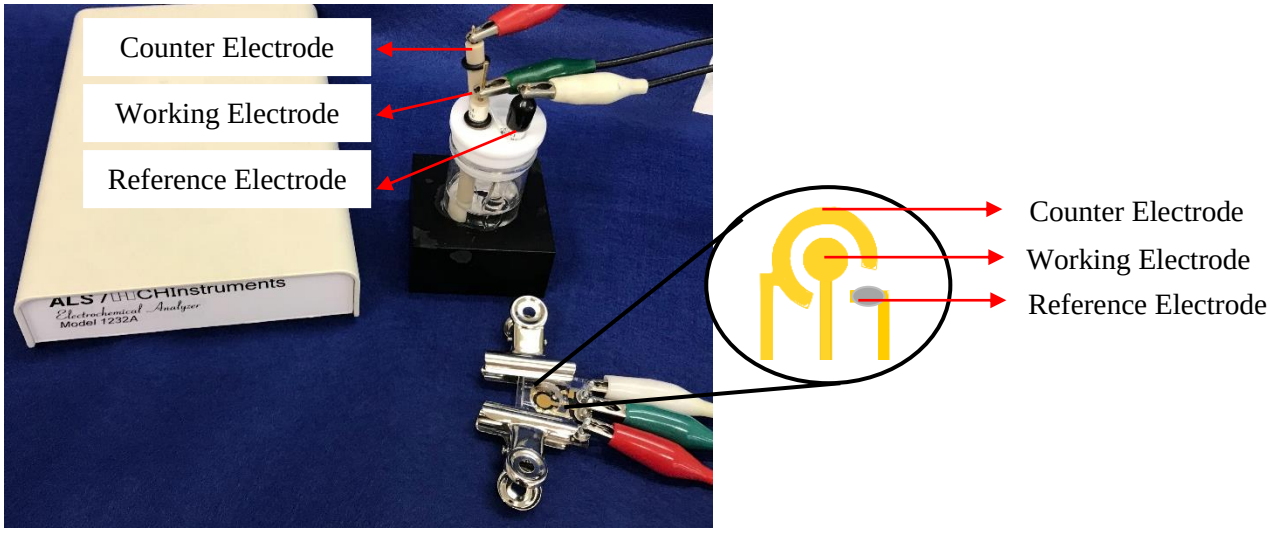

Figure 3-2. The electrochemical system used in this study contains an ALS 1232a electrochemical analyzer, conventional electrodes, and the microfabricated electrodes.

3.3 Result and Discussion

3.3.1 Principle of the Sensor

In the present study, the whole analytical process takes advantage of a high affinity of the aptamer with OTA and a structure switching of the aptamer that its complex formation triggered. There have been several reports on the detection of OTA with structure switching of aptamers [13, 25], which were based on the target-induced dissociation (TID) that produces a decreased signal after binding with OTA. The TID-based sensor promises a very sensitive detection, however, the decreased signal due to aptamer binding with the target or other external factors such as contaminant, poor of sensing layer electrode were

indistinguishable. Consequently, a false negative result may determine as OTA concentration and the measurement become unreliable. The drawback of this method can be eliminated by change the principle detection from signal-off to signal-on detection. In the signal-on, the target binding changes the conformation of the aptamer and alters the electron transfer efficiency between MB and the electrode surface that increasing the signal currents. This method follows a Langmuir binding isotherm as illustrated in figure 3-3. The process of building a sensing layer on the electrode surface was simple, we only used one aptamer strand without a covalently labeled redox probe as previously reported [25, 26]. Instead, the MB was incubated on the aptamer-modified electrode. The π-π interaction between MB molecules and guanine bases of aptamer has established a redox probe on the sensor [19, 27, 28]. In step C, the MB molecules and electrode surface are situated in stable proximity and allowed electron transfer that obtained as low peak current by electrochemical, also this condition called as background signal current. Introduction of target OTA to the sensor could induce structural switching of aptamer caused by target binding to form G-quadruplex conformation [29]. Furthermore, the distance of MB to the electrode surface will be closer and generating a higher peak current than the background (step D). The high current obtained can be attributed to the enhancement of electron transfer efficiency from MB to the electrode surface as a result of complex aptamer-OTA. Therefore, OTA concentration can be accurately quantified by the measurement of the peak current. Notably, the formation of complex aptamer-OTA structure that increases the peak current will guarantee a reproducible result.

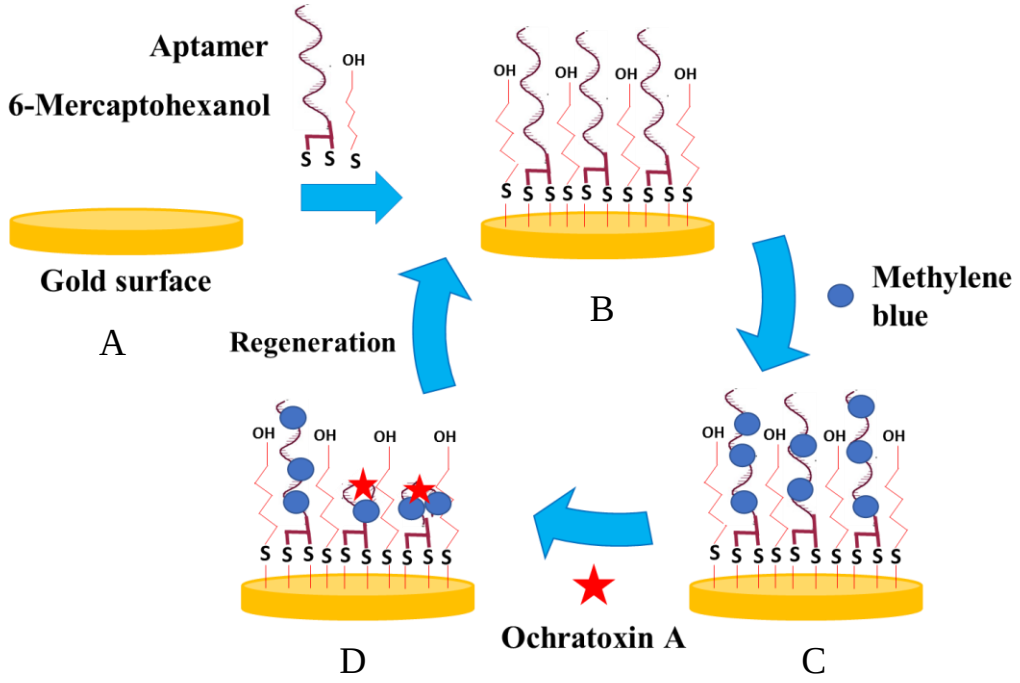

Figure 3-3. Schematic illustration of the modified electrode based on structure switching signal-on aptasensor and sensor regeneration.

3.3.2 Aptamer Immobilization

The self-assembly of alkanethiols onto a gold surface is occurred by chemisorption, and we previously reported immobilization of an aptamer with a monothiol-based linker having a sequence that hybridized with an aptamer [24]. The bond energy between thiol-gold interaction is 30 – 45 kcal/mol, which is relatively weak, compared with covalent bonds (100 – 150 kcal/mol) [21]. Liepold *et al* reported that the gold surface functionalized via thiol anchoring was subjected to "stress condition" by adding other thiol-containing compounds, which may displace the original thiol [21]. For example, after adding the filling agent such as 6-mercaptohexanol (MCH), the signal typically decreases or was even lost because MCH displace the aptamer on the gold surface. Frequently this displacement was happened on mono-thiol anchored aptamer which has similar binding energy to MCH.

Since the mechanism of the proposed sensor relies on the electron transfer efficiency between MB on the aptamer and the gold surface of the electrode, the stable anchoring of thiol is essential to obtain reproducible results. To demonstrate our approach, we used DTPA modification with two thiol groups per unit aptamer to make a stable anchoring along the gold surface (Figure 3-4).

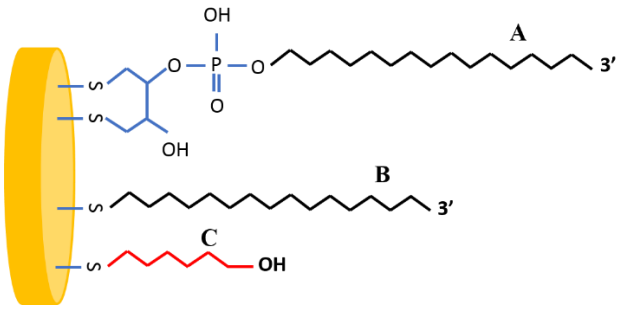

Figure 3-4. Modification of the gold surface with (A) dithiol based-aptamer, (B) monothiol based-aptamer, and (C) 6-mercaptohexanol.

To investigate the effect of the MCH on the dithiol modified aptamer, two electrodes were used which modified with and without MCH. Figure 3-5 shows the signal currents of both electrodes were increased. When the aptamer was displaced with MCH, the signal supposed to lose because the MB could not bind to MCH. Moreover, the potential of an electrode that modified without MCH shift to -0.35 V and any signal was detected on potential -0.69 V due to any unspecific absorption on the electrode surface.

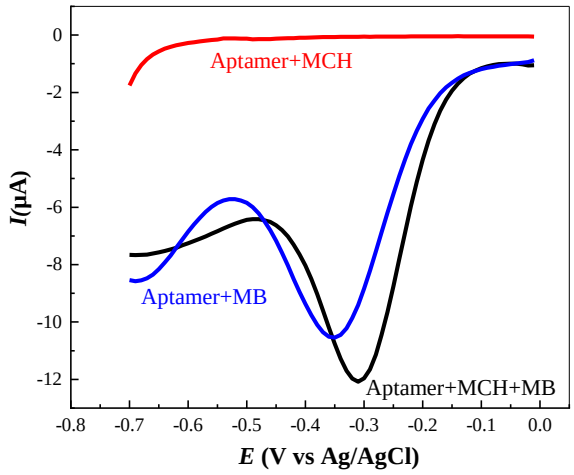

Figure 3-5. The effect of MCH to the dithiol modified aptamer on the electrode surface

In addition, we tried to confirm the stability of modified aptamer in the above experiment with different six electrodes. As shown in figure 3-6, the current signals of the sensor after immobilization with aptamer and MCH followed incubation with MB was increased. This result confirmed that dithiol modification attached strongly in the gold surface and has no effect in the presence of MCH.

We also examined a variety of the aptamer immobilization process with and without reduction by TCEP solution. The entire protocol had the same steps except for incubation of the aptamer with TCEP, then the results were compared. In figure 3-7, both aptamers were successfully immobilized on the gold surface with evidence of exhibit a current signal. Although the potential shifted for the aptamer without TCEP incubation, the peak current intensity was almost similar around 10 μA. This result indicating that the bond between DTPA and gold surface has a probability to formed spontaneously. A future investigation was needed with topography instrument to confirm the bonding between DTPA molecules on the gold surface.

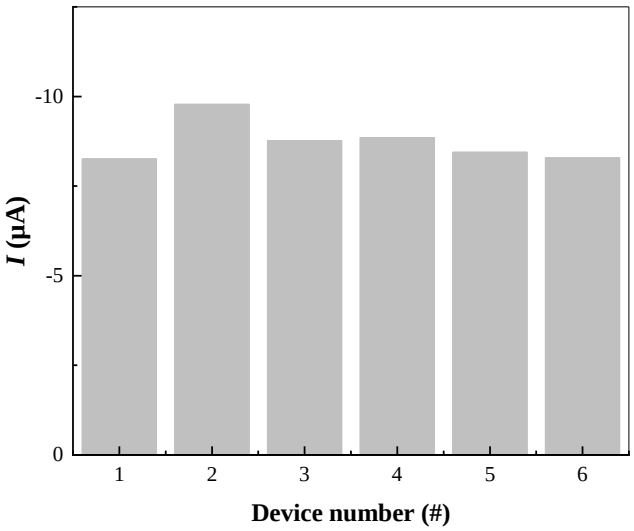

Figure 3-6. The currents after incubating with MB on six sensors separately fabricated. All electrodes have same tendency after incubation with MB.

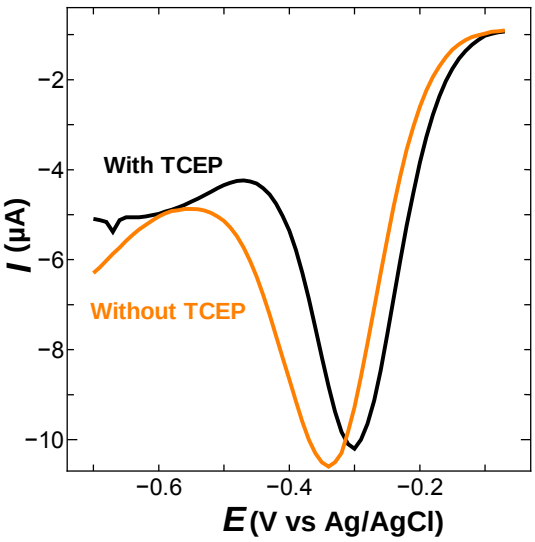

Figure 3-7. Comparison of the current responses obtained with sensors immobilized with aptamers with and without TCEP treatment.

3.3.3 Characterization of Electrochemical Aptasensor

To characterize the affinity of the dithio-modified aptamer with OTA, we determined the dissociation constant of the aptamer-OTA complex. We made assumption that there is negligible intermolecular interaction of aptamers, having equal binding energy, and uniform

binding sites between them on the surface of gold electrode. The equilibrium and disocciation constant can be written as follows:

$$A + T \rightleftharpoons C \qquad (1)$$

$$K_d = \frac{[A][T]}{[C]} \qquad (2)$$

where [A], [T], [C], and K_d are the free aptamer concentration on the electrode surface, the free OTA concentration in solution, the concentration of aptamer-target complex at the electrode, and the dissociation constant, respectively. Equation 3 can be derived from Equation 2 as follows [Ref 23]:

$$\frac{[C]}{[A]_T} = \frac{-\sqrt{[T]_T{}^2+(2Kd-2[A]_T)[T]_T+Kd^2+2[A]_T\,Kd+[A]_T^2}+[T]_T+Kd+[A]_T}{2[A]_T} \qquad (3)$$

where $[A]_T$ and $[T]_T$ are the total concentrations of aptamer and OTA.

The fraction of the complex concentration on the surface [C] to total aptamer concentration $[A]_T$ ($[C]/[A]_T$) can be obtained as the function of the peak current as the $(I_0 - I_t)/(Imax - Imin)$.

The Kd value was determined by fitting the experimental data to Equation 3 using the nonlinear regretion method and *OriginPro* 2019 software (Massachusetts, USA) (Figure 3-8). The dissociation constant (Kd) was 12.6 nM, which was close to the values previously published for electrochemical aptasensor for OTA (9 nM) [23].

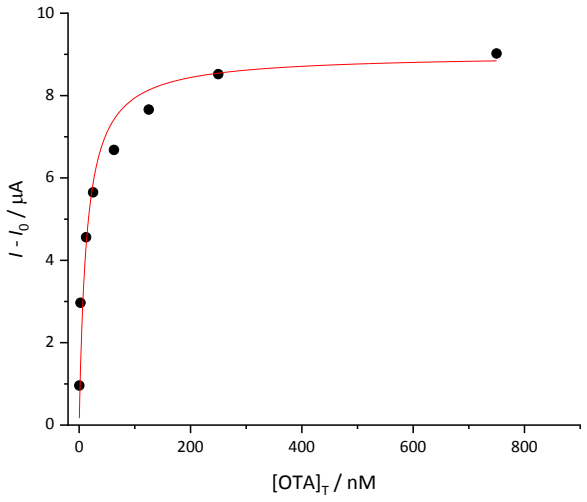

Figure 3-8. Plot of ratio complex concentration and total aptamer as a function of OTA concentration to the determination of the dissociation constant (Kd) on the microfabricated electrode.

The modification of the electrode was electrochemically monitored in a stepwise manner with DPV in PBS containing 1 mM $MgCl_2$. As shown in figure 3-9, a bare electrode exhibited peak currents (curve a), which were probably due to the reduction of oxidized surface because the electrode surface was cleaned at high potentials. Next, immobilizing the aptamer and MCH provided no peak current (curve b), indicating that the electrode surface was fully covered with those compounds. Afterwards, the electrode was incubated in an MB solution for 10 min and washed with PBS buffer. The modified electrode exhibited a peak current at a potential -0.3 V vs Ag/AgCl (curve c). This peak current was attributed to the remaining MB molecules intercalated with the aptamer immobilized on the electrode surface. The MB molecules specifically bind only with guanine bases through electrostatic interaction. The similar results were revealed in previous research [19, 20, 28, 31].

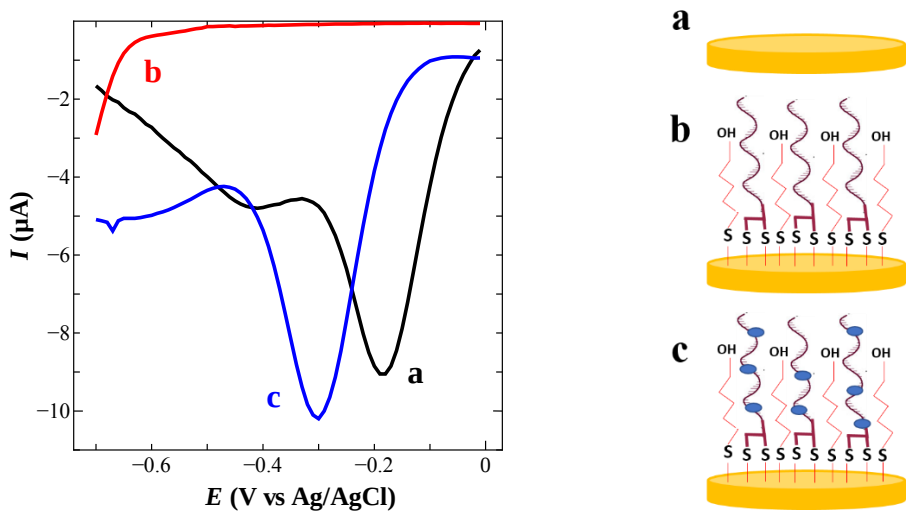

Figure 3-9. The current responses obtained before and after electrode modification: a) bare electrode; b) aptamer-and MCH modified electrode; c) MB-modified electrode. These responses were obtained in PBS containing 1 mM $MgCl_2$.

We examined the electrode-modification scheme with the dithiol-modified aptamer in different electrode systems including conventional and microfabricated electrodes. The current responses were measured by DPV in response to different concentrations of OTA. In the electrode system consisted of conventional electrode, a peak current was observed at a potential of -0.34 V vs Ag/AgCl with a current of -9.18 µA in the absence of OTA, as shown in figure 3-10A. Increasing the concentration of OTA from 0.25 to 125 nM increased the peak current. Figure 3-10C displays a linear relationship between the peak current and the logarithm of the concentration in the OTA concentration range of 0.25 to 125 nM with the coefficient of correlation of 0.976 (Figure 3-10C). The current reached a plateau at the OTA concentration above 125 nM, which indicated that the aptamer was saturated with OTA. The limit of detection was 81 pM (32 pg mL^{-1}), at which the signal current equaled to the background signal plus 3 standard deviations of the background. Meanwhile, the microfabricated electrode exhibited a wider detection range of 0.25 – 750 nM with the coefficient of correlation of 0.990 (Figure 3-10B) because the diameter of the microfabricated

working electrode was 3 mm greater than that of the conventional one. The limit of detection was 113 pM (45 pg mL^{-1}) in the microfabricated system. Although the proposed microfabricated system offered a higher limit of detection than those systems presented in previous works [13, 15, 25], it satisfies the required minimum amount of OTA considered safe for human consumption (2−10 ng mL^{-1}) without signal amplification. Furthermore, this versatile modification strategy can be applied to any type of platforms, such as screen-printing gold electrode and carbon nanotubes with gold nanoparticles for aptamer-based sensors that require stable anchoring of aptamer.

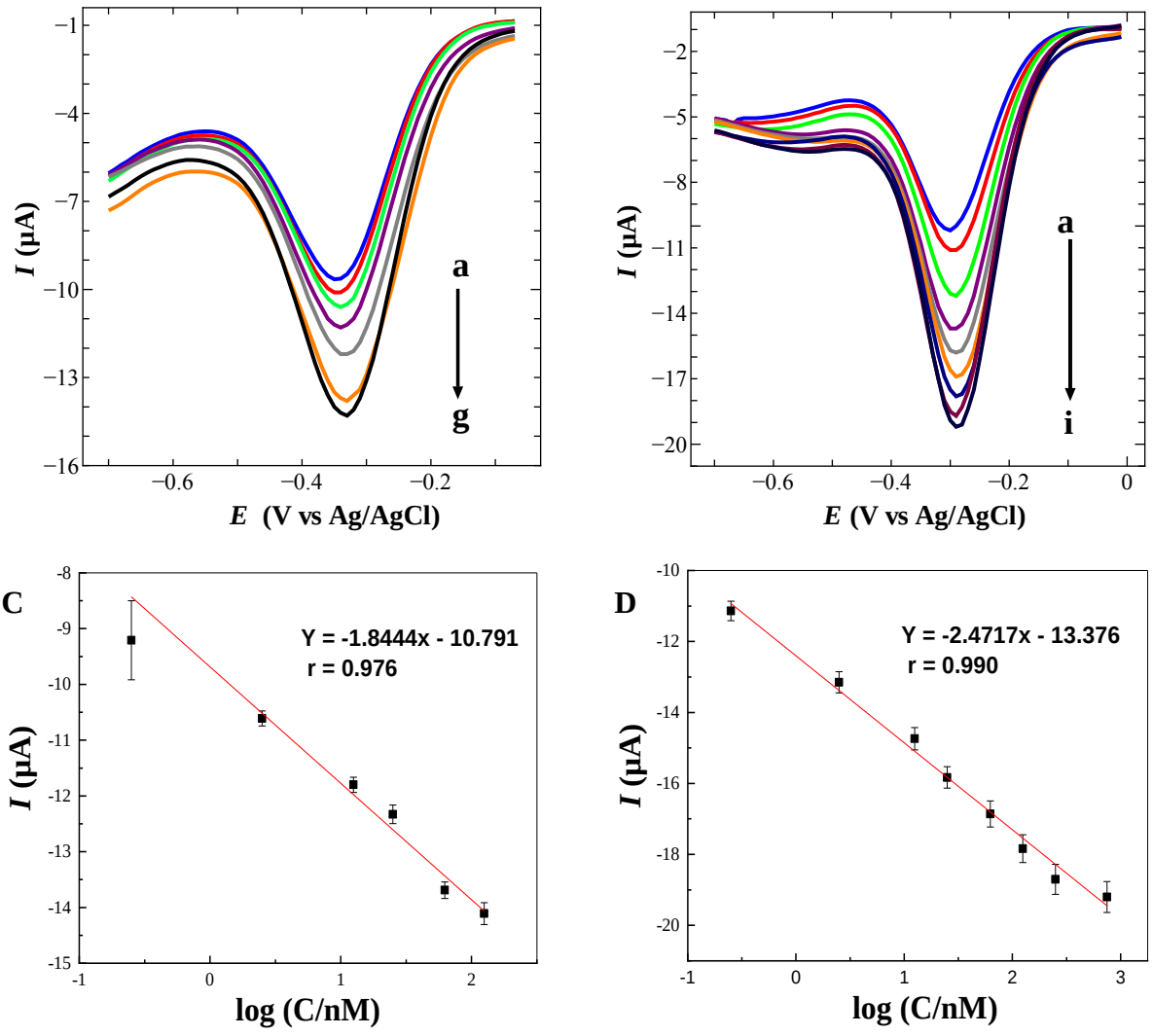

Figure 3-10. DPV signal currents in response to various OTA concentrations for (A) conventional electrode and (B) microfabricated electrode. The OTA concentrations (nM): (A) (a) 0, (b) 0.25, (c) 2.5, (d) 12.5, (e) 25, (f) 62.5, (g) 125; (B) (a) 0, (b) 0.25, (c) 2.5, (d) 12.5, (e) 25, (f) 62.5, (g) 125, (h) 250, (i) 750. Logarithmic dependences of current responses upon OTA concentration for the conventional electrode (C) and microfabricated electrode (D). All data points are presented as the mean ± standard deviation (n = 3).

3.3.4 Selectivity Test with Mycotoxins

Since many fungi can produce more than one mycotoxin under similar environmental conditions, sensors are required to have specificity to the target mycotoxin to avoid false-positive result. Aflatoxin B1 (AFB1) and deoxynivalenol (DON) are the most common toxins that coexist with OTA and the structure of toxins are depicted in figure 3-11. They have similar molecular weight and functional groups, such as phenyl, hydroxyl, and methyl groups. To evaluate the specificity of the proposed sensor, the DPV curves were measured at a potential of -0.3 V vs Ag/AgCl in several experimental runs. For this purpose, the proposed sensor was exposed to separately prepared solutions and the mixture of the mycotoxin. As shown in figure 3-12, a less significant increase in the current was observed for each AFB1 and DON solution, while the current greatly increased in an OTA solution. The specific binding of the aptasensor to OTA was further tested with a mixture of AFB1, DON, and OTA at each concentration of 250 nM. Similar current signal was observed in the mixture, compared with the signal obtained in the former experiment. These results indicate that the proposed sensor had a high specificity to OTA against other mycotoxins.

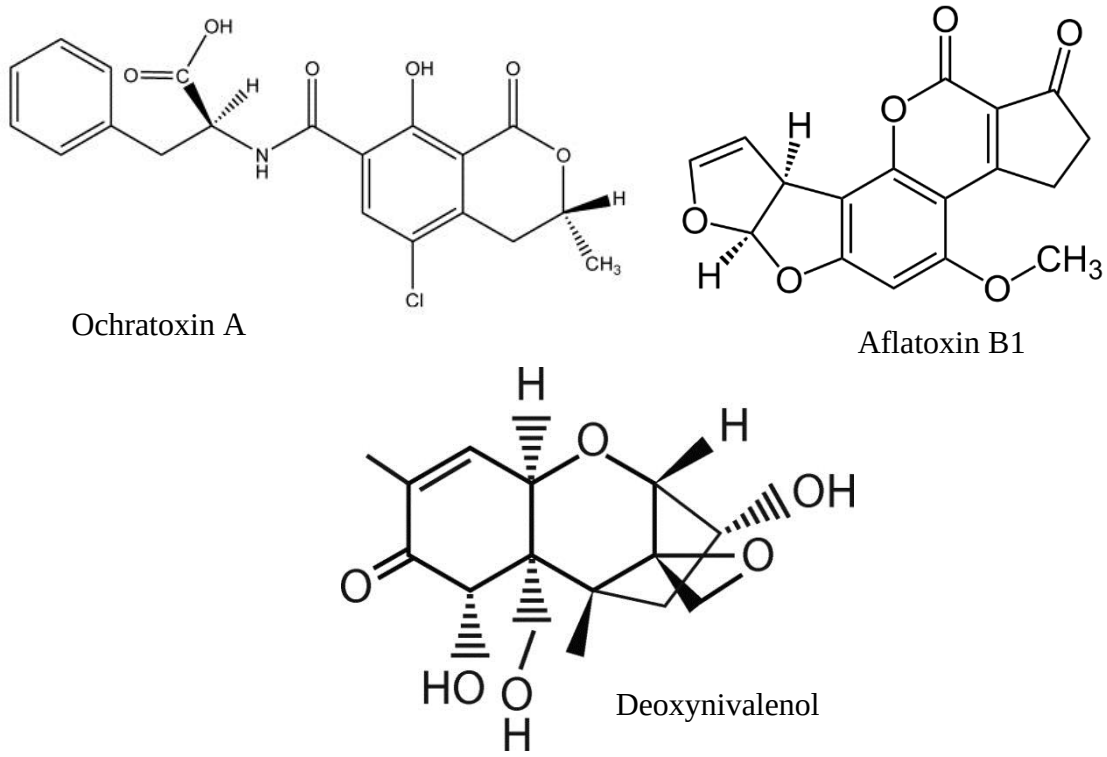

Figure 3-11. Chemical structure of OTA, AFB1 and DON

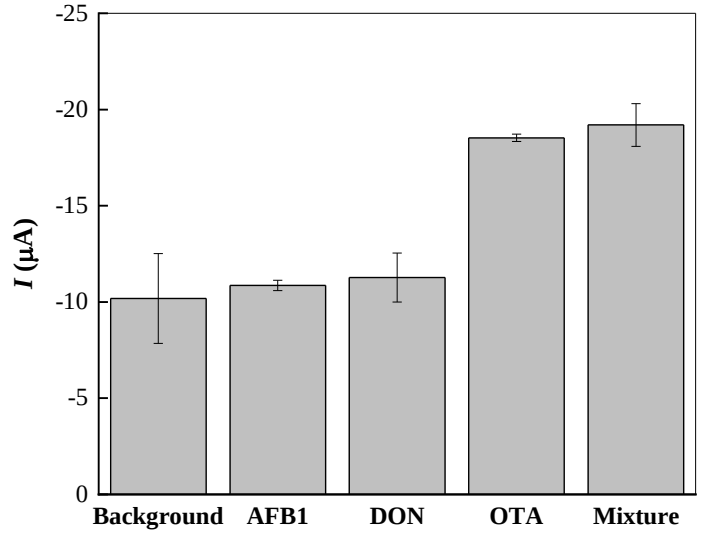

Figure 3-12. Selectivity of the proposed sensor toward OTA. The concentrations of AFB1, DON, and OTA were 250 nM in this experiment and the background corresponding to the signal current without mycotoxin. The mixture contains AFB1, DON, and OTA. All bars are presented as the mean ± standard deviation (*n* = 3).

3.3.5 Regeneration of Sensing Layer

Reusability of the sensor was another advantage of the electrochemical aptasensor. In this work, the proposed sensor was regenerated under Experimental section. Briefly, the sensor was incubated with 50 mM NaOH, which was an efficient denaturant reagent for aptamer [34] and disturbs the interaction between aptamer and OTA by shifting the pH. Denaturation promoted OTA release without influence the affinity of the surface-bound aptamer. Furthermore, the aptamer was renatured with PBS buffer and incubated again with an MB solution (see Figure 3-3). Figure 3-13 shows the currents measured without and with 250 nM OTA after regeneration of the sensor. Repeating six regenerations offered a constant current with the coefficient of variation of 3.7%, indicating that the aptamer still retains on the surface of the electrode after at least five regenerations. This suggested a high stability of the dithiol-modified aptamer immobilized on the electrode surface. However, when the sensor was regenerated for more than five times, the counter electrode was damaged as shown in Figure 3-14, and the current considerably decreased as shown in Table 3-1. It is still a challenge for microfabricated thin film and opportunity for improvement in the future.

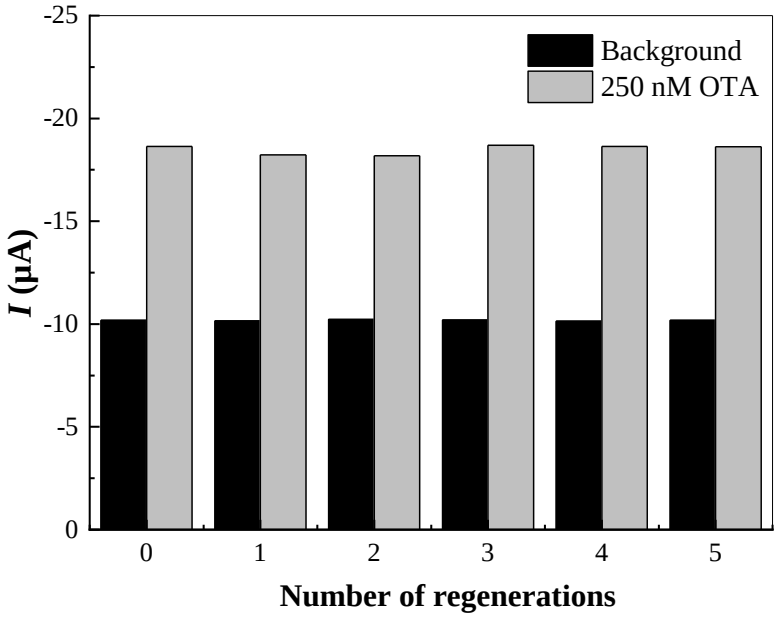

Figure 3-13. Regeneration of microfabricated electrochemical aptasensor under stepwise incubation with MB and 250 nM OTA. The black bars represent the background currents recorded in the absence of OTA after the regeneration, while the gray bars represent the currents recorded in the presence of OTA with the regenerated sensor.

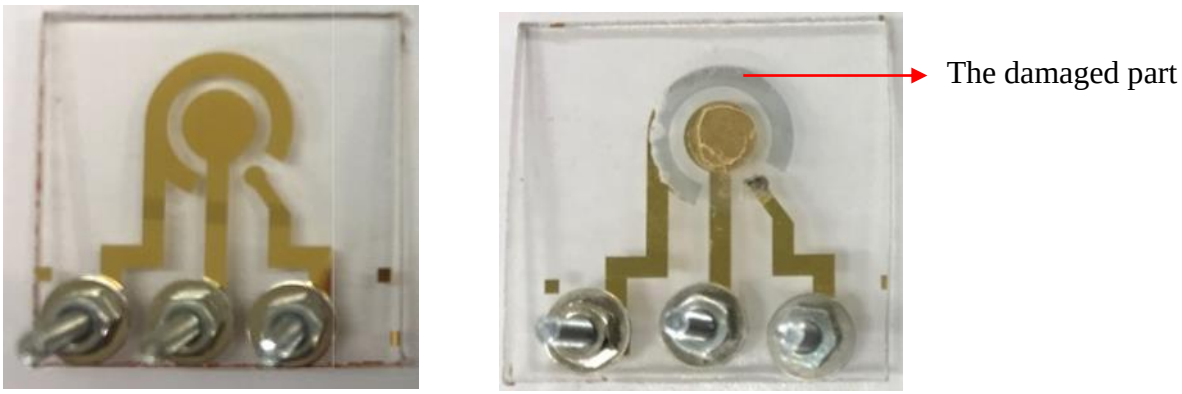

Figure 3-14. The microfabricated electrode that used in this experiment. (A) The new electrode, (B) After six times regeneration.

Table 3-1. Regeneration of microfabricated electrode

Cycle number (#)	Current values (µA)	
	Without OTA	With OTA
1	-10.18	-18.66
2	-10.15	-18.62
3	-10.23	-18.69
4	-10.20	-18.71
5	-10.16	-18.64
6	-10.14	-18.62
7	-4.16	-0.31
8	-0.08	-0.02
% SD (1 - 6 #)		3.72

We have regenerated the microfabricated electrode several times. However, after regeneration six times, the current value significantly decreased and the detection of OTA not sensitive as before. After carefully investigated this problem, we found the reason why the electrode was damage is that the gold layer reacts with chlorine that contained in PBS buffer. The gold form trihalides gold (III) chloride and dissolve in the PBS buffer as follow:

$$2\ Au + 3\ Cl_2 \longrightarrow 2\ AuCl_3$$

This reaction was happened only in the counter electrode (CE) because of electrode surface was not covered with aptamer (only working electrode covered by aptamer).

3.3.6 Performance of Proposed Sensor Comparing with Other Electrochemical Aptasensors

Although the proposed microfabricated system offered a higher limit of detection than those systems presented in previous works [13, 15, 25], it satisfies the required minimum amount of OTA considered safe for human consumption (2−10 ng mL^{-1}) without signal amplification. Furthermore, this versatile modification strategy can be applied to any type of platforms, such as screen-printing electrode, microbeads, and carbon nanotubes, for aptamer-based sensors that require stable anchoring of aptamer.

According to the previous reports, most of the electrochemical aptasensor has a focused on lower detection limits and wider linear range of detection, only a few papers discussed the stability of the sensing layer. It is noteworthy that the stability of immobilized aptamer in the electrode is very important to make reproducible and avoid a bias result. Although the sensitivity of the proposed sensor was not significantly higher than those of other sensors (Table 3-2), the proposed sensor demonstrated advantages of the simple fabrication and good reproducibility with DTPA modified aptamer in microfabricated system.

Table 3-2. Performance comparisons of electrochemical aptasensor for OTA detection

Platform	Detection limit (pg mL^{-1})	Linear range (ng mL^{-1})	Reproducibility CV%	Label / probe	Signal amplifier	Ref
SPCE modified with thionine	5.6	0.004 – 40	N/A	Label-free / Impedance	IrO_2NPs	10
Conventional electrode	0.005	5×10^{-6} - 5×10^{-4}	N/A	Label-free / MB	AuNPs	13
Conventional electrode	1	0.005 – 10	N/A	Covalently labeled ferrocene	Exonuclease	15
Conventional electrode	21	N/A	N/A	Covalently labeled MB	SWCNTs	16
Fe_3O_4 Au Magnetic beads	5.4	0.015 -100	5.3	Covalently labeled fluorescence	HFNPs Quantum Dots	17
Microfabricated electrode	45	0.1 – 300	5.9	Label-free / MB	Not used	This work

SPCE = Screen printed carbon electrode
IrO_2NPs = Iridium oxide nanoparticles
SWCNTs = Single-walled carbon nanotubes
HFNPs = Hybrid fluorescent nanoparticles
N/A = Not available. The data were not provided in the paper.

3.4 Conclusion

Herein the signal-on microfabricated electrochemical sensor based on dithiol-modified aptamer for the detection of OTA has been developed. We perform the modified aptamer not only on the proposed sensor but also in the conventional electrode that frequently used on electrochemical aptasensor. The conventional and microfabricated electrode was treated with the same modification, entailing non-covalent interaction between MB and aptamer bearing a dithiol modification for attachment to the gold surface. We have used MB attached to the aptamer and generate a stable redox signal without specific signal enhancer in both electrodes. In addition, we proposed the use of the end-site modification of aptamer with dithiol as anchor site, which provided good stability and reproducibility of the sensing layer after adding the backfilling agent. Both electrodes were shown a quantitative response to various OTA concentrations as proven by fitting well to the linear curve. The proposed sensor also provided good selectivity and reusability. Moreover, this characteristic offered a

potential tool for simple and portable on-site detection for the universal platform by changing the corresponding aptamer. Future research will be directed to the extension of the stability of immobilized aptamer by modifying the anchoring group with triple DTPA then integrating into a microfluidic device.

References

[1] S.M. Taghdisi, N.M. Danesh, P. Lavaee, M. Ramezani, K. Abnous, An electrochemical aptasensor based on gold nanoparticles, thionine and hairpin structure of complementary strand of aptamer for ultrasensitive detection of lead, *Sensors Actuators, B Chem*. 2016, 234, 462–469. doi:10.1016/j.snb.2016.05.017.

[2] N.Y. Jayanath, L.T. Nguyen, T.T. Vu, L.D. Tran, Development of a portable electrochemical loop mediated isothermal amplification (LAMP) device for detection of hepatitis B virus, *RSC Adv*. 2018, 8, 34954–34959. doi:10.1039/c8ra07235c.

[3] A. Ishida, M. Fujii, T. Fujimoto, S. Sasaki, I. Yanagisawa, H. Tani, M. Tokeshi, A Portable Liquid Chromatograph with a Battery-operated Compact Electroosmotic Pump and a Microfluidic Chip Device with a Reversed Phase Packed Column, *Anal. Sci*. 2015, 31, 1163–1169. doi:10.2116/analsci.31.1163.

[4] M. Akbar, M. Restaino, M. Agah, Chip-scale gas chromatography: From injection through detection, *Microsystems Nanoeng*. 2015, 1, 15039. doi:10.1038/micronano.2015.39.

[5] R. McKendrick, R. Parasuraman, H. Ayaz, Wearable functional near infrared spectroscopy (fNIRS) and transcranial direct current stimulation (tDCS): expanding vistas for neurocognitive augmentation, *Front. Syst. Neurosci*. 2015, 9, 1–14. doi:10.3389/fnsys.2015.00027.

[6] G. Koukouvinos, P.S. Petrou, K. Misiakos, D. Drygiannakis, I. Raptis, D. Goustouridis, S.E. Kakabakos, A label-free flow-through immunosensor for determination of total- and free-PSA in human serum samples based on white-light reflectance spectroscopy, *Sensors Actuators, B Chem*. 2015, 209, 1041–1048. doi:10.1016/j.snb.2014.11.104.

[7] D. Hao, C. Hu, J. Grant, A. Glidle, D.R.S. Cumming, Hybrid localized surface plasmon resonance and quartz crystal microbalance sensor for label free biosensing, *Biosens. Bioelectron*. 2018, 100, 23–27. doi:10.1016/j.bios.2017.08.038.

[8] Zhou, L., Lu, P., Zhu, M., Li, B., Yang, P., Cai, J. Silver nanocluster-based sensitivity amplification of a quartz crystal microbalance gene sensor. *Microchim Acta*. 2016, 183, 881-887. doi:10.1007/s00604-015-1728-9

[9] D.N. Mazaafrianto, M. Maeki, A. Ishida, H. Tani, Recent Microdevice-based Aptamer Sensors, *Micromachines*. 2018, 9. doi:10.3390/mi9050202.

[10] L. Rivas, C.C. Mayorga-Martinez, D. Quesada-González, A. Zamora-Gálvez, A. De La Escosura-Muñiz, A. Merkoçi, Label-free impedimetric aptasensor for ochratoxin-A detection using iridium oxide nanoparticles, *Anal. Chem*. 2015, 87, 5167–5172. doi:10.1021/acs.analchem.5b00890.

[11] S.D. Jayasena, Aptamers: An emerging class of molecules that rival antibodies in diagnostics, *Clin. Chem*. 1999, 45, 1628–1650. doi:10.1038/mtna.2014.74.

[12] D. Irvine, C. Tuerk, L. Gold, Selexion. Systematic evolution of ligands by exponential enrichment with integrated optimization by non-linear analysis, *J. Mol. Biol*. 1991, 222, 739–761. doi:10.1016/0022-2836(91)90509-5.

[13] M. Wei, S. Feng, A signal-off aptasensor for the determination of Ochratoxin A by differential pulse voltammetry at modified Au electrode using methylene blue as electrochemical probe, *Anal. Methods*. 2017. doi:10.1039/C7AY01735A.

[14] J. Zhang, Y.K. Xia, M. Chen, D.Z. Wu, S.X. Cai, M.M. Liu, W.H. He, J.H. Chen, A fluorescent aptasensor based on DNA-scaffolded silver nanoclusters coupling with Zn(II)-ion signal-enhancement for simultaneous detection of OTA and AFB1, *Sensors Actuators, B Chem*. 2016, 235, 79–85. doi:10.1016/j.snb.2016.05.061.

[15] P. Tong, L. Zhang, J.J. Xu, H.Y. Chen, Simply amplified electrochemical aptasensor of Ochratoxin A based on exonuclease-catalyzed target recycling, *Biosens. Bioelectron.* 2011, 29, 97–101. doi:10.1016/j.bios.2011.07.075.

[16] Abnous, K., Danesh, N.M., Alibolandi, M. et al. Amperometric aptasensor for ochratoxin A based on the use of a gold electrode modified with aptamer, complementary DNA, SWCNTs and the redox marker Methylene Blue. *Microchim Acta*. 2017, 184, 1151-1159. doi:10.1007/s00604-017-2113-7.

[17] C. Wang, J. Qian, K. Wang, K. Wang, Q. Liu, X. Dong, C. Wang, X. Huang, Magnetic-fluorescent-targeting multifunctional aptasensorfor highly sensitive and one-step rapid detection of ochratoxin A, *Biosens. Bioelectron*. 2015, 68, 783–790. doi:10.1016/j.bios.2015.02.008.

[18] E. Gonzalez-Fernandez, N. Avlonitis, A.F. Murray, A.R. Mount, M. Bradley, Methylene blue not ferrocene: Optimal reporters for electrochemical detection of protease activity, *Biosens. Bioelectron.* 2015, 84, 82–88. doi:10.1016/j.bios.2015.11.088.

[19] W. Yang, M. Ozsoz, D.B. Hibbert, J.J. Gooding, Evidence for the direct interaction between methylene blue and guanine bases using DNA-modified carbon paste electrodes, *Electroanalysis*. 2002, 14, 1299–1302.

[20] Pheeney, C. G.; Barton, J. K. DNA Electrochemistry with Tethered Methylene Blue. *Langmuir*. 2012, 28, 7063–7070. doi:10.1021/la300566x.

[21] P. Liepold, T. Kratzmüller, N. Persike, M. Bandilla, M. Hinz, H. Wieder, H. Hillebrandt, E. Ferrer, G. Hartwich, Electrically detected displacement assay (EDDA): A practical approach to nucleic acid testing in clinical or medical diagnosis, *Anal. Bioanal. Chem*. 2008, 391, 1759–1772. doi:10.1007/s00216-008-2045-5.

[22] N. Garg, A. Mohanty, N. Lazarus, L. Schultz, T.R. Rozzi, S. Santhanam, L. Weiss, J.L. Snyder, G.K. Fedder, R. Jin, Robust gold nanoparticles stabilized by trithiol for application in chemiresistive sensors, *Nanotechnology*. 2010, 21. doi:10.1088/0957-4484/21/40/405501.

[23] J.A. Cruz-Aguado, G. Penner, Determination of ochratoxin A with a DNA aptamer, *J. Agric. Food Chem*. 2008, 56, 10456–10461. doi:10.1021/jf801957h.

[24] D.N. Mazaafrianto, A. Ishida, M. Maeki, H. Tani, M. Tokeshi, Label-Free Electrochemical Sensor for Ochratoxin A Using a Microfabricated Electrode with Immobilized Aptamer, *ACS Omega*. 2018, 3, 16823–16830. doi:10.1021/acsomega.8b01996.

[25] J. Chen, Z. Fang, J. Liu, L. Zeng, A simple and rapid biosensor for ochratoxin A based on a structure-switching signaling aptamer, *Food Control*. 2012, 25, 555–560. doi:10.1016/j.foodcont.2011.11.039.

[26] Y. Xiao, R.Y. Lai, K.W. Plaxco, Preparation of electrode-immobilized, redox-modified oligonucleotides for electrochemical DNA and aptamer-based sensing., *Nat. Protoc*. 2007, 2, 2875–80. doi:10.1038/nprot.2007.413.

[27] X. Lin, Y. Ni, S. Kokot, An electrochemical DNA-sensor developed with the use of methylene blue as a redox indicator for the detection of DNA damage induced by endocrine-disrupting compounds, *Anal. Chim. Acta*. 2015, 867, 29–37. doi:10.1016/j.aca.2015.02.050.

[28] E. Papadopoulou, N. Gale, J.F. Thompson, T.A. Fleming, T. Brown, P.N. Bartlett, Specifically horizontally tethered DNA probes on Au surfaces allow labelled and label-free DNA detection using SERS and electrochemically driven melting, *Chem. Sci.* 2015, 7, 386–393. doi:10.1039/c5sc03185k.

[29] K.L. Fadock, R.A. Manderville, DNA Aptamer–Target Binding Motif Revealed Using a Fluorescent Guanine Probe: Implications for Food Toxin Detection, *ACS Omega*. 2017, 2, 4955–4963. doi:10.1021/acsomega.7b00782.

[30] H. Kuang, W. Chen, D. Xu, L. Xu, Y. Zhu, L. Liu, H. Chu, C. Peng, C. Xu, S. Zhu, Fabricated aptamer-based electrochemical "signal-off" sensor of ochratoxin A, *Biosens. Bioelectron*. 2010, 26, 710–716. doi:10.1016/2010.06.058.

[31] E. Doğru, E. Erhan, O.A. Arikan, A Recent Approach for Monitoring Interactions Between Methylene Blue and DNA Using Carbon Fiber Based DNA Biosensor. *Int. J. Electrochem. Sci*. 2016, 11, 829–839. doi:10.20964/2017.12.104.

[32] Zhao, Q., Geng, X. & Wang, H. Anal Bioanal Chem. 405 (2013).6281. https://doi.org/10.1007/s00216-013-7047-2

[33] A. Rhouati, C. Yang, A. Hayat, J.L. Marty, Aptamers: A promosing tool for ochratoxin a detection in food analysis, Toxins (Basel). 5 (2013) 1988–2008. doi:10.3390/toxins5111988.

[34] K. Lee, J. Ahn, S. Lee, S.S. Sekhon, D. Kim, J. Min, Y. Kim, Aptamer-based sandwich assay and its clinical outlooks for detecting lipocalin-2 in hepatocellular carcinoma (HCC), Nat. Publ. Gr. (2015) 1–13. doi:10.1038/srep10897

CHAPTER 4 Competitive Fluorescence Polarization Aptamerassay for Ochratoxin A Detection Using a Miniaturized Analyzer

4.1 Introduction

In the last decade, the trend of sensing platform based on affinity and specific recognition of analyte toward to more convenient instruments. In particular, the combination of micro-design and conventional biosensor technologies has led to the invention of miniaturized platforms with many favorable properties, such as high-throughput analysis, portability, low reagent consumption, and disposability [1, 2]. These miniaturized biosensors have numerous advantages such as minimal handling of hazardous materials, detection of several samples in parallel, and design flexibility [3]. Moreover, development in this area not only in physical instrument, but also detection methodologies of the sensor [4].

The homogenous technique that utilize of affinity and specific biorecognition both antibody and aptamer are fluorescence polarization (FP) or fluorescence anisotropy (FA). This method observed when the fluorescent molecule is excited with plane polarized light, light is emitted in the same polarized plane, provided that the molecule remains stationary throughout the excited state [5]. The polarization (*P*) depending on the measured emission intensities parallel and perpendicular to the plane of the vertically polarized excitation light, can interchangeably be used for determining the polarization degree of a fluorescent rotating species. Moreover, *P* value reflect to the concentration of the target molecules, according to equation:

$$\mathrm{P} = \frac{(I_{\parallel} - I_{\perp})}{(I_{\parallel} + I_{\perp})} \qquad (1)$$

where (I_{II}) and ($I_{\perp}$) are fluorescence intensities between the parallel and perpendicular polarization, respectively. The FP is related to the rate and extent of rotational diffusion and

the lifetime of fluorescent molecules. Fluorescent molecules with higher rates of rotation usually give lower polarization values, while fluorescent molecules with lower rates of rotation give higher polarization values [6].

Application of the FP method to detection of mycotoxin has several advantages. First, simple sample preparation because does not require separation and washing step. The yield of mycotoxin target will be high. Second, the FP assay has low reagent consumption. Third, the biorecognition of this method can be modified with aptamer that more attractive. [7,8,9] In addition, incorporated of the FP method with miniatured instrument and multiplex analysis format will give more benefit in practical application [10].

Analysis of mycotoxin, especially ochratoxin A (OTA) with FP immunoassay (FPIA) has been reported [7,11]. Typically, detection uses a fluorophore-labelled antigen conjugate (tracer) that having low FP values in an unbound state and high values when it is included in the complex with antibodies. The presence of a target/antigen in the sample leads to its competition with the tracer for binding sites of antibodies. This competition reduces FP at increased target concentrations up to the FP value which corresponds to the state of the tracer. Taking advantages of the FP method as described above, development of FP aptamerassay (FPAA) will improving the detection mechanism such as aptamers can be precisely labeled with single fluorophores on specific sites through chemical reactions, which facilitates the generation of fluorescence polarization signals. Besides, the structures of aptamers possible to switch depending on the presence or absence of target binding [12,13]. The principle of FPAA method in this research were described in figure 4-1.

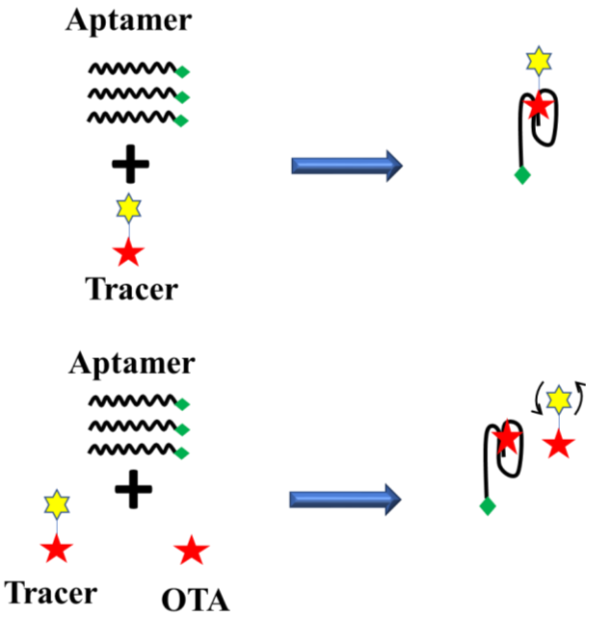

Figure 4-1. Working principle of competitive FPAA method for OTA detection. In the absent of OTA, all the aptamer will bind with tracer resulting high *P* value (above). However, when the target was present, the tracer and OTA competitively bind to the aptamer (below) and the *P* value depends on the OTA concentration.

In spite of the ease of analyzing target, the FPAA method remains challenging for small molecule analysis because the binding of small target only brings a negligible mass change of aptamer. Furthermore, application FPAA in miniaturized FP analyzer is never been reported, then the parameter of FP components should be optimized before measurement. We will compare the performance between conventional and miniaturized FP analyzer for OTA detection.

4.2 Experimental

4.2.1 Reagents and Materials

The anti-OTA aptamer, poly A-T-C-G oligonucleotides used in this experiment were custom-synthesized and purified by Integrated DNA Technologies (IDT; Coralville, USA), OTA-labeled antigen (tracer) was obtained from FPIA kit (Ochratoxin A FPIA kit, Aokin

AG., Berlin, Germany). Ochratoxin A standard solution (10 μgmL^{-1} in acetonitrile, ≥99%), tris (hydroxymethyl)aminomethane, sodium chloride, potassium chloride, and calcium chloride were purchased from Wako Pure Chemical Industries, Ltd, Japan. The aptamer contains 36 bases and designed refer to literature [14] (5'- Biotin-GAT CGG GTG TGG GTG GCG TAA AGG GAG CAT CGG ACA-3').

4.2.2 Instrument

Detection of FP was conducted using conventional and miniaturized FP analyzer that developed in our lab [10,15]. The measurement based on LC-CCD camera that synchronized from measurements of AC and DC values. Then, the fluorescein has a maximum absorption wavelength of 494 nm and maximum emission wavelength of 521 nm. The sample was introduced in microdevice (channel width = 200 μm, depth = 900 μm) that fabricated by standard soft-lithography techniques with PDMS and a glass slide (figure 4-1) [15].

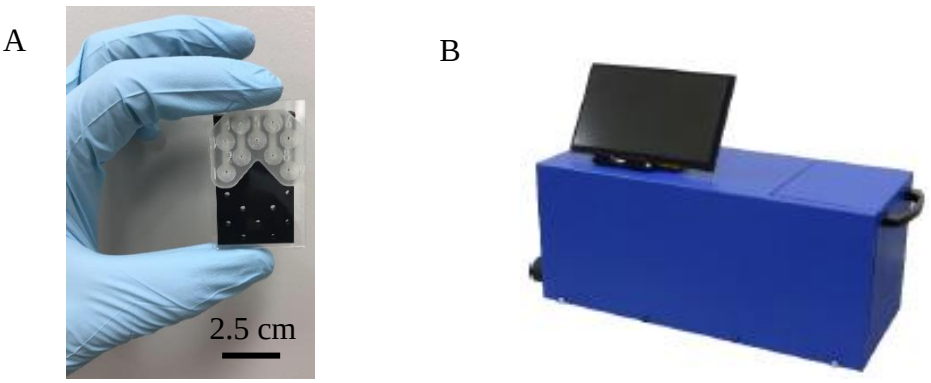

Figure 4-2. (A) Microdevice chip enable to detect up to nine samples simultaneously. (B) Miniaturized fluorescence polarization analyzer

The conventional method for OTA detection was performed using 96-well microplate with the FP microplate reader (TECAN Infinite 200 Pro, Switzerland) (figure 4-3) at emission wavelength 535 nm and absorption wavelength 485 nm.

Figure 4-3. Conventional fluorescence polarization instrument.

4.2.3 Fluorescence Polarization Measurement

The competitive FPAA method were carried out in the microplate and microdevice chip with total volume per well was 150 µL. The target OTA dilutions in tris buffer were prepared in concentration ranging from 0.1 ppb to 1500 ppb. The microplate wells were filled with 120 µL of tris buffer, 10 µL of OTA and 10 µL of tracer, and then 10 µL of aptamer was added in the last step. The mixture was incubated for 15 min at 4ºC, followed by measurement using FP analyzer [7]. For miniaturized FP analyzer, the 20 µL of mixing solution was injected to microdevice chip, then put into the holder. Each analysis has included several controls. First, maximum *P* value which obtained from aptamer-tracer solution in the absence of OTA, this condition revealed that all aptamer bound with tracer. Second, minimum *P* value determined when no aptamer in the mixing solution.

4.2.4 Statistical Analysis

The concentration of OTA was calculated after fitting the standard curve using the four-parameter logistic (4-PL) model using *MedCalc* for Windows, version 15.0 (MedCalc Software, Ostend, Belgium). Sigmoidal fits of FP data were performed using *OriginPro 2019* software (Massachusetts, USA).

The equation for the 4-parameter logistic model is as follows:

$$y = d + \frac{a-d}{1+(\frac{x}{c})^b} \qquad \text{or} \qquad x = c\,(\frac{a-d}{y-d} - 1)^{\frac{1}{b}}$$

where: a = Minimum asymptote, it can be thought of as the response value at 0 standard concentration

b = Hill's slope refers to steepness of the curve

c = Inflection point. it is defined as the point on the curve where the curvature changes direction or signs

d = Maximum asymptote, it can be thought of as the response value for infinite standard concentration.

4.3 Result and Discussion

4.3.1 Optimization of Aptamer Concentration

The reagents component of FP aptamerassay contains of an aptamer, tracer, target (OTA), and tris buffer. The first step was to obtain optimum concentration of aptamer when the tracer is constant. The optimal concentration for aptamer to perform competitive assay with higher FP intensity were selected based on figure 4-4.

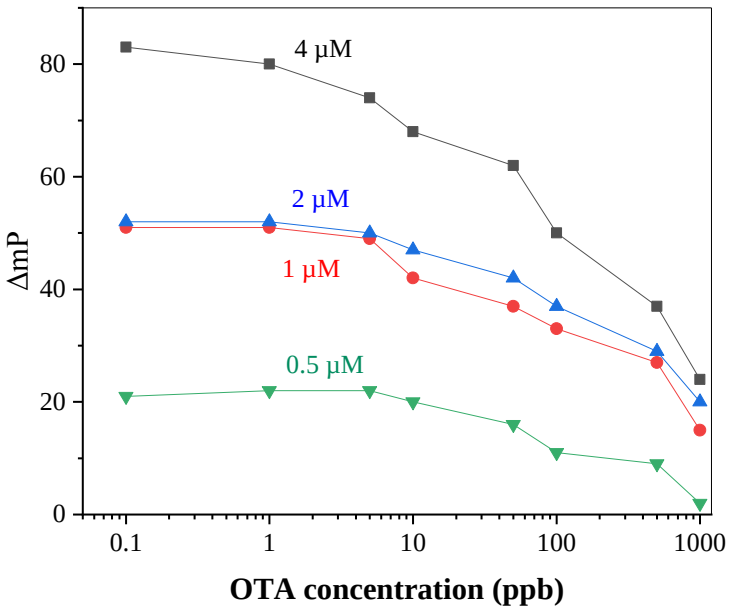

Figure 4-4. FP intensity dependencies of aptamer concentration from 0.5 µM to 4 µM. The higher intensity was reached with aptamer concentration 4 µM.

4.3.2 FPAA Performance

We demonstrated competitive FPAA method for OTA detection by using conventional and miniaturized FP analyzer. Under the optimized binding condition, 4 µM of aptamer, tracer and varying concentrations of OTA were mixed together and FP was measured. When OTA did not exist, the binding of tracer and aptamer led to a high FP intensity. With addition of increasing concentration of OTA, the FP value gradually decreased as the OTA bound to the aptamer. The calibration curve for FPAA to OTA detection between two instruments were described in the figure 4-5.

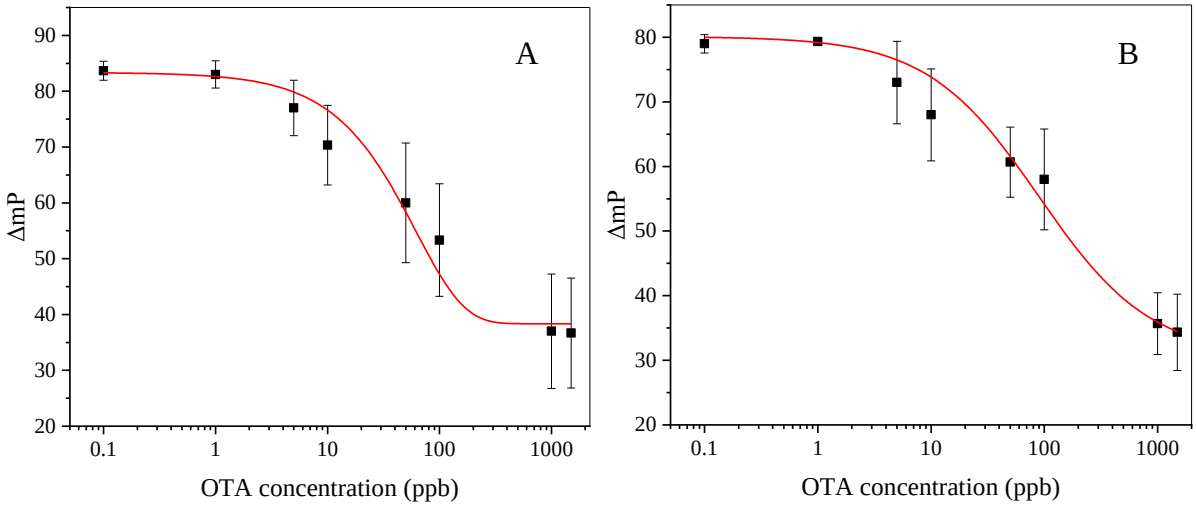

Figure 4-5. Calibration curve of FPAA method against OTA concentration in the range of 0.1 – 1500 ppb obtained from conventional (A) and miniaturized FP analyzer (B). The measurement was performed in triplicates.

According to the above figure, the minimum and maximum *P* value between both instruments are not significantly differed, it was about 35 until 80. The sensitivity of the instrument was determined as the lowest concentration of OTA that could be detect with the system, on other hand we perform three times of blank then measure the signal and standard deviation. The blank was defined as aptamer and tracer in the absence of OTA. The detection

limits based on a signal to noise ratio (S/N = 3), was comprised between 0.9 ppb and 1 ppb for conventional and miniaturized FP analyzer, respectively.

4.3.3 Selectivity of FPAA Method

To evaluate the selectivity of FPAA method in the miniaturized FP analyzer, we used 500 ppb concentration of AFB1 and DON as the non-specific interferences to substitute the OTA. These nonspecific interferences are included the mycotoxin group and analogous molecules of OTA. As shown in figure 4-6 A, the *P* value of the aptamer-tracer complex does not significantly decrease when AFB1 or DON was existed in the mixing solution. This result shows the tracer only competitively bound to the aptamer when OTA was present that indicating the good selectivity of the aptamer toward these mycotoxins.

In order to further investigate whether our FPAA method shows response to other oligonucleotide, we tested the FP response of tracer toward various oligonucleotides poly A-T-C-G without aptamer. As shown in figure 4-6 B, In the presence of poly A-T-C-G, intensity of FP does not increase highly. The results have proven that the tracer only binds with the aptamer with high selectivity.

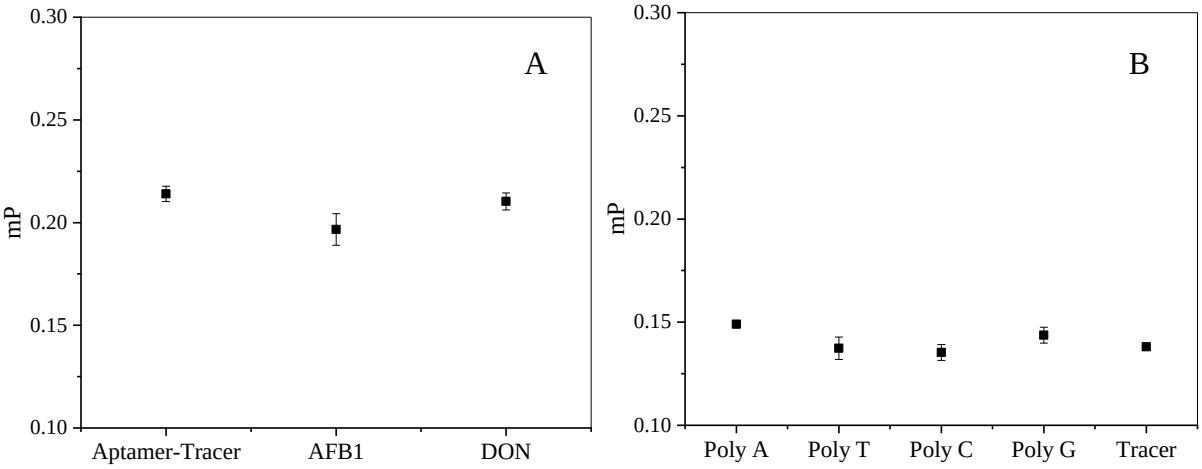

Figure 4-6. Selectivity of FPAA method toward any nonspecific binding. In the present of : A).analogeus molecules mycotoxins AFB1 and DON. B) Other oligonucleotides poly A-T-C-G.

3.4 Conclusion

In summary, we apply a simple competitive fluorescence polarization aptamer assay to detection ochratoxin A by using miniaturized FP analyzer. The binding of fluorescence-labeled OTA (tracer) to aptamer causes an increase of molecular volume and restriction of rotation, so a high *P* value is induced. the performance of FPAA method between conventional and miniaturized FP analyzer was studies through FP analysis. In addition, good selectivity test using other mycotoxins (AFB1 and DON) and oligonucleotides allowed the FPAA method to apply in the complex matrix samples.

References

[1] L. Syedmoradi, M. Daneshpour, M. Alvandipour, F.A. Gomez, H. Hajghassem, K. Omidfar,. Point of care testing: The impact of nanotechnology. *Biosen and Bioelectron.* 2017, 87, 373–387.

[2] C. Maragos, Fluorescence polarization immunoassay of mycotoxins: a review, *Toxins* (Basel). 2009, 1, 196–207.

[3] E. Esen, G. Kokturk, H. Ozer, T. Muhammad, Z. Olcer, H.I. Oktay, S. Simsek, S. Barut, M.Y. Gok, *Talanta*, Lab-on-a-chip based biosensor for the real-time detection of aflatoxin, 2016, 160, 381–388.

[4] D.S. Smith, S.A. Eremin, Fluorescence polarization immunoassays and related methods for simple, high-throughput screening of small molecules, *Anal. Bioanal. Chem*, 2016, 391, 1499–1507.

[5] S. Perrier, V. Guieu, B. Chovelon, C. Ravelet, E. Peyrin, Panoply of Fluorescence Polarization/Anisotropy Signaling Mechanisms for Functional Nucleic Acid-Based Sensing Platforms, *Anal. Chem*, 2018, 90, 4236–4248.

[6] Q. Zhao, J. Tao, J.S. Uppal, H. Peng, H. Wang, X.C. Le, Nucleic acid aptamers improving fluorescence anisotropy and fluorescence polarization assays for small molecules, *TrAC - Trends Anal. Chem*, 2019, 110, 401–409.

[7] A. V. Samokhvalov, I. V. Safenkova, S.A. Eremin, A. V. Zherdev, B.B. Dzantiev, Use of anchor protein modules in fluorescence polarisation aptamer assay for ochratoxin A determination, *Anal. Chim. Acta*, 2017, 962, 80–87.

[8] L. Sun, Q. Zhao, Direct fluorescence anisotropy approach for aflatoxin B1 detection and affinity binding study by using single tetramethylrhodamine labeled aptamer, *Talanta*, 2018, 189, 442–450.

[9] X. Zhang, S.A. Eremin, K. Wen, X. Yu, C. Li, Y. Ke, H. Jiang, J. Shen, Z. Wang, Fluorescence Polarization Immunoassay Based on a New Monoclonal Antibody for the Detection of the Zearalenone Class of Mycotoxins in Maize, *J. Agric. Food Chem*, 2017, 65, 2240–2247.

[10] O. Wakao, K. Satou, A. Nakamura, K. Sumiyoshi, M. Shirokawa, C. Mizokuchi, K. Shiota, M. Maeki, A. Ishida, H. Tani, K. Shigemura, A. Hibara, M. Tokeshi, A compact fluorescence polarization analyzer with high-transmittance liquid crystal layer, *Rev. Sci. Instrum*, 2018, 89, 1-4.

[11] F. Zezza, F. Longobardi, M. Pascale, S.A. Eremin, A. Visconti, Fluorescence polarization immunoassay for rapid screening of ochratoxin A in red wine, *Anal. Bioanal. Chem*, 2009, 395, 1317–1323.

[12] J.A. Cruz-Aguado, G. Penner, Fluorescence polarization-based displacement assay for the determination of small molecules with aptamers, *Anal. Chem*, 2018, 80, 8853–8855.

[13] A. V. Samokhvalov, I. V. Safenkova, S.A. Eremin, A. V. Zherdev, B.B. Dzantiev, Measurement of (Aptamer-Small Target) KD Using the Competition between Fluorescently Labeled and Unlabeled Targets and the Detection of Fluorescence Anisotropy, *Anal. Chem*, 2018, 90, 9189–9198.

[14] Cruz-Aguado, J. A.; Penner, G. Determination of Ochratoxin A with a DNA aptamer. *J. Agric. Food Chem*. 2008, 56, 10456−10461.

[15] O. Wakao, M. Maeki, A. Ishida, H. Tani, A. Hibara, M. Tokeshi, Sensitive fluorescent polarization immunoassay by optimizing synchronization mismatch condition, *Sens Act B Chem*, 2019, 285, 418–422.

CHAPTER 5 Conclusion and Future Prospects

5.1 Conclusive Remarks

The main goal of this thesis is to develop simple and effective strategies to exploit the advantages of the DNA aptamers in the microdevice systems, overcome of their weaknesses when used in such assays and employ these molecules for ochratoxin A detection. The result of this thesis can be concluded in three parts. In the first part, we describe the development of aptasensor on the microfabricated electrochemical system and determined the optimum condition to immobilized aptamer on the gold surface. The proposed sensor constructed on a polystyrene substrate which provides simple and cost-effective for on-site detection. In addition, the surface of the working electrode was not polished with alumina and underwent no treatment with highly oxidizing solutions such as piranha solution and aqua regia as is done on conventional electrode. Instead, the electrode surface was treated by repeated potential scanning under acidic and basic conditions, this treatment makes it easier and safer. We used methylene blue (MB) as a redox indicator because of the ability to interact with the guanine base and the backbone of DNA aptamer proposed a label-free detection. The principle of detection in the first experiment was TID (target induced dissociation) or signal-off, the aptamers that bound with OTA was folded and dissociated from the linker-attached on the electrode surface resulting decreased signal. The findings obtained using the proposed sensor shown wide detection range from 0.1 to 300 ng mL^{-1} with detection limit 78.3 pg mL^{-1}. The proposed sensor also successfully applied to the analysis of spiked coffee and beer samples within the acceptable range (86.4−107%).

In the second part, we developed a miniaturized electrochemical sensor with a dithiol-modified aptamer. we considered to modifying the aptamer through increasing the number of thiol groups on the anchoring sites of the aptamer. This modification aptamer can produce

much stronger interaction with the gold surface, and hence the sensor can provide good reproducible signals. The non-covalently labeled MB was used as a redox probe similar with the previous part. However, here, the mechanism of detection was signal-on. The aptamer would trigger structure switching in the presence of OTA which causes the MB molecule became closer to the electrode surface then generating a higher current. The stability of the dithiol-modified aptamer immobilized on the gold surface was tested by adding another thiol-containing compound such MCH. The DPV response same signal with and without MCH that indicates dithiol-modified aptamer was not affected by adding the monothiol blocking agent. Furthermore, the reproducibility of sensor using six different electrodes obtained 5.9% coefficient of variation. To investigate versatility of the dithiol-modified aptamer, we also applied to the conventional rod electrode. Both electrodes exhibited quantitative responses to a wide concentration range of OTA and provided good linearity in their standard curve. Moreover, this characteristic offered a potential tool for simple and portable on-site detection for the universal platform by changing the corresponding aptamer.

In third part, key features of the aptamer to detection of OTA have broadened by using fluorescence polarization (FP). Application of this method relied on competitive binding between target and tracer to aptamer. The dependency of fluorescence signal with a molecular weight of complex aptamer-target in FPAA was examined in conventional and miniaturized FP analyzer. Performance between two instruments is very satisfactory and revealed that the FPAA method has good sensitivity on a different platform. In addition, this method allowed to detection of OTA in the complex matrix sample, because this method provide excellent selectivity.

5.2 Future Prospects

A miniaturized label-free electrochemical aptasensor has attracted due to their remarkable features of simple and portable instrumentation, wide detection range, good sensitivity, selectivity, and low-cost. However, in a physiological environment, the gold surfaces functionalized via thiol anchoring aptamer will be subjected to stress by other thiol-containing molecules, which may displace the original thiol anchored loading of the surface. Though this displacement is common for mono thiol and can be significantly reduced by use of DTPA. The DTPA can be inserted into an oligonucleotide at the 5'-end position, internally or at the 3-end' position. In addition, it can be inserted in series (two, three or more dithiol-groups) to increase the efficiency of ligand/surface interaction. Future research will be directed to the extension of the stability of the immobilized aptamer by modifying the anchoring group with triple DTPA, and then integrating it into a microfluidic device system. Robust and high stability of the sensing layer could extend regeneration capability of the sensor thus increasing efficiency of measurement. Moreover, the sensing layer will be resistance into chemical and thermal condition for real sample application. In addition, another prospect is to incorporated other substrate such as paper-based device with screen printing technique, polymer film that provides thin and flexible electrode to applied in wearable sensor for personal health or using "pin" as electrode. Combining the microfabricated electrode to a portable potentiostat with wireless connectivity to smartphones would facilitate electrochemical analysis at the point-of-use and in the field, where access to a computer or wired connection to a device is difficult or impossible.

Another future prospect was addressed in the FPAA method. We have designed a biotinylated aptamer that has an affinity to bind with OTA. The relationship between molecular weight of complex aptamer-target or aptamer tracer toward signal intensity will be a potential issue that interest to be examined. Moreover, research related combination of

FPAA with nanomaterials are still quite limited. Hence, exploring and constructing more novel nanomaterials based on different family members is necessary. It is highly desired to establish FPAA based on nanomaterials with low toxicities, desirable stability, non-quenched activity. In addition, most of the established FPAA sensors based on nanomaterials still limited at the stage of laboratory scale and not yet reach a commercial level, it may be caused by the complexity of the real biological matrix samples, which makes the detection result susceptible to the influence of unexpected events. In response to these challenges and opportunities, it is highly demanded to prepare more new nanomaterials with high physicochemical properties combined with other paths as FPAA enhancers. Development FPAA method to large number of target analytes in medical diagnosis, food safety, environmental monitoring was also preferable effort in this field.

Along with the great progress in the micro total analysis system (μTAS) as well as biosensor technology, I believe that aptamer-based microdevice instrument will bring about promising future and play a critical role in the various applications in the coming years.